# Chloride initiated reinforcement corrosion in marine concrete

Sandberg, Paul

1998

LUND UNIVERSITY
LUND INSTITUTE OF TECHNOLOGY
Division of Building Materials

# Chloride initiated reinforcement corrosion in marine concrete

Paul Sandberg

Report TVBM-1015 Lund, Sweden, 1998

LUND UNIVERSITY
LUND INSTITUTE OF TECHNOLOGY
Division of Building Materials

# Chloride initiated reinforcement corrosion in marine concrete

Paul Sandberg

Report TVBM-1015 Lund, Sweden, 1998

Cover Photo: The Great Belt Bridge in Denmark, Göran Hedenblad, Lund, Sweden

ISRN LUTVDG/TVBM--98/1015--SE(1-86)
ISSN 0348-7911 TVBM

Lund Institute of Technology
Division of Building Materials
Box 118
S-221 00 Lund, Sweden

Telephone: 46-46-2227415
Telefax: 46-46-2224427

## PREFACE

This thesis is to a large extent based on analyses and discussion of data collected by a group of researchers working within the project Durability of Marine Concrete Structures (BMB), including the following persons, to whom the author is very grateful:

Göran Fagerlund, Lund Institute of Technology (LTH); Kyösti Tuutti, Cementa AB and Skanska AB; Karin Pettersson and Kerstin Woltze, the Swedish Cement and Concrete Research Institute (CBI); Hans Arup Consultant, Denmark; Ervin Poulsen, Jens Frederiksen and Henrik Sörensen, AEC Consulting Engineers, Denmark; Lars-Olof Nilsson and Alf Andersen, Chalmers University of Technology; Johan Larsson, Scancem Research AB / Lund Institute of Technology; Per-Erik Pettersson and Tang Luping, the Swedish Research and Testing Institute (SP).

The following persons have also contributed significantly to the project: Gert-Olof Johansson, Sten Hjelm and Catrine Ewertsson, SP; Tord Lundgren, Stefan Backe and Sture Sahlén, LTH; Mats Rodhe and Juhan Avik, Chalmers. I also want to thank Britt Andersson, LTH, for all the help with my figures!

The BMB project has been a joint research project based on an annual 2 MSEK research grant from Cementa AB and the Euroc/Scancem Development and Research Fund.

The work by the present author has been funded by Scancem/Cementa AB from 1991 to 1998. During 1997 and 1998 the work by the author has partially been funded as a part of the infrastructure project "Industriprogram Infrastruktur" which was funded by NUTEK, the industry and universities in Sweden.

Lund, April 1998

Paul Sandberg

**CONTENTS** **page**

## SUMMARY


### Topics

The thesis covers the following topics:

A) A review of the electrochemistry of steel in concrete (Chapter 2).
B) Principles of field testing for service life prediction (Chapter 3).
C) Chloride thresholds for steel in concrete (Chapter 4-5).
D) Experimental work chloride threshold in marine concrete (Chapter 6).
E) Experimental work on chloride binding in field exposed marine concrete (Chapter 7).
F) Experimental data on chloride transport rates in marine concrete (Chapter 8).
G) Simple prediction of chloride ingress in marine concrete (Chapter 9).
H) Service life prediction (Chapter 10).

### Chloride thresholds for reinforced concrete exposed in a marine environment

The chloride threshold for initiation of pitting corrosion in reinforced concrete depends on the exposure conditions, the cover thickness, the presence of defects at the steel surface, the microstructure and w/c ratio of the concrete, and the type of binder used. The relative effects of these parameters have been evaluated. It was found that the chloride threshold for uncracked concrete based on sulfate resisting portland cement (SRPC) with w/c ratio 0.3-0.5 and exposed in the splash zone is in the range of 1.1 to 1.5 % total chloride by weight of binder. Assuming a normal frequency distribution, the corresponding chloride threshold with 95 % confidence is 1.0 to 1.3 % total chloride by weight of binder for plain SRPC concrete and 0.8 to 1.0 % total chloride by weight of binder for SRPC concrete with 5 % silica fume in the binder. It was estimated from the results from exposure tests on specially designed corrosion cells that the chloride threshold is approximately 2 times higher in fully submerged concrete than in the splash zone. It was also estimated that the chloride threshold can be increased by 40-75 % by the removal of voids 0.1-2 mm in the concrete at the steel surface. The chloride threshold for slag cement concrete exposed in the splash zone was estimated to be 60 % of the chloride threshold for SRPC concrete with 5 % silica fume. The corresponding chloride threshold for concrete with 10-20 % fly ash in the binder was estimated to be 80 % of the threshold for SRPC concrete with 5 % silica fume.

### Chloride binding in concrete exposed in a marine environment

A linear relationship between free and total chlorides was found in concrete submerged in sea water or exposed in the splash zone close to the water line, for ½ to 2 years. Concentration profiles measured for the chloride and hydroxide ion concentration indicated that these ions penetrate concrete in opposite directions but at approximately the same rate. It was suggested that hydroxide counter diffusion increases the chloride binding close to the exposed uncarbonated surface, which leads to a more linear relationship between free and total chlorides in marine concrete than that observed under ideal laboratory conditions with no hydroxide gradient in the concrete pore solution.

Chloride transport in concrete exposed in a marine environment

After 5 years of field exposure, most profiles of total chloride measured fitted well to a theoretical profile calculated by fitting experimentally obtained chloride concentrations to a solution to Fick's second law of diffusion assuming linear chloride binding and constant diffusivity. However, the calculated effective chloride diffusivity obtained by the curve fitting of total chloride concentrations measured at different exposure times, decreases over time in field exposed concrete. The effective chloride diffusivity can be reduced by a factor of 3-5 by using 5 % silica fume in the form of a well dispersed slurry in the binder fraction of the concrete, as compared to a plain SRPC concrete. If on the other hand the w/c ratio is reduced from 0.40 to 0.30 besides the introduction of 5 % silica fume in the binder, it seems that the effective chloride diffusivity can be reduced by a factor of 8-10.

Service life prediction

The predicted required minimum cover is much more sensitive to variations in parameters affecting the chloride transport rate than to variations in the chloride threshold. The calculations of the required minimum cover thickness indicate that the use of 5% silica fume and a reduction of the w/c ratio from 0.40 to 0.30 would reduce the required minimum cover by approximately 50 % as compared to a normal Swedish "bridge concrete" of w/c 0.40 and no pozzolans. It is however important to point out that other durability issues such as the durability to freezing and thawing may completely alter the overall judgement of the most durable concrete mix. Considering the durability to both reinforcement corrosion and freezing and thawing, the optimum binder is probably a mix with SRPC and 5% silica fume, as this relatively small amount of pozzolan has a strong positive effect on the resistance to chloride penetration, but only a small negative effect on the chloride threshold. Furthermore, it is relatively easy to produce a concrete with SRPC and 5% silica fume, which is resistant to freezing and thawing in a saline environment.

Service life prediction based both on prediction of the initiation time in uncracked concrete and prediction of the permissible time of active corrosion in cracks appears to be more useful than predictions based on only the initiation time in uncracked concrete. However, data on the permissible loss of reinforcement cross section at a corrosion pit in a crack is lacking. Some speculations on the corrosion rate and the permissible loss of reinforcement cross section were undertaken in order to demonstrate the suggested theory for service life prediction.

Potentially it would be of great interest to consider high performance concrete with 5-10 % silica fume in the binder and a maximum w/c ratio of 0.30 for concrete structures exposed in very aggressive saline environments. This concrete would be highly resistant to chloride penetration and would suppress active corrosion rates to very low levels, as a result of the very high resistivity of the concrete. However, concrete with such low w/c ratios are more sensitive to cracking than normal concrete. Further research is therefore needed on the effects of active corrosion in cracks on the service life of high performance concrete structures.

Organisation of the thesis

The thesis is composed of, (i) a report summarising the total work, (ii) 7 papers and reports that are either published or submitted for publication in international journals or conference proceedings, (iii) 4 institutional reports including the licentiate thesis.

The summarising report presents and discusses the main results obtained and concludes by a theory for service life prediction with regard to reinforcement corrosion in uncracked and cracked marine concrete.

The 11 supplementing papers and reports are listed below. They contain the following:

- The 7 papers (I, II, IV, VI-IX) Presents selected experimental data and evaluations of chloride thresholds, chloride binding and chloride transport rates.

- 3 of the 4 institutional reports (II, V, X) include compilations of chloride thresholds and chloride transport rates measured within the project. Attempts to use the data for service life prediction are also undertaken.

- The licentiate thesis (paper XI) describes the overall picture of the problem, including a literature review of the mechanisms involved and speculations on factors affecting the chloride threshold. Some experimental data are available in the licentiate thesis on chloride binding and chloride transport rates in concrete.

The papers, institutional reports and the licentiate thesis included in this doctorate thesis are referred to by Roman numerals as follows:

I: Sandberg, P., " Factors affecting the chloride thresholds for uncracked reinforced concrete exposed in a marine environment. Part I: Field exposure tests of reinforced concrete", submitted for publication in Advanced Cement Based Materials.

II: Sandberg, P. and Sørensen, H. E., " Factors affecting the chloride thresholds for uncracked reinforced concrete exposed in a marine environment. Part II: Laboratory- and field exposure of corrosion cells", submitted for publication in Advanced Cement Based Materials.

III: Sandberg, P., The effect of defects at the steel – concrete interface, exposure regime and cement type on pitting corrosion in concrete, Report TVBM-3081, 1998, Lund Institute of Technology, Division of Building Materials.

IV: Sandberg, P., "Studies of chloride binding in concrete exposed in a marine environment", submitted for publication in Cement and Concrete Research.

V: Sandberg, P., Recurrent studies of chloride ingress in uncracked marine concrete, Report TVBM-3080, 1998, Lund Institute of Technology, Division of Building Materials.

VI: Sandberg, P., Luping, T. and Andersen, A., "Recurrent studies of chloride ingress in uncracked concrete at various exposure times and –elevations", submitted for publication in Cement and Concrete Research.

VII: Sandberg, P., Pettersson, K., Jørgensen, O., "Field studies of chloride transport into high performance concrete", in Concrete in Marine Environment, ACI SP-163, ed: V. M. Malhotra , ACI, Michigan, 1996, pp. 233-254.

VIII: Sandberg, P., Tang, L., "A field study of the penetration of chlorides and other ions into a high quality concrete marine bridge column", in Durability of Concrete, ACI SP-145, ed: V. M. Malhotra, ACI, Michigan, 1994, pp. 557-571.

IX: Sandberg, P., Pettersson, K., Arup, H., Tuutti, K., "Cost-effective design of high performance concrete structures exposed in saline environment", in Concrete Repair, Rehabilitation and Protection, ed: R K Dhir and M R Jones, E&FN Spon, London 1996, pp 779-789.

X: Sandberg, P., "Service life prediction of reinforced concrete structures in saline environment", in Selected Research Studies from Scandinavia, ed: K. Tuutti, Report TVBM-3078, 1997, Lund Institute of Technology, Division of Building Materials, pp.139-152.

XI: Sandberg, P., Critical evaluation of factors affecting chloride initiated reinforcement corrosion in concrete, Licentiate thesis, Report TVBM-3068, 1995, Lund Institute of Technology, Division of Building Materials.

## NOTATIONS AND ABBREVIATIONS

A list of notations and abbreviations with descriptions or definitions as used in this thesis is shown in Table i.

Table i. Notations

| Text or symbol | Unit | Description or definitions used in this thesis |
|---|---|---|
| Active corrosion | | A corrosion rate for freely corroding reinforcement > 1 $\mu A/cm^2$, or for specially designed steel electrodes under potential control, Chapter 6.4.1.4, a current >100 $\mu A$ needed to maintain a given potential. |
| Aq | | Aqueous solution |
| AEC | | AEC Consulting Engineers, Vedbaek, Denmark |
| AISI 316 | | Austenitic standard stainless steel according to ASTM (AISI), see (paper XI) |
| Atm. or Atmosph. | | Exposure in the atmospheric exposure zone which is seldom affected by wave action |
| BMB | | Durability of Marine Concrete Structures. Cementa/Scancem sponsored project on field and laboratory exposure tests of marine concrete. |
| C (capital) | $kg/m^3$ | Cement (portland or slag cement) content in concrete |
| c | mm | Cover thickness |
| Chalmers | | Division of Building Materials, Chalmers University of Technology |
| Chloride threshold | % wt of binder | Concentration of total chloride needed to initiate and maintain active corrosion for 2 consecutive weeks (also called Ccrit). |
| $[Cl^-]$ or Cl | Mol/l | Chloride ions in concrete pore solution (also called free chlorides) |
| Cmax | % wt of binder | Measured maximum total chloride concentration in a profile of total chloride |
| Cscalc | % wt of binder | Calculated apparent surface total chloride concentration used when fitting a theoretical profile of total chloride according to Fick´s $2^{nd}$ law of diffusion to a measured profile of total chloride |
| $C_3A$ | | Aluminate phase in portland cement |
| $C_3AF$ | | Ferrite phase in portland cement |
| $C_3S$, $C_3S$ | | Tri-calcium silicate, di-calcium silicate; schematic formula for the principal strength giving compounds alite and belite in portland cement |
| CBI | | Swedish Cement and Concrete Research Institute |
| DeCl | | Calculated effective chloride diffusivity by fitting a theoretical profile of total chloride according to Fick´s $2^{nd}$ law of diffusion to a measured profile of total chloride, assuming linear chloride binding and constant diffusivity |
| dry | | Indicates silica fume added as a compacted powder, see Table 8.1 |
| E | V | Potential, relative to a reference electrode (SCE, $MnO_2$, AgCl or SHE) |
| FA | | Fly ash, see Table 6.1 |
| f´c 28 d | MPa | Compressive cube strength after 28 days standard curing |
| Filter paper defect | | Artificially produced defects at the steel-concrete interface in corrosion cells, by means of a standard filter paper, see Figure 6.6. |
| HPC | | High performance concrete, w/c ratio ≤ 0.40 |
| i | A | Electrical current |
| $i_{corr}$ | | Corrosion current for freely corroding steel (no potentiostatic control) |
| LTH | | Division of Building Materials, Lund Institute of Technology |
| M | Mol/l | Molarity, concentration of a given ion in solution |

Table i. Notations (continued)

| | | |
|---|---|---|
| N.A. | | Not analysed |
| NPC | | Normal performance concrete, w/c ratio > 0.40 |
| $[OH^-]$ or OH | Mol/l | Hydroxide ions in concrete pore solution |
| OPC | | Ordinary portland cement, see Table 7.1 |
| Passivity | | State of corrosion with the corrosion rate depressed to insignificant levels by the formation of a barrier of oxides on the steel surface. |
| Polarisation | | Shift in steel potential caused by an impressed current or by changes in the resistance against the anodic or cathodic reactions to proceed |
| Potentiostatic control | | Method of maintaining a constant value of the steel potential by an impressed current controlled by a potentiostat |
| Pozzolan | | Siliceous material which reacts with calcium hydroxide to form a cementitious binder (normally silica fume, fly ash or granulated blast furnace slag) |
| $R^2$ | | Correlation coefficient calculated by the least square method when fitting a trend line to measured data |
| RH | % | Relative humidity |
| SF | | Silica fume, see Table 6.1 |
| Slag cem. | | 50 % granulated blast furnace slag interground with portland cement, see Table 6.1 |
| Slu or slurry | | Indicates silica fume added as a 50 % slurry, see Table 8.1 |
| Spl. or Splash | | Exposure in the splash zone which is frequently exposed to wave action |
| SRPC | | Sulfate resisting portland cement (high iron oxide content), see Table 6.1 |
| Steel electrode | | Model reinforcement in corrosion cells, see Figure 6.5 |
| SP | | Swedish Research and Testing Institute |
| Subm. | | Exposure in the submerged zone |
| Total Cl or Tot. Cl | % wt of binder | Total chloride (free and bound chlorides) concentration by weight of binder |
| w | $kg/m^3$ | Water (tap water) content in concrete |
| w/c | | Water to binder ratio = w/(C+SF+0.3FA) |
| > x | Tot Cl % wt of binder | Minimum chloride threshold, related to the total chloride concentration at depth of a passive steel electrode at the end of exposure |
| Ø | | Diameter |

# 1. INTRODUCTION

## 1.1 Background

Chloride initiated reinforcement corrosion is one of the major causes of distress in marine concrete structures and in several on shore concrete structures exposed to de-icing salt. In USA, the costs for rehabilitation of deteriorated bridges has been estimated to $ 90-150 billion. Most of the deterioration has been linked to the use of de-icing salts causing either salt frost attack on the concrete surface and/or reinforcement corrosion /1,2/.

Steel reinforcement in chloride free alkaline concrete is protected by a passive iron oxide layer which depresses the corrosion rate to insignificant levels. Chloride ions however penetrate the concrete cover at a rate which depends on the exposure conditions, the pore structure, the homogeneity and the moisture state of the concrete cover. At a critical chloride concentration, the chloride threshold, the passivity of the steel is interrupted and active corrosion is initiated.

Considerable research work has been carried out on factors affecting chloride transport in concrete with the aim to predict the chloride penetration rate in concrete structures. On the other hand, relatively little research work has been carried out on the factors affecting the chloride threshold level for steel reinforcement in concrete exposed under various conditions.

## 1.2 Aim of project and of this study

This doctoral thesis was carried out as a part of a larger experimental program "Durability Reinforced Concrete Structures in Marine Environment" (BMB) carried out in Sweden in 1991-1997 and involving also Danish researchers. One of the main objectives was to establish and run a marine field station where many different concrete mixes were exposed to natural marine conditions. Thereby important field data to be used in service life prediction were obtained and service life models were calibrated against reality. The present author was co-ordinating the BMB project.

The aim of this doctoral thesis was to quantify and evaluate the relative importance of factors affecting the chloride threshold and the chloride transport rate in concrete exposed in a marine environment. The new field station established in the BMB project should be used for field exposure tests and the results should be evaluated against parallel laboratory exposure tests on similar concrete. Field exposure data from real structures should be established and evaluated when appropriate. Relatively little attention has been drawn to the testing and mathematical modelling of chloride transport in concrete as this topic was covered by Tang Luping et. al. at Chalmers University of Technology; see /3/.

## 1.3 Funding

The BMB project has been a joint research project based on an annual 2 MSEK research grant from Cementa AB and the Euroc/Scancem Development and Research Fund. Each party as listed in Table 1.1 has contributed with additional internal research funding to cover internal research and other activities connected to the BMB project.

The work by the present author has been funded by Scancem/Cementa AB from 1991 to 1998. During 1997 and 1998 the work by the author has partially been funded as a part of the infrastructure project "Industriprogram Infrastruktur" which was funded by NUTEK, the industry and universities in Sweden.

## 1.4 Organisation of the project

The project has involved a number of institutions and research activities co-ordinated by the present author which during the work was employed by Cementa AB, Table 1.1. Much of the data presented in this thesis originates from different institutions. The present author, however, has been heavily involved in the work done, as initiator or as researcher. The data presented has been subjected to careful quality control by the author before they were presented.

Table 1.1. Organisation of research and other activities in the project

| **LTH**[1] | **Chalmers**[2] | **CBI**[3] | **SP**[4] | **AEC**[5] | **Scancem Res.**[7] |
|---|---|---|---|---|---|
| Chloride threshold | Moisture and chloride transport | Chloride threshold | Operation of field station | Modelling of chloride transport | Pore solution chemistry |
| Chloride binding | Rapid migration tests | Corrosion rates | Casting of concrete specimens | Chloride threshold[6] | Chloride binding |
| Moisture and chloride transport | Modelling of chloride transport | Pore solution chemistry | Freezing and thawing | Standard test methods[6] | |
| Freezing and thawing | Chloride binding | Chloride binding | | Casting of concrete specimens | |

[1] Division of Building Materials, Lund Institute of Technology
[2] Division of Building Materials, Chalmers University of Technology
[3] Swedish Cement and Concrete Research Institute
[4] Swedish Research and Testing Institute
[5] AEC Consulting Engineers, Denmark
[6] Method for testing of chloride threshold supervised by Hans Arup Consult, Denmark
[7] Scancem Research AB

## 2. ELECTROCHEMISTRY OF STEEL IN CONCRETE

### 2.1 General

Normally, steel in concrete is passive in a moist, alkaline environment which is free of chlorides and other aggressive ions /4/. The term passivity denotes that although ordinary steel reinforcement in concrete is thermodynamically not stable, the corrosion rate is depressed to an insignificant low level by the formation of a barrier of iron oxides on the steel surface.

The passive state is maintained until the concrete in contact with the reinforcement becomes carbonated, or until a sufficient concentration, the chloride threshold, of aggressive ions (normally chlorides) has reached the steel surface. The aggressive ions (e.g. chlorides) then trigger the dissolution of the iron oxide layer and later on the dissolution of steel.

In the following the basic electrochemistry of steel passivation and -corrosion in concrete is reviewed. The chemical equations given are simplified but should help to describe the corrosion phenomena in concrete. A more comprehensive description of the passivation and corrosion processes for steel in concrete can be found in /5/ and in the Licentiate Thesis (paper XI). General descriptions of the electrochemistry of corrosion can be found in textbooks such as /6,7/.

### 2.2 The basic anodic- and cathodic reactions

Concrete is an inhomogeneous material with local variations in the alkalinity, the moisture content and bonding at the interface between concrete and steel. The steel is therefore divided into several anodic and cathodic areas. The electrons released in the anodic reaction, eq.1, has to be consumed in cathodic reaction, eq. 2, in order to maintain electrical neutrality. Therefore the anodic- and cathodic reactions are always proceeding at the same rate.

$Fe \rightarrow Fe^{2+} + 2e^-$ eq. 1, anodic oxidation of iron.

$O_2 + 2H_2O + 4e^- \rightarrow 4OH^-$ eq. 2, cathodic reduction of oxygen.

The basic anodic and cathodic reactions, eqs 1-2, are the same in both the passive and the active state, but the reaction rate is higher by orders of magnitudes in the active state.

### 2.3 The passive state

As long as the steel is passive, the anodic oxidation of iron leads to the formation of insoluble iron oxide which helps to build up and maintain the passive layer, eq. 3-5. However, the passive layer on steel in concrete does not consist of $Fe_2O_3$ only, but rather a mixture of the iron oxides $Fe_2O_3$ and $Fe_3O_4$ intermixed with cement hydrates (paper XI). $Fe_3O_4$ is not a passive oxide as its porosity can be very high as compared to $Fe_2O_3$. The formation of $Fe_3O_4$ can schematically be described by eq. 6-7. The anodic formation of the iron oxide layer on passive steel in concrete is relatively slow because of the impermeability of the passive layer.

$4Fe^{2+} \rightarrow 4Fe^{3+} + 4e^-$
$3O_2 + 12e^- \rightarrow 6O^{2-}$ eq. 3-5, formation of passive iron oxide $Fe_2O_3$
$4Fe^{3+} + 6O^{2-} \rightarrow 2Fe_2O_3$

$2O_2 + 8e^- \rightarrow 4O^{2-}$ eq. 6-7, formation of iron oxide $Fe_3O_4$
$2Fe^{3+} + Fe^{2+} + 4O^{2-} \rightarrow Fe_3O_4$

## 2.4 The active state

### *2.4.1 Corrosion products formed in an oxygen rich environment*

Once active corrosion has been initiated, the formation of $Fe_3O_4$, or other corrosion products with a much higher porosity as compared to $Fe_2O_3$, is accelerated. If enough oxygen is available at the anode, solid corrosion products "red rust" are formed, thus replacing eq. 6-7 with eq. 8-10. The formation of red rust is more expansive than the formation of $Fe_3O_4$ and may cause cracking and spalling of the concrete cover.

$Fe^{2+} + 2OH^- \rightarrow Fe(OH)_2$ eq. 8, formation of ferrous hydroxide
$4Fe(OH)_2 + O_2 + 2H_2O \rightarrow 4Fe(OH)_3$ eq. 9, formation of ferric hydroxide
$2Fe(OH)_3 \rightarrow Fe_2O_3{*}H_2O + 2H_2O$ eq. 10, formation of hydrated ferric oxide

### *2.4.2 Corrosion products formed in an environment low in oxygen*

Corrosion in concrete with a lack of oxygen such as in concrete submerged in seawater, leads to the formation of non- or little expansive rust as the oxygen required in eq. 9 is lacking. Thus no spalling takes place and the corrosion may continue without being visible from the outside of the concrete. The corrosion products formed can be solid black rust, eq. 6-7, soluble black or green rust due to the formation of iron complexes sometimes containing chlorides, or solid white ferrous hydroxide. These corrosion products are not stable in oxygen rich concrete, see the Licentiate Thesis (paper XI).

## 2.5 The catalytic effect of chloride ions

Chloride ions trigger and accelerate the dissolution of the passive iron oxide layer. The chloride attack starts with pitting at "weak spots" at the steel-concrete interface. A "weak spot" may occur due to a local pH drop, a compaction void, or a crack in the concrete, or a defect in the steel scale. The formation of local anodes at weak spots create potential differences which attract chlorides. Eventually pitting corrosion initiates at the weak spot as illustrated in Figure 2.1 /8/. As oxygen is removed from the emerging pit, eq. 9, the steel surface below the solid corrosion products becomes acidified as described by eq. 11.

$Fe^{2+} + H_2O \rightarrow FeOH^+ + H^+$ eq. 11, acidification inside corrosion pit.

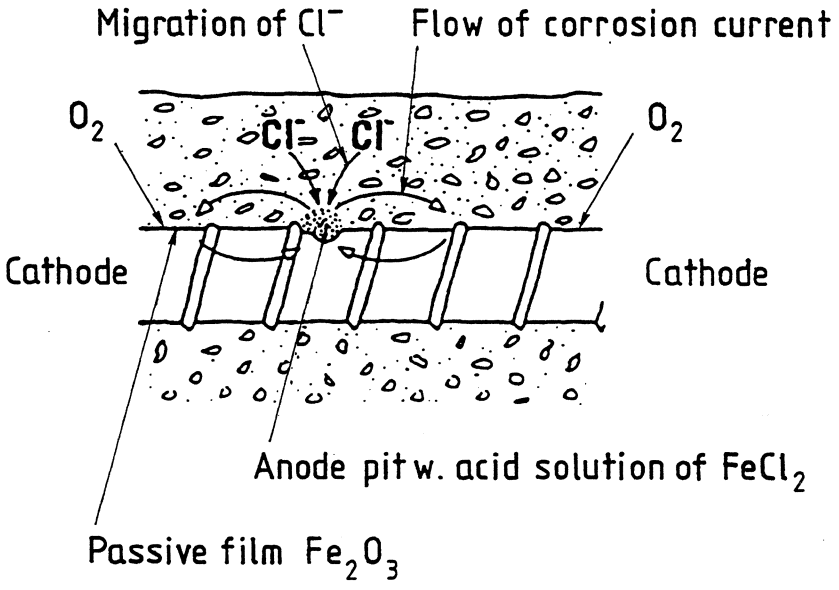


Figure 2.1. Mechanism of pitting corrosion in concrete /8/.

Several mechanisms may contribute to the catalytic effect of chloride ions. Chloride ions form soluble complexes with iron ions which favour the dissolution of iron oxide. The reactions described in eq. 5 and 7 go almost completely to the right as indicated by the arrows. The formation of chloride ion complexes may however consume the free iron ions in solution, and change the equilibrium which would trigger the dissolution of iron oxide. The presence of chloride ions also increases the solubility of the passive layer which further accelerates its dissolution.

The catalytic effect of chlorides is stronger in concrete exposed to oxygen as discussed in (paper XI). This effect is due to the breakdown of the chloride iron complexes as they diffuse away from a corrosion pit which is low in oxygen into oxygen rich concrete. The chloride iron complexes are not stable in the presence of oxygen as described by eq. 12.

$4FeCl_2(aq) + O_2 + 6H_2O \rightarrow 4FeOOH + 8HCl(aq)$ eq. 12, breakdown of chloride iron complex and acidification of pit.

The net result is a further acidification and a release of chloride ions. Both effects accelerate the corrosion attack. pH as low as 1.0 inside corrosion pits in concrete has been reported /8/. At such low pH, the acid dissolution of the steel can be much more rapid than the electrochemical corrosion.

## 2.6 Steel potentials in concrete

The (measured) steel potential in concrete represents a balance of cathodic reactions, anodic reactions and any external current from other metals or other electrical sources connected to

the steel. The steel potential is measured relative to a standard reference electrode with a known potential.

The anodic reaction (eq. 1) tends to increase the steel potential while the cathodic reaction (eq. 2) tends to decrease it. This phenomena is called polarisation and reflects the difficulty for the anodic- and cathodic reactions to proceed. Figure 2.2 illustrates a concrete in a given exposure condition, i.e. at a given cathodic oxygen reduction capacity, but with two different anodic polarisation curves representing a passive and an active state. As indicated in Figure 2.2, the anodic polarisation curve is very steep in the passive state (because of the impermeability of the passive oxide layer) which leads to a very low corrosion rate as compared to the active state. Figure 2.3 illustrates the steel polarisation and the corrosion rate in a fully submerged concrete with a very low availability of oxygen at the steel surface.

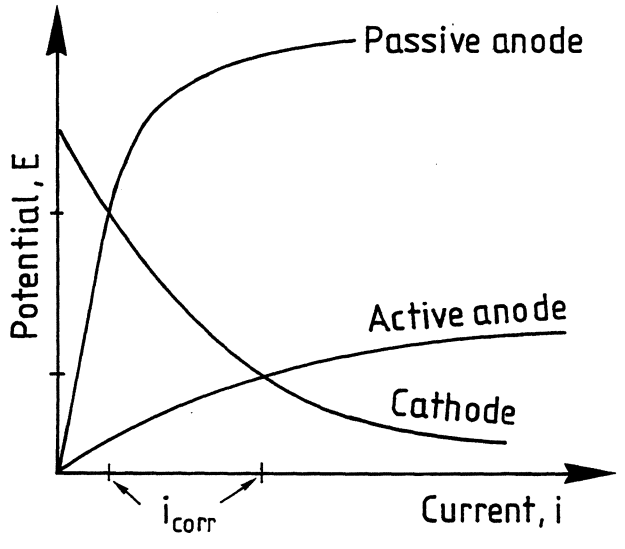


Figure 2.2. Anodic polarisation in the passive and in the active state /6/.

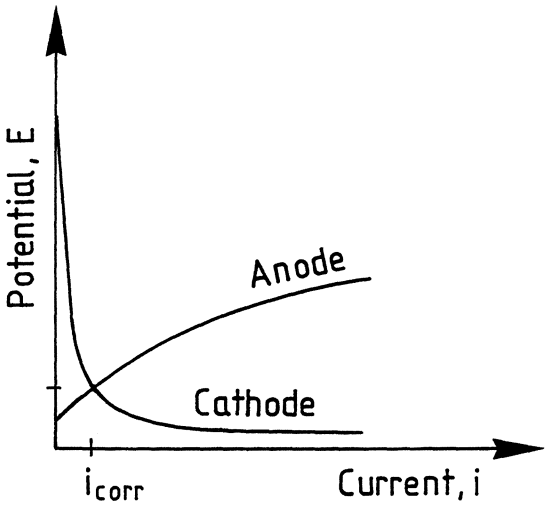


Figure 2.3. Cathodic polarisation in submerged concrete /6/.

## 2.7 Driving force for corrosion

The driving force for corrosion of steel in concrete may schematically be illustrated in a Potential - pH diagram as shown in Figure 2.4 taken from the Licentiate Thesis (paper XI) for iron in aqueous solutions at + 25 °C. The dotted lines a and b represent the limits of water stability. As uncarbonated concrete has a pore solution with pH in the range of 12.5 - 14, steel in concrete is found in the "Passivity" region in Figure 2.4, between the lines a and b in the pH range 12.5 - 14. As opposed to the situation in the "Immunity" region, there is a driving force for corrosion in the "Passivity" region, but the formation of iron oxide may protect the steel. The chloride iso-concentration lines indicate the approximate chloride ion concentration necessary to destroy the passive iron oxide layer. Once a corrosion pit has been established, the pH drops inside the pit and active pitting corrosion occurs locally in the "$Fe^{2+}/Fe^{3+}$" region shown in Figure 2.4.

As indicated in Figures 2.3 and 2.4, the potential for non corroding steel in concrete is to a large extent controlled by the availability of oxygen in the concrete at the depth of the

reinforcement. A fully submerged concrete has a very low oxygen permeability, and therefore the availability of oxygen at the reinforcement quickly becomes very low and hence the steel potential drops into a region of higher resistance to chloride initiated corrosion. The potential drop represents the basis for cathodic protection. A complete cathodic protection implies that the steel potential is brought down into the "Immunity" region by an imposed electrical current.

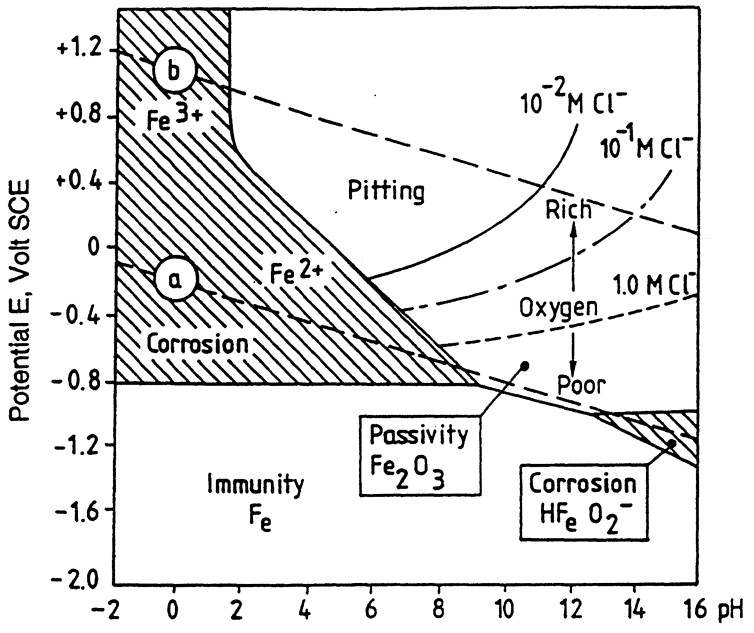


Figure 2.4. Potential – pH diagram for black steel in aqueous solution (paper XI).

## 2.8 Corrosion rate

As opposed to Figures 2.2 and 2.3, the potential-pH diagram in Figure 2.4 gives no information on the corrosion rate. The corrosion region "$HFeO_2^-$" in Figure 2.4 indicates that corrosion can be initiated in the absence of chlorides at very low steel potentials. But as seen in Figure 2.3, the corrosion rate is very low as long as the cathodic reaction is restricted by a low availability of oxygen at the steel surface.

The corrosion rate in fully submerged concrete members is usually very low because the oxygen transport to the cathode is restricted as described in the Licentiate Thesis (paper XI). The phenomena is called cathodic control. However, if the reinforcement in the submerged concrete is in metallic contact with reinforcement (or another metal) in concrete exposed to the atmosphere, a corrosion macrocell may form with very high corrosion rates. In this case a very efficient cathode formed in the oxygen rich concrete exposed to the atmosphere may boost the anodic reaction in the submerged concrete. The only limiting factor would be the resistivity of the concrete between the anode and the cathode. But the resistivity of wet, chloride contamined concrete is often relatively low, especially in porous concrete with a high w/c ratio.

The corrosion rate in concrete members exposed to the atmosphere is not limited by the availability of oxygen. Instead the formation of solid rust at the anode and the resistivity in the

often relatively dry concrete between the cathode and the anode limit the corrosion rate. The formation of solid rust at the anode represents a diffusion barrier with a function similar to, but not as efficient as, the iron oxide layer on passive steel.

## 2.9 Assessment of corrosion state (active or passive)

The steel potential alone does not give a definite indication of the corrosion state. As illustrated in Figure 2.5 /8/, a passive reinforcement with steep polarisation curves but a very low corrosion current, may have a similar potential as an active reinforcement with a high corrosion rate. As indicated in Figure 2.5, studies of the polarisation behaviour of the reinforcement gives a more reliable indication of the corrosion state. A small current induced in a passive reinforcement would result in a relatively high polarisation, i.e. change of steel potential, as compared to when the same small current is induced in an active reinforcement. This principle forms the basis for studies of corrosion rates by means of polarisation resistance and galvanostatic pulse /8/.

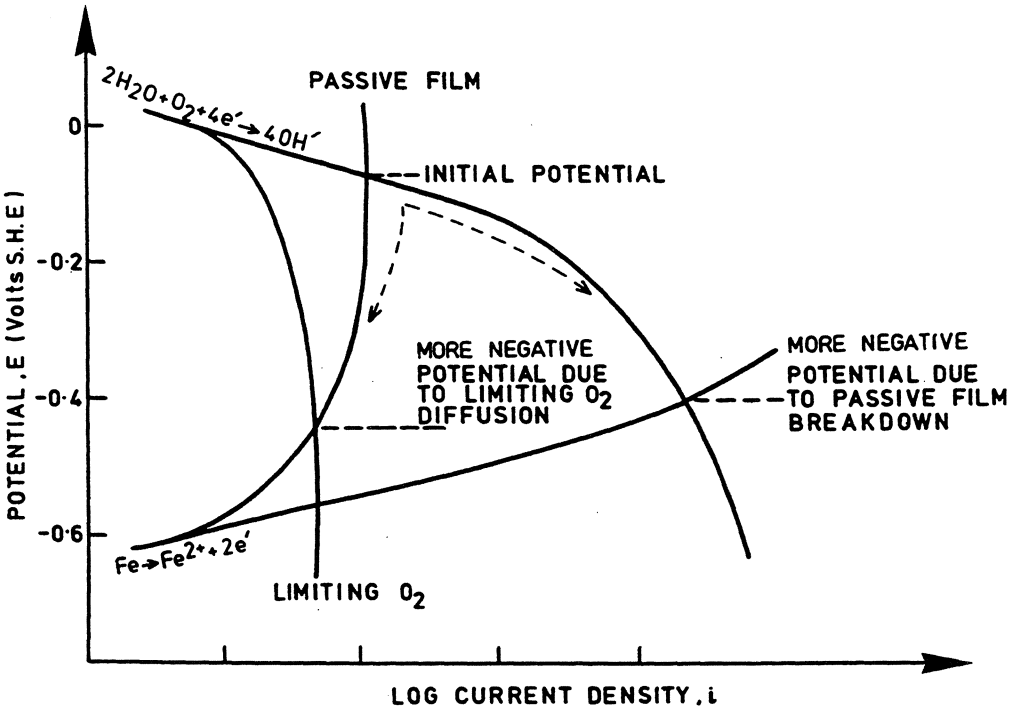


Figure 2.5. Active and passive polarisation curves for steel in concrete.

# 3. PRINCIPLES OF FIELD TESTING FOR SERVICE LIFE PREDICTION

## 3.1 General procedure for collecting data for service life prediction

Several long-term field studies of concrete have revealed the need for a systematic approach for collecting field data for service life prediction of concrete structures /9-12/. These field studies among others indicated that field testing of concrete will generate a wide spread of data for a given concrete mix, depending mainly on the exposure conditions on the micro level, and on the exposure length.

Most laboratory testing of the potential durability of concrete involves accelerated and simplified exposure conditions. Tests for the evaluation of chloride permeability, for instance, are usually accelerated by the use of an electrical field or immersion in very strong chloride solutions. Such laboratory testing produces some permeability-related results, which are only valid for that specimen at the testing age and the specific exposure conditions used. Today it is obvious that laboratory tests cannot be used for service life prediction unless they are carefully calibrated against long term experience from field exposure tests. General procedures for the development of testing methods for service life prediction, by simultaneous field and laboratory testing, have been presented by CIB/RILEM and ASTM /13-14/, Figure 3.1. This procedure was adopted as far as possible in the work on which this thesis is based.

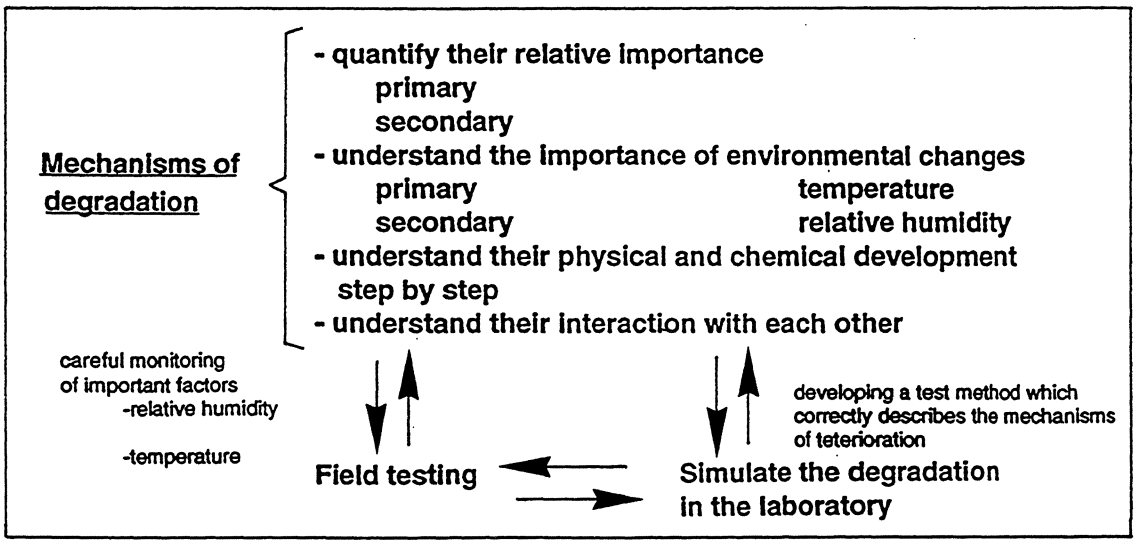


Figure 3.1. General procedure for the development of testing methods for service life prediction; derived from recommendations by CIB/RILEM and ASTM /13-14/.

It has become evident from field testing combined with laboratory testing that concrete in most cases perform better in the field as compared to the expected performance based on results from laboratory testing /10/. When considering chloride transport rates in marine exposed concrete, there is a substantial decrease in the chloride transport rate over time /10-12/. The effect is illustrated in Figure 3.2, with the chloride transport coefficient evaluated as a diffusion coefficient by fitting measured chloride profiles to a solution to Fick's second law of diffusion, assuming constant diffusivity and linear chloride binding when calculating the diffusivity at each exposure time considered.

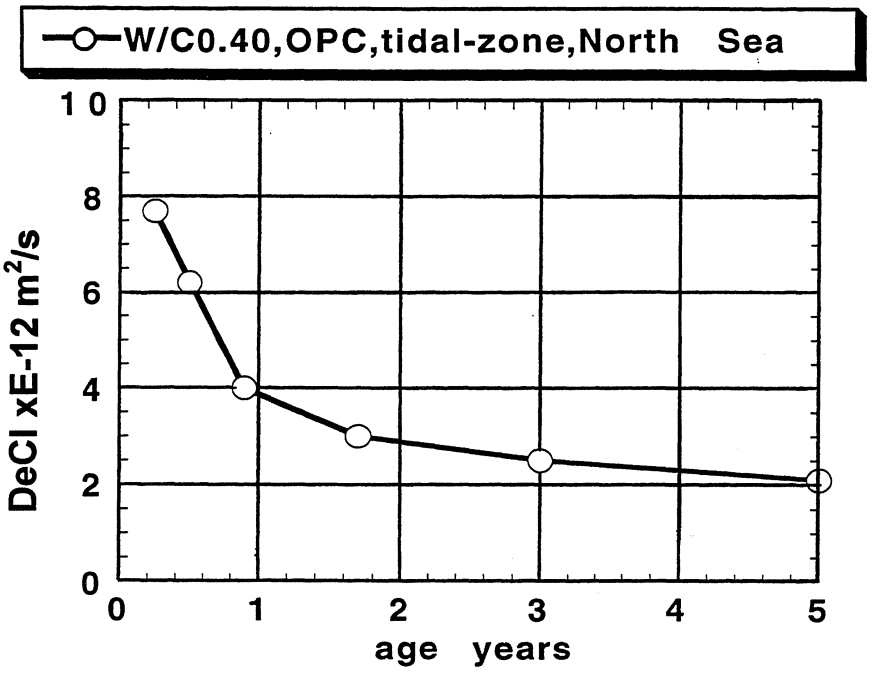


Figure 3.2. The relationship between the "effective diffusion coefficient and time for a concrete exposed in the tidal zone in the North Sea /11/.

The need for reliable field data for service life prediction lead to the establishment of a marine field station at Träslövsläge on the Swedish west coast in the end of 1991, Figure 3.3. More than 50 different concrete qualities, with water to binder ratios ranging from 0.25 to 0.75, have been field exposed at the Träslövsläge Marine Field Station since 1991.

## 3.2 Exposure zones considered

The main factors affecting the degradation rate of a given reinforced concrete structure are the moisture state and the temperature. The moisture state controls the transport of moisture and aggressive ions through a given concrete, thereby affecting chemical and physical degradation of concrete. The moisture state also controls the resistivity and the oxygen permeability of the concrete. Oxygen is needed for the cathodic part of the corrosion process to proceed at a significant rate. The temperature affects the transport of aggressive ions, the chloride threshold for corrosion initiation, and the active corrosion rate of steel in concrete.

As a consequence, it is practical to subdivide a given reinforced concrete structure into different exposure zones, reflecting mainly the variations in the concrete moisture state in the different zones. A marine structure partly exposed in sea water can de subdivided into a continuously submerged zone, a tidal zone with daily immersion and drying, a splash zone with significant wave action, and an atmospheric zone with windburn salt as the main source of salt.

## 3.3 Design of the field station and concrete specimens

The Träslövsläge Marine Field Station is based on 3 floating pontoons carrying the concrete specimens mounted on the sides, Figure 3.3 and 3.4. The use of floating pontoons allows the lower parts of the specimens to be continuously submerged in sea water. The pontoons are situated in the harbour of the village Träslövsläge on the Swedish west coast, protected from the open sea by a breakwater. This design facilitates a well defined and continuously submerged "submerged zone", a relatively small "splash zone" close to the water line, and an "atmospheric zone" which is seldom affected by wave action but affected by air borne chloride from the sea outside the breakwater.

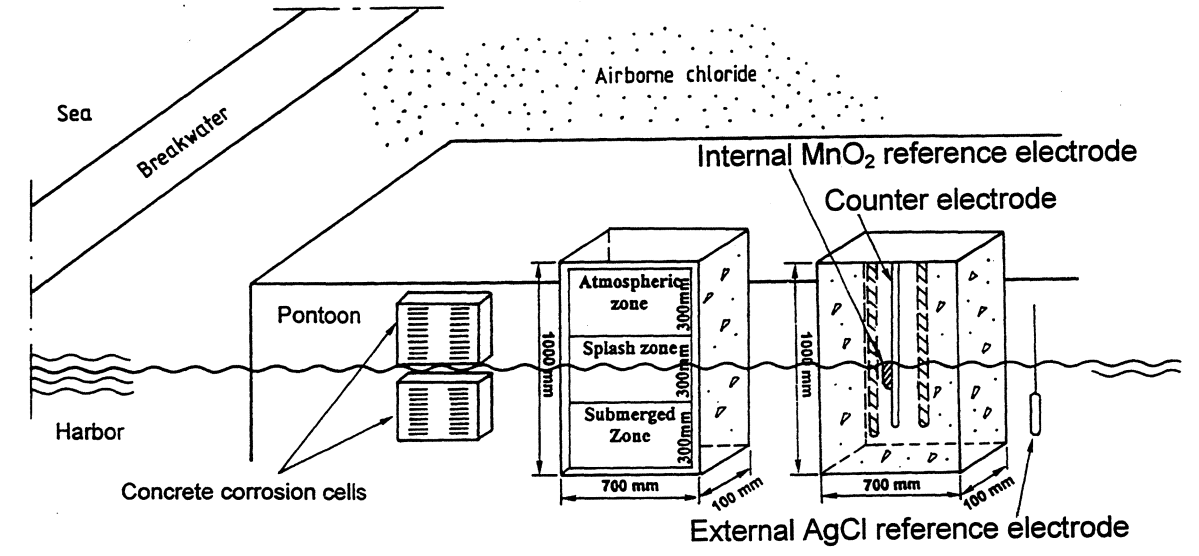


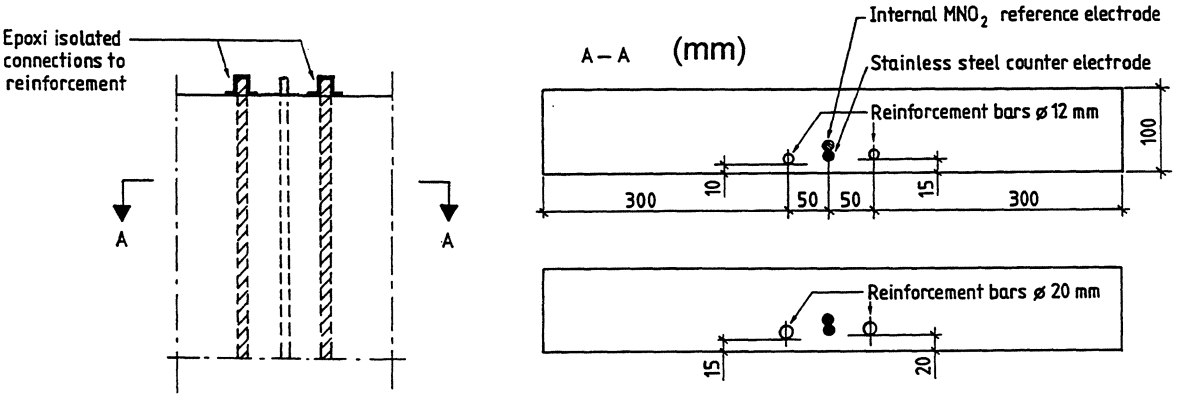


Figure 3.3. Exposure conditions at the Träslövsläge Marine Field Station.

Figure 3.4. Photograph of the newly established Träslövsläge Marine Field Station in 1992. A third pontoon was added to the field station in 1993.

The field exposed concrete specimens have the following dimensions and exposure conditions, Figure 3.3:

A) Reinforced concrete slabs, height 100 cm, width 70 cm, thickness 10 or 20 cm. Two ordinary reinforcement bars, one AISI 316 stainless steel counter electrode, and one $MnO_2$ reference electrode were cast in. The slabs are accompanied by 4 external AgCl reference electrodes immersed into the sea. See Chapter 6.3 for covers.

B) Concrete corrosion cells, 34 x 34 cm, thickness 9 cm. The corrosion cells include 20 mild steel electrodes, two titanium mesh counter electrodes, and one $MnO_2$ reference electrode. A further description is given in Chapter 5.

One of the 3 pontoons is equipped with a datalogger system, which enables the potentials of the steel in the concrete specimens to be monitored continuously relative to both the internal cast in $MnO_2$ reference electrodes and relative to the external AgCl reference electrodes. In addition, studies of the polarisation resistance of the reinforcement in concrete slabs can be carried out through the datalogger system using a galvanostatic pulse.

# 4. CHLORIDE THRESHOLDS FOR STEEL IN CONCRETE

## 4.1 General

The service life with respect to reinforcement corrosion of uncracked reinforced concrete exposed to chlorides may be described by an initiation- and a propagation phase. In the initiation phase chloride ions penetrate the concrete cover to reach the reinforcement in the initially chloride free concrete. In the propagation phase active reinforcement corrosion has already been initiated by chloride ions /4/.

Normally, steel in concrete is passive in a moist, alkaline environment which is free of chlorides and other aggressive ions /4/. The term passivity denotes that although ordinary steel reinforcement in concrete is thermodynamically not stable, the corrosion rate is depressed to an insignificant low level by the formation of a barrier of iron oxides on the steel surface /6/. The passive state is maintained until the concrete in contact with the reinforcement becomes carbonated, or until a sufficient concentration, the chloride threshold, of aggressive ions (normally chlorides) has reached the steel surface. The aggressive ions then trigger the dissolution of the iron oxide layer and later the steel (paper XI). Once active corrosion has been initiated, the corrosion rate can be very high and thus the remaining service life very short.

## 4.2 Chlorides in concrete

Only external chlorides which penetrate into originally chloride free concrete are considered in this thesis.

Hydrated cement paste binds chloride ions both physically and chemically. Experimental data was presented in the Licentiate Thesis (paper XI) which indicated that most of the bound chlorides are physically bound, probably by adsorption on the surface of the calcium silicate hydrates and the aluminate phases. Chlorides in concrete can be divided into free, physically bound and chemically bound chlorides, with the total chloride concentration referring to the sum of free and bound chlorides. A further discussion of factors affecting the relative proportion of free and bound chlorides is available in Chapter 7 (paper IV) and in /3, 28/.

## 4.3 Accuracy in reported chloride thresholds

Chloride thresholds reported in the literature are confusing as they vary extensively depending on if they refer to total or free chlorides. Chloride thresholds also vary depending on the experimental methods, the exposure conditions, the concrete quality and the cement type used. A review of chloride thresholds in the literature performed by Glass and Buenfeld /15/ indicates free chloride thresholds expressed as the ratio $[Cl^-]/[OH^-]$ in the range of 0.26 to 40. The authors suggested that a major reason for the inconsistency in reported results is the difficulties associated with methods for extracting and analysing the free ions in the concrete pore solution close to an emerging corrosion pit. No accurate method exists for studies of the pore solution composition in concrete with w/c ratio less than approximately 0.45, see the Licentiate Thesis (paper XI) and /30/.

On the other hand chloride thresholds based on the total chloride content seems more consistent, in the range of 0.17 to 2.2 % total Cl by weight of binder. As a consequence chloride thresholds are often reported as total chloride content by weight of binder although direct measurements of the ions in the pore solution would be desirable.

It can be argued that the total chloride concentration by weight of binder reflects the ratio of $[Cl^-]/[OH^-]$ in the concrete pore solution for a given binder type, provided that the hydroxide concentration at the depth of the reinforcement is relatively unaffected by leaching. This assumption is based experimental data indicating a similar transport rate for hydroxide ions as for chloride ions (papers IV and XI). If the assumption is correct, the chloride threshold expressed as total chloride content by weight of binder reflects the probability of corrosion initiation for a given concrete in a given exposure condition.

## 4.4 Definition of the chloride threshold

It is generally believed that only the concentration of free chlorides affect the chloride threshold as it is assumed that the bound chlorides do not affect the passivity /4,17/. This assumption was questioned recently in /15/. It was suggested that the normal cycles of activation and repassivation, i.e. electrochemical noise, see the Licentiate Thesis (paper XI), can locally release bound chlorides close to a repassivating pit and thereby influence the next activation of the pit.

The chloride threshold was defined so that normal electrochemical noise should not be considered when evaluating the chloride threshold. The chloride threshold was therefore considered as reached and active corrosion initiated only when the active corrosion rate was remaining higher than 1 $\mu A/cm^2$ for freely corroding steel, or higher than 10 $\mu A/cm^2$ for steel under potentiostatic control (100 mV rel $MnO_2$), for 2 consecutive weeks.

In this study the chloride threshold was defined as the mass ratio between the measured total (bound + free) aggressive substance (chloride) and the measured inhibiting substance (binder) necessary to maintain active corrosion in a pit. This definition was adopted because it is relatively easy to measure the total chloride concentration, and also because the suggested effect of cycles of activation and repassivation/15/ would influence less on the total chloride concentration as compared to the free chlorides. If not otherwise stated, the chloride threshold in this thesis refers to the total chloride concentration by weight of binder.

# 5 FACTORS AFFECTING THE IDENTIFICATION AND USE OF CHLORIDE THRESHOLDS

## 5.1 General

The chloride threshold for mild steel in a given concrete quality depends on both the micro structure /16/ and the micro climate (papers I-III, XI) at the concrete-steel interface.

## 5.2. The effect of micro structure at the concrete - steel interface

Hausmann /17/ has measured the free chloride threshold for ordinary steel exposed to alkaline chloride solutions reflecting typical concrete pore solutions. Hausmann reported that the free chloride threshold expressed as the ratio $[Cl^-]/[OH^-]$ is approximately 0.6 under these conditions. On the other hand steel in chloride contamined concrete is normally much more chloride resistant as compared to when the same steel is exposed to a bulk solution of the same composition as the concrete pore solution. The difference in calculated free chloride thresholds can be orders of magnitude /18/.

The reasons for the improved chloride resistance for steel in concrete as compared to steel in alkaline solutions, are not fully understood. Experimental work by Yonezawa /16/, including variations in bond between the steel and the cement matrix, have indicated that the effect of physical adhesion between cement hydrates and iron oxides formed on the steel surface is important. It was concluded that the formation of voids at the steel-mortar interface is a necessary condition for active corrosion to start in water saturated concrete containing a moderate chloride content. Furthermore, observations of a protective effect of calcium hydroxide precipitated at the steel surface were reported. The protective effect of calcium hydroxide was attributed to the dissolution of calcium hydroxide crystals close to emerging pits, thereby preventing the pH drop required for the further propagation of the corrosion pit.

Mammoliti et al /19/ on the other hand found that the tendency for pitting of steel exposed to alkaline solutions was controlled by the surface roughness of the steel and by the pH of the solution. At pH 13.3 continued pitting was not possible to initiate on any steel surface independently of the surface roughness. It was again suggested that testing of steel in solutions is not representative for the inhomogeneous material concrete. Concrete is likely to exhibit local variations in the pH of the pore solution at the steel surface as opposed to well stirred solutions.

## 5.3 The effect of micro climate at the concrete - steel interface

Chloride thresholds vary with the exposure conditions (paper XI). The moisture state is of especially big importance as experimentally shown for mild steel in mortar specimens conditioned at different RH by Pettersson, Figure 5.1 /20/. Very high chloride thresholds have been found for steel in concrete exposed fully submerged in the laboratory with no changes in the exposure regime (paper II). A varying moisture state at the depth of the reinforcement caused by wetting and drying of concrete has been suggested to result in a substantially lower chloride threshold (paper XI), which was confirmed by the findings in (paper II). The results in (papers I,II) confirmed that a more stable micro environment, as achieved by an increased

cover size and/or a lower w/c ratio, or by a non-varying exposure condition, may result in a higher chloride threshold.

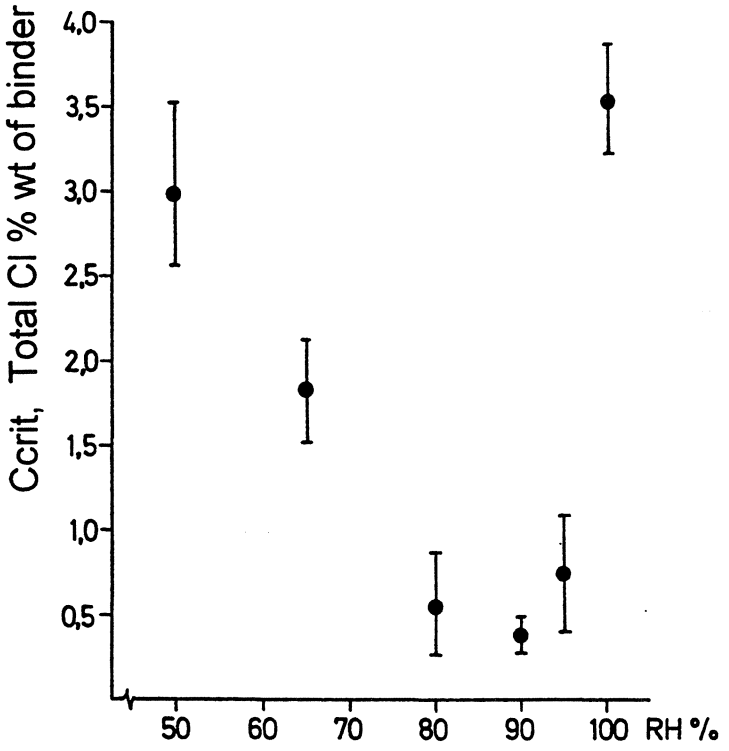


Figure 5.1. Total chloride thresholds measured for mild steel bars in mortar, w/c 0.50, conditioned at different RH /20/. A sulphate resisting Portland cement was used, Table 6.1.

# 6 EXPERIMETAL WORK ON CHLORIDE THRESHOLDS

## 6.1 General

Experimental work on total chloride thresholds was carried out by field exposure tests on reinforced concrete slabs and by field- and laboratory exposure tests on concrete corrosion cells. The field exposure tests were carried out at the Träslövsläge Marine Field Station while the laboratory tests were carried out at LTH and at AEC, see Table 1.1.

## 6.2 Binders

A sulfate resisting portland cement with a high iron oxide content (SRPC), a slag cement based on 50 % portland cement and 50 % interground granulated blast furnace slag, silica fume (SF) and fly ash (FA) were used as specified in Table 6.1. Fly ash was only used in field tests on reinforced concrete slabs.

The w/c ratio was defined as the ratio w/(C+SF+0.3FA) by weight, with w = water, C = cement (sulfate resisting portland cement or slag cement), SF = silica fume, FA = fly ash.

Table 6.1. Details of cementing materials used

| **Material** | | **Sulfate resisting Portland cement (SRPC)** | **Slag cement 50 % slag** | **Silica fume (SF)** | **Fly ash (FA)** |
|---|---|---|---|---|---|
| Fineness - % passing | 45 µm | 85.9 | 100 | 100 | 73 |
| | 20 µm | 51.3 | 72.0 | | |
| | 10 µm | 33.1 | 45.3 | | |
| | 5 µm | 19.5 | 33.8 | | |
| | 1 µm | 3.8 | 8.2 | | |
| Specific surface $m^2/kg$ | Blaine | 300 | 410 | | 227 |
| | BET | | | 23 000 | 625 |
| Compressive Strength | 1 day | 10.1 | 4.0 | | |
| of standard 40 mm | 7 days | 35.6 | 29.7 | | |
| mortar cubes, MPa | 28 days | 56.2 | 49.8 | | |
| Chemical analysis % | CaO | 63.8 | 43.3 | 0.4 | 1.87 |
| | $SiO_2$ | 22.8 | 28.5 | 94.2* | 57.0 |
| | $Al_2O_3$ | 3.5 | 11.9 | 0.62 | 29.1 |
| | $Fe_2O_3$ | 4.7 | 1.1 | 0.95 | 6.56 |
| | MgO | 0.80 | 9.0 | 0.65 | 0.79 |
| | $SO_3$ | 1.9 | 4.7 | 0.33 | 0.21 |
| | $K_2O$ | 0.55 | 0.55 | 0.5 | 1.76 |
| | $Na_2O$ | 0.06 | 0.26 | 0.2 | 0.28 |
| | Loss of ignition | 0.55 | 0 | 1.8 | 1.9 |
| Bogue potential | $C_3S$ | 51.5 | | | |
| compounds -% | $C_2S$ | 25.5 | | | |
| | $C_3A$ | 1.3 | | | |
| | $C_4AF$ | 14.3 | | | |

*amorphous silica content

## 6.3 Field exposure tests of reinforced concrete slabs

### *6.3.1 Concrete mix designs and types of binder for reinforced concrete slabs*

Cementing materials according to Table 6.1 were used. 16 different concrete qualities including 7 different binder compositions were tested in this study of total chloride thresholds, with w/c ratios between 0.30 to 0.75 according to Table 6.2. Additional total and free chloride thresholds were studied by Pettersson at CBI, some results are available in /20/.

Table 6.2. Experimental data for concrete slabs exposed at the Träslövsläge Marine Field Station and tested for chloride thresholds.

| | **w/(C+SF+0.3FA)** | | | | |
|---|---|---|---|---|---|
| **Mix design** | **0.30** | **0.35** | **0.40** | **0.50** | **0.75** |
| **SRPC**<br>C kg/m3<br>f'c 28d / air content | 2 slabs<br>492<br>96 MPa / 2 % | 2 slabs<br>50<br>70 MPa / 6 % | 4 slabs<br>420<br>58 MPa / 6 % | 2 slabs<br>370<br>41 MPa / 6 % | 2 slabs<br>240<br>21 MPa / 6 % |
| **SRPC 5 % SF**<br>C kg/m3<br>f'c 28d / air content | 1 slab<br>475<br>112 MPa / 1% | 2 slabs<br>428<br>72 MPa / 6 % | 4 slabs<br>399<br>61 MPa / 6 % | 2 slabs<br>351<br>45 MPa / 6 % | 2 slabs<br>233<br>21 MPa / 6 % |
| **SRPC 10 % SF**<br>C kg/m3<br>f'c 28d / air content | 1 slab<br>450<br>117 MPa / 1% | *Not tested* | 2 slabs<br>378<br>65 MPa / 6 % | *Not tested* | *Not tested* |
| **SRPC**<br>**5 % SF, 17%FA** C kg/m3<br>f'c 28d / air content | *Not tested* | *Not tested* | 2 slabs<br><br>345<br>69 MPa / 6 % | *Not tested* | *Not tested* |
| **SRPC**<br>**5 % SF, 10%FA**<br>C kg/m3<br>f'c 28d / air content | *Not tested* | 2 slabs<br><br>382<br>84 MPa / 6 % | *Not tested* | *Not tested* | *Not tested* |
| **SRPC 20%FA**<br>C kg/m3<br>f'c 28d / air content | 2 slabs<br>493<br>98 MPa / 1 % | *Not tested* | *Not tested* | *Not tested* | *Not tested* |
| **Slag cement**<br>C kg/m3<br>f'c 28d / air content | *Not tested* | *Not tested* | 2 slabs<br>440<br>54 MPa / 6 % | *Not tested* | *Not tested* |

f'c 28d = compressive cube strength (MPa) after 28 days of standard curing.
The percentage of SF or FA is by weight of the total binder content.

### *6.3.2 Field exposure of reinforced concrete slabs in a marine environment*

Reinforced concrete slabs, height 100 cm, width 70 cm, thickness 10 cm, Chapter 3.3, were cast and moist cured for 10 days prior to marine exposure in 1992. The reinforcement used were diameter 20 mm and 12 mm ordinary ribbed mild steel bars, as received from the supplier, used with 10, 15 and 20 mm cover, Figure 3.3. 20 cm thick slabs with SRPC and 0 or 5 % silica fume, w/c ratio 0.35 and 0.40, were cast with 30, 40 and 55 mm cover. No active corrosion has yet been indicated in these slabs and they are not included in this study.

The slabs were mounted on a floating pontoon in the harbour of the village Träslövsläge on the Swedish west coast. The bottom half of each slab was submerged in order to achieve exposure conditions with relatively rapid chloride penetration in the submerged part and unlimited availability of oxygen in the upper part, Figure 3.4. The use of a floating pontoon allowed the lower half of each slab to be continuously submerged in sea water. The concrete slabs were protected from waves by a breakwater.

None of the slabs were considered as exposed fully submerged with respect to the chloride threshold, as all reinforcement were in contact with oxygen rich concrete exposed to the atmosphere. Therefore the exposure was considered relevant for structural parts of concrete structures exposed in the splash zone even if the corrosion initiation occurred below the water table.

### *6.3.3 Method of identification of the corrosion initiation in reinforced concrete slabs*

External AgCl-electrodes and cast-in $MnO_2$-electrodes were used simultaneously as reference electrodes. 4 AgCl electrodes were submerged into the sea while each concrete slab had one $MnO_2$-electrode in the concrete at the depth of the stainless steel counter electrode, i.e. 12 or 17 mm from the concrete surface. The AgCl and $MnO_2$ reference electrodes nominally read + 44 mV SCE and + 142 mV SCE respectively. Both electrode types experienced a slow drift in the range of 50 mV over a time period of 2 months. The drift was evaluated by comparing the relative potentials between the reference electrodes. The drift did not affect the method of corrosion initiation as this was based on a larger and more rapid potential shift, and a control of the polarisation resistance, as described below.

The steel potentials relative to the external AgCl- and the internal $MnO_2$-electrodes were recorded on an hourly basis by a datalogger. When a potential shift indicated corrosion initiation, the active/passive corrosion state was checked by means of the following electrochemical methods:

i) polarisation resistance measurements as described in detail in /21/ and

ii) the response of the reinforcement to a galvanostatic pulse of 0.1 mA introduced into the surrounding sea water. The technique is described in detail in /21,22/.

The purpose of these studies was not to calculate corrosion rates but only to give an indication on the active/passive state of the reinforcement. Both methods are based on studies of how easy it is to polarise steel in concrete. Passive steel is polarised to a much larger extent than active steel, as described in chapter 2.9.

Typical steel potentials in SRPC concrete, w/c ratio 0.40 are shown in Figure 6.1, for a passive steel with 15 mm cover and a corroding steel with 10 mm cover. The changes in the passive potential over time was interpreted as being related to changes in the moisture state at the reinforcement as influenced by rain, intensive splashing, changes in the temperature, etc.

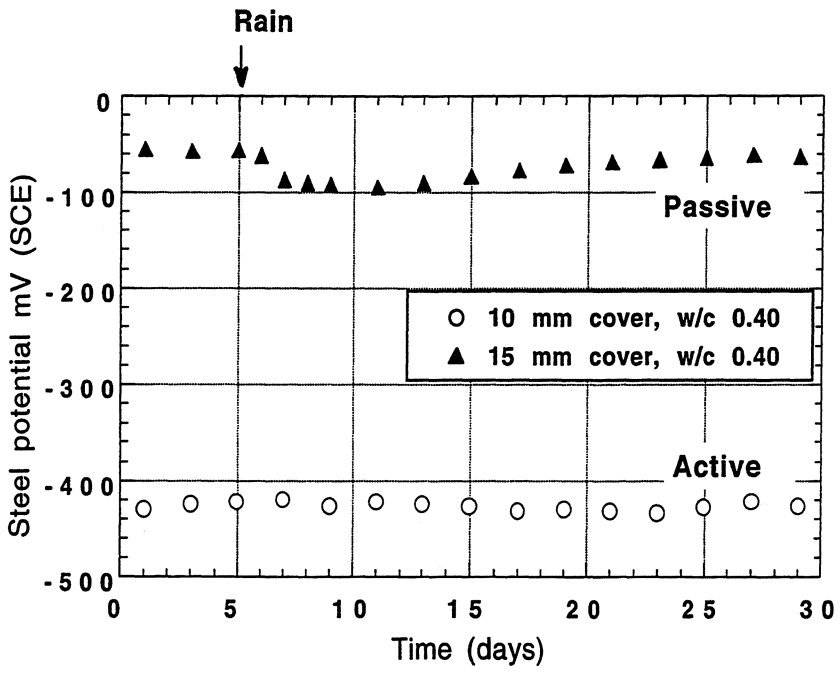


Figure 6.1. Example of steel potentials for passive and active steel reinforcement in SRPC concrete, w/c ratio 0.40, with 15 and 10 mm cover respectively, exposed at the Träslövsläge Marine Field Station. The passive reinforcement has the less negative potential.

A typical active/passive response to the galvanostatic pulse is shown in Figure 6.2. As expected /22/, the passive reinforcement is polarised more easily than the active reinforcement, because of the higher resistance in the passive corrosion cell.

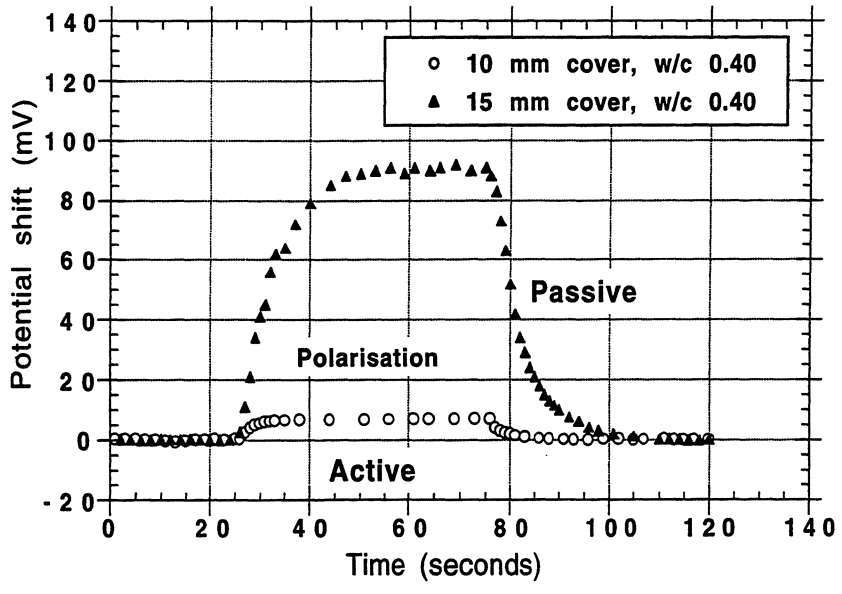


Figure 6.2. Active/passive response of a SRPC concrete, w/c ratio 0.40, exposed at the Träslövsläge Marine Field Station, to a 0.1 mA galvanostatic pulse. The active reinforcement is less polarised than the passive reinforcement.

Finally, a visual inspection of the degree of corrosion was carried out in order to confirm the existence, position and the approximate age (size) of the corrosion pit.

### *6.3.4 Analysis of chloride and binder profiles*

Profiles of total chloride were analysed in the non reinforced parts of each concrete slab, after 7 months, 12 months, 2 years, and 5 years exposure. Once active corrosion was detected profiles of total chloride were also analysed right on to the corroding steel.

Cylinders with diameter 100 mm were drilled from the concrete slabs at more than 50 mm distance from the edges, see Figure 3.3. The concrete cylinders were immediately sealed in airtight bags and brought to the laboratory for processing and analyses:

The concrete cover was abraded from the exposed surface and inwards in steps of 1 mm using a diamond tool according to the Nordic standard NT Build 443 /23/. The pulverised samples were analysed for total chloride content according to AASHTO T 260-A, by potentiometric titration using a chloride ion selective electrode and a silver nitrate solution of 0.01 N.

After chloride titration, 5 ml of 1:2 diluted triethanolamine was added to the sample solution and the pH value was adjusted to pH > 12 using sodium hydroxide. The calcium content was determined by potentiometric titration using a calcium ion selective electrode and a 0.1 N EDTA solution /24/. As the aggregate contained no acid soluble calcium, the binder content in each 1 mm fraction of concrete was calculated from the measured calcium content in each fraction. The result was presented as total chloride by weight of binder for each 1 mm fraction.

The chloride profiles obtained after 7 months, 12 months, 2 years, and 5 years exposure were used for estimations of the chloride transport rate and of the chloride content at the depth of the reinforcement at any exposure time. Thus it was possible to estimate the total chloride content at the depth of the reinforcement at the time of corrosion activation. The total chloride profile measured right on to the steel once active corrosion was detected, served as a control of the calculated values.

The profiles of total chloride were analysed at the following laboratories: AEC, Chalmers, LTH, CBI and SP, see Table 1.1 for the full names of the laboratories.

The polarisation resistance measurements on the reinforcement was carried out by the CBI using a commercially available GEOCOR 6 instrument.

*6.3.5 Results on chloride thresholds in field exposed concrete slabs*

All chloride thresholds measured in reinforced concrete slabs exposed at the Träslövsläge Field Station are shown in Table 6.3.

Table 6.3. Chloride thresholds expressed as % total Cl by weight of binder. Reinforced concrete slabs, splash zone exposure as defined in Chapter 6.3.2.

| | **W/(C+SF+0.3FA)** | | | | | | | | | | | | | | |
|---|---|---|---|---|---|---|---|---|---|---|---|---|---|---|---|
| | **0.30** | | | **0.35** | | | **0.40** | | | **0.50** | | | **0.75** | | |
| **Cover → mm** | **10** | **15** | **20** | **10** | **15** | **20** | **10** | **15** | **20** | **10** | **15** | **20** | **10** | **15** | **20** |
| **SRPC plain** | 1.1 | 1.1<br>1.3* | 1.5* | 1.0* | 1.2<br>1.4* | 1.4* | 0.9*<br>1.0 | 1.0<br>1.1*<br>1.2*<br>1.2 | 1.2<br>1.4* | 0.7* | 1.3*<br>1.0 | 1.1 | 0.6 | 0.8<br>1.1* | 1.0 |
| **SRPC 5 % SF** | 1.0* | 1.2 | | 0.7 | 1.2<br>1.3* | 1.1* | 0.8<br>1.1* | 0.8<br>1.0<br>1.2*<br>1.3* | 1.1*<br>1.4 | 0.6 | 1.1*<br>1.2 | 1.2* | 0.5 | 0.9*<br>1.0 | 0.9 |
| **SRPC 10 % SF** | *No corrosion initiated* | | | *Not tested* | | | 1.0* | 1.0<br>1.2* | | *Not tested* | | | *Not tested* | | |
| **SRPC 5 % SF 17 % FA** | *Not tested* | | | *Not tested* | | | 0.6 | 1.1<br>1.3* | 1.1* | *Not tested* | | | *Not tested* | | |
| **SRPC 5 % SF 10 % FA** | *Not tested* | | | 0.6 | 1.0<br>1.3* | 1.1* | *Not tested* | | | *Not tested* | | | *Not tested* | | |
| **SRPC 20 % FA** | 1.0* | 0.8<br>1.2* | | *Not tested* | | | *Not tested* | | | *Not tested* | | | *Not tested* | | |
| **Slag cement** | *Not tested* | | | *Not tested* | | | 0.4*<br>0.6*<br>0.5*<br>0.9* | | | *Not tested* | | | *Not tested* | | |

* The total chloride threshold has been actually verified by the measurement of a total chloride profile at the corrosion pit within 2 months from the corrosion initiation, as indicated by a potential shift and a measurement of the corrosion activity by polarisation resistance and/or galvanostatic pulse. The other values are interpolated at the time of corrosion initiation from chloride profiles measured at different ages.

The effects of cover and w/c ratio on the measured chloride thresholds are indicated in Figure 6.3 for A) Plain SRPC concrete, and B) Comparable concrete with 5% silica fume as cement replacement.

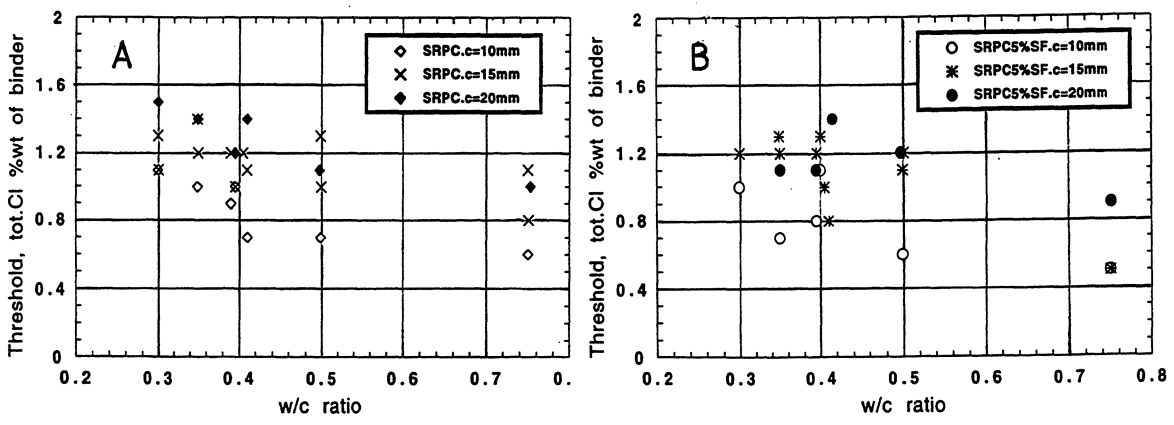


Figure 6.3. The effect of cover on the measured chloride thresholds for A) Plain SRPC-based concrete, and B) for similar concrete with 5% silica fume as cement replacement.

The effects of binder type and w/c ratio on the measured chloride thresholds are indicated in Figure 6.4 for A) 10 mm cover, B) 15 mm cover, C) 20 mm cover.

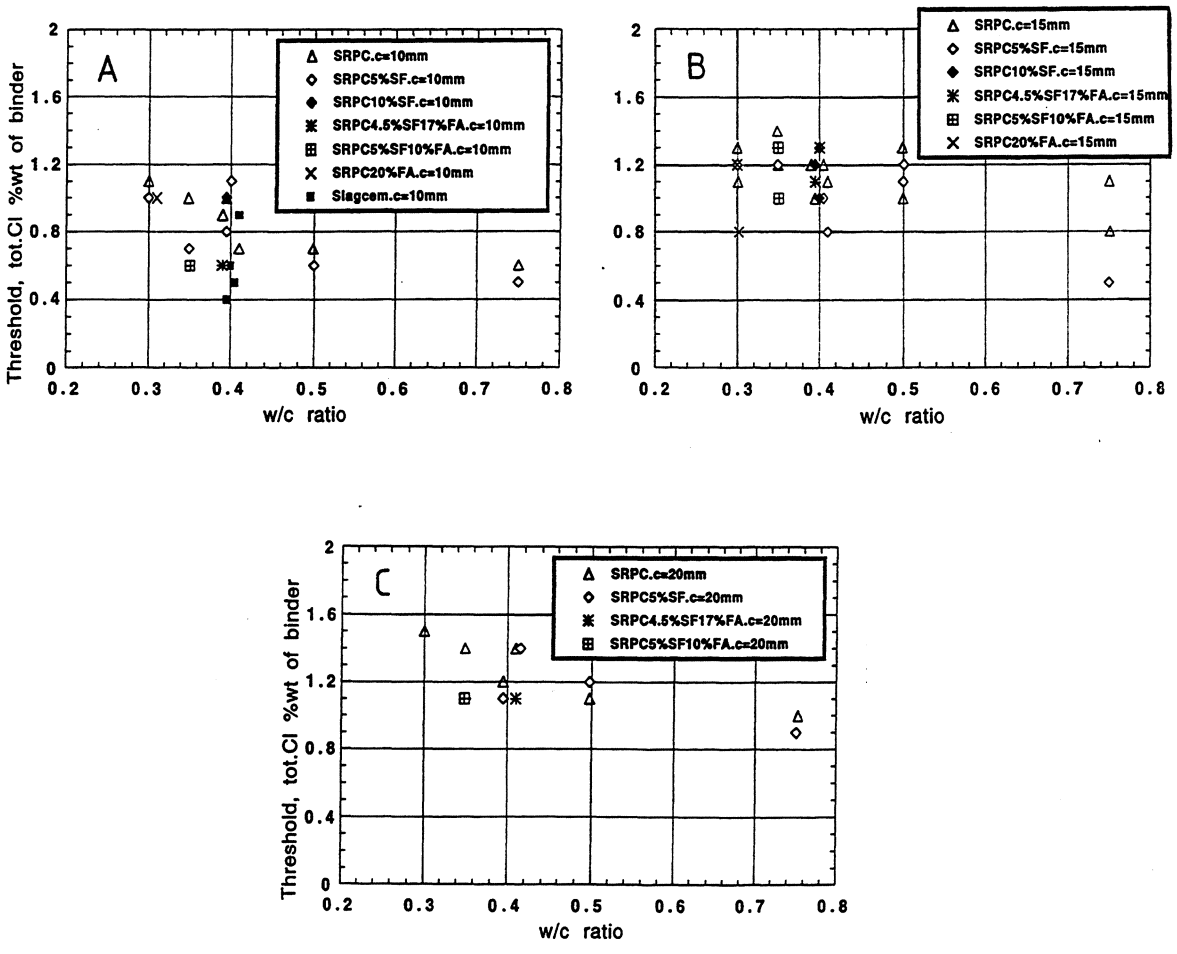


Figure 6.4. The effects of binder type and w/c ratio on the measured chloride thresholds for A) 10 mm cover, B) 15 mm cover, C) 20 mm cover.

## 6.4 Laboratory and field exposure tests of specially designed concrete corrosion cells

### *6.4.1 Design and use of standard corrosion cells*

#### 6.4.1.1 General

A standard corrosion cell for testing of chloride thresholds in concrete /25/ was developed by Hans Arup, in co-operation with Henrik Sørensen at AEC, Denmark and the present author /25/. The test unit consists of 20 U-shaped smooth 8 mm mild steel electrodes, 2 titanium mesh counter electrodes and a $MnO_2$ reference electrode which were very accurately positioned into a cement based precast specimen holder of Densit, as shown in Figure 6.5. The $MnO_2$ reference electrode reads + 142 mV SCE. Some of the electrodes were connected to a potentiostat and kept under potentiostatic control, Tables 6.5-6.8.

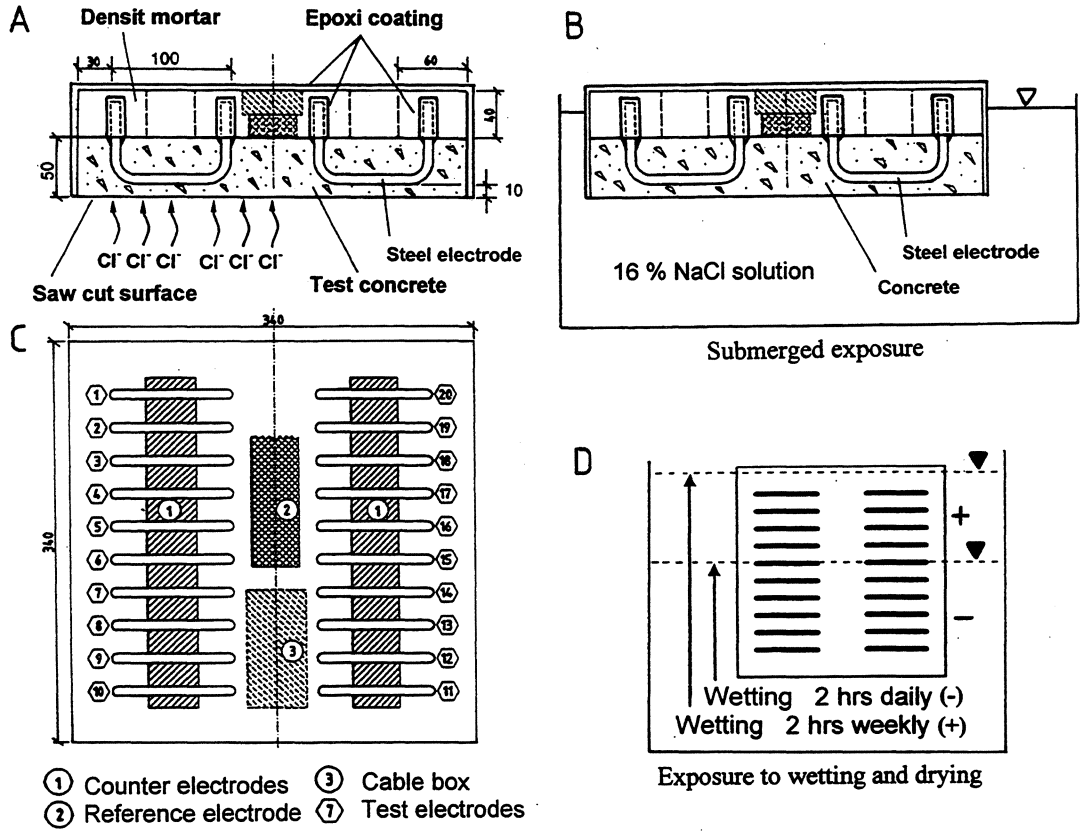


Figure 6.5. Standard corrosion cell. All measures are given in millimetres /25/. A) Cross-section, B) View, C) Immersed laboratory exposure, D) Exposed to wetting and drying.

The U-shaped steel electrodes have epoxy coated legs facing away from the exposed concrete surface in order to prevent corrosion initiation on the legs. The $MnO_2$ reference electrode and the counter electrodes were cast into mortar bars before assembling the standard unit.

The steel electrodes were cast in the concrete or mortar to be tested. The placing and compacting of concrete were carried out carefully as described in /26/. After demoulding and moist curing for 14 days the concrete surface to be exposed was cut open using a large water-cooled diamond saw to obtain a cover to the steel electrodes of nominally 10 mm. A chloride proof coating was applied to the test unit on all sides except the saw-cut face to be exposed.

Nine "dummy" concrete specimens were made from the cut off concrete plate. These specimens were handled in exactly the same manner as the test unit containing the embedded steel. All surfaces were coated except for the surface opponent to the exposed surface on the test unit. The test unit and the dummy concrete specimens were then stored in a saturated calcium hydroxide solution at room temperature for 2 weeks prior to the saline exposure.

Steel-, counter- and reference electrodes were connected to a datalogger for monitoring the corrosion activity. A potentiostat was used for potentiostatic control of passive steel electrodes.

6.4.1.2 Introduction of artificially produced defects at the steel – concrete interface

A standard filter paper was applied on the surface on some steel electrodes according to Figure 6.6 and Tables 6.5-6.8, with the purpose to produce artificial defects at the steel-concrete interface, following the procedure by Yonezawa in /16/. The filter paper used was a Schleicher & Schuell, Filter Paper Circles no. 589-1, Black Ribbon, Ashless, diameter 110 mm, Ref. No. 300 010. The filter paper (white area in Figure 6.6) was mounted in 2 layers on the steel surface and fixed by a 0.40 mm nylon string. The filter paper was soaked in a 0.4 M KOH solution immediately before the casting of concrete or mortar on top of the steel electrodes coated by filter paper. The KOH soaked filter paper was used with the aim to simulate a situation with the steel in contact with a simulated pore solution but without physical contact with cement hydrates.

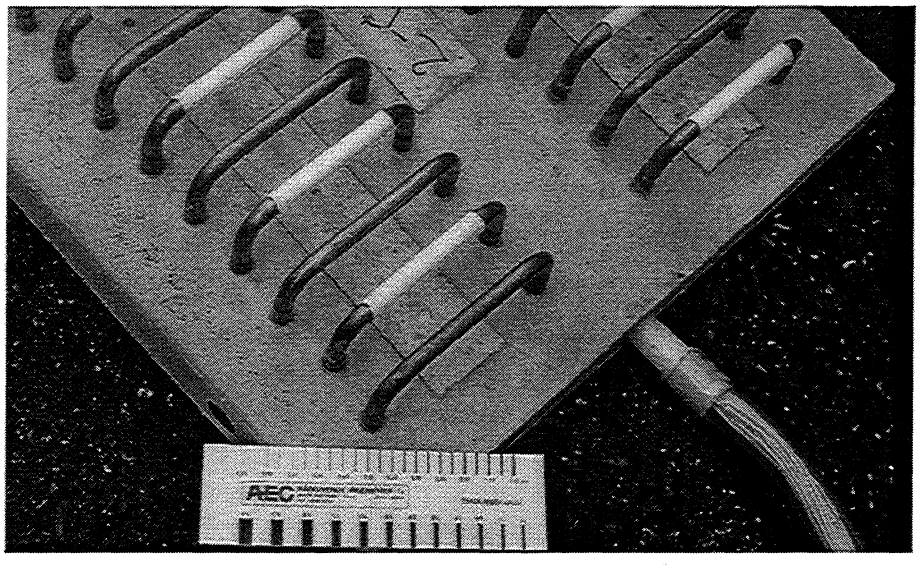

Figure 6.6. Application of filter paper defect on the surface of every second steel electrode.

6.4.1.3 Compaction voids at the steel – concrete interface

All concrete mixes were cast, compacted and cured in a similar way as recommended in /26/. All in all, 35 of 210 electrodes investigated were despite this found to be affected by visible compaction voids, approximately 0.1-0.5 mm wide, at the steel surface. 17 or approximately 50 % of these electrodes in "defect" concrete were found in slag cement concrete. A few voids were found to be wider than 0.5 mm at the steel surface.

6.4.1.4 Registration of corrosion activity in concrete corrosion cells

The corrosion activity in electrodes under potentiostatic control was recorded by a datalogger on a hourly basis by measuring the electrical current needed to maintain the steel electrodes at their controlled potentials. The current was in the range of 0-10 μA when the steel electrodes were passive. Note that the current needed to maintain a given potential should not be confused with the corrosion current defined as the threshold for active corrosion in freely corroding steel as described in Chapter 4.4.

The initiation of active corrosion was detected by an increase in the current needed to maintain a given potential to more than 100 μA as illustrated in Figure 6.7 /25/.

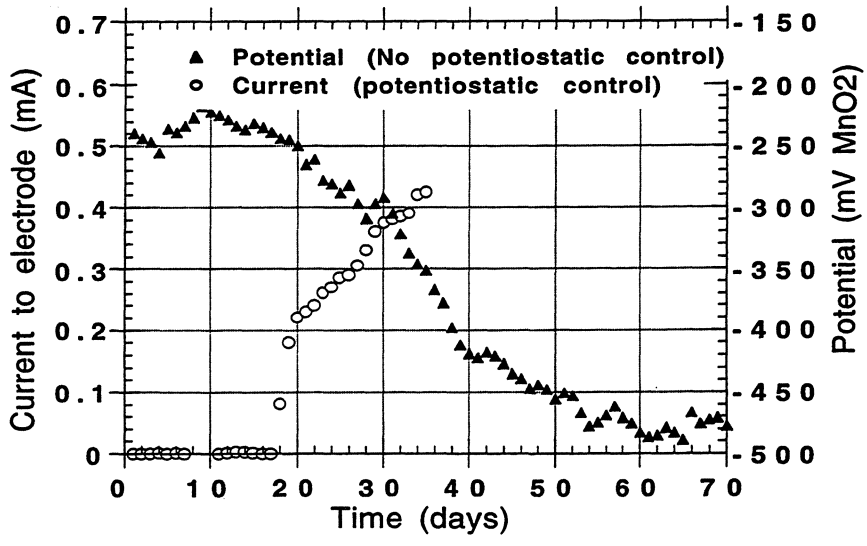


Figure 6.7. Detection of corrosion initiation on electrodes with and without potentiostatic control /25/.

After corrosion initiation, the potentiostatic control was switched off and the steel electrode was allowed to corrode freely with the free potential recorded by the datalogger. If repassivation occurred as indicated by a shift in the order of 200-500 mV to a less negative potential, the corrosion status was checked by switching on the potentiostatic control. Repassivation was confirmed by the return to very low electrical currents in the range of 0-10 μA needed to maintain the steel electrode at the controlled potential. If the status of repassivation was confirmed, the steel electrode was kept under potentiostatic control until initiation of active corrosion was again detected by an increase in the current needed to maintain the given potential to more than 100 μA.

The corrosion activity in electrodes under no potentiostatic control was recorded by a datalogger simply by recording the steel potentials. Corrosion initiation was detected by a shift in the order of 200-500 mV to a more negative potential as illustrated in Figure 6.7 /25/. The active or passive state of electrodes under no potentiostatic control was confirmed by a potentiostatic test carried out as previously described, by measuring the current needed to maintain the potential at - 100 mV ($MnO_2$).

Passive steel electrodes under no potentiostatic control experienced potential shifts in the range of 0-50 mV as induced by electrochemical noise (paper XI) or, if present, by varying exposure conditions. A more detailed description of the standard test cell is given in /25/.

6.4.1.5 Control of degree of corrosion and location of corrosion pit

At terminated exposure of a test cell, electrodes were removed from the cell and carefully examined visually in order to confirm the position and the approximate size of the corrosion pit. The evaluation was carried out as indicated in Figure 6.8.

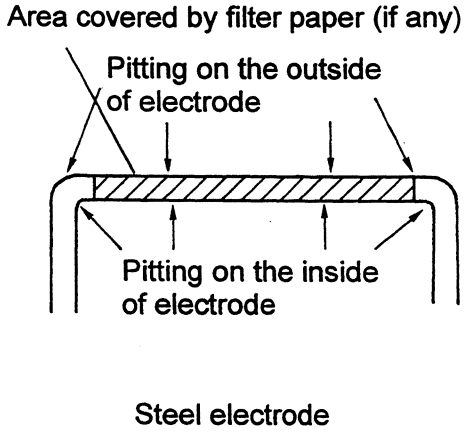


| Degree of corrosion | Description of corrosion pit |
|---|---|
| 0 | None |
| 1 | Very small pit, 0-1 % of steel surface, only surface corrosion |
| 2 | Small pit, 1-10 % of steel surface, max 0.5 mm deep |
| 3 | Corrosion in 10-50 % of steel surface, max 1.0 mm deep |
| 4 | Corrosion in 50-100 % of steel surface, > 1.0 mm deep |

Figure 6.8. Control of degree of corrosion and location of corrosion pit.

6.4.1.6 Evaluation of defects in the concrete microstructure close to the steel surface

The concrete surrounding each electrode was examined for the existence of visible voids close to the steel electrode. This was aided by a visual examination of the distribution of chlorides in the surrounding concrete, by spraying freshly cut surfaces with a 0.1 M $AgNO_3$ solution. The formation of light grey AgCl precipitate at chloride rich voids provided a visual indication of chloride rich areas in concrete surrounding the steel electrodes. Photographs with examples of the microstructure of concrete and chloride penetration depths in concrete corrosion cells exposed at various exposure regimes are shown in the Appendix.

6.4.1.7 Analysis of chloride and binder profiles

Total chloride- and binder profiles were analysed on a concrete dummy exposed parallel to the corrosion cell at the time of the first confirmed corrosion initiation; the corrosion cell and the corresponding dummies were cast at the same time with the same materials as previously described.) Profiles of total chloride were also analysed after confirmed corrosion initiation in 25% and 50% of the steel electrodes. If no corrosion initiation was confirmed, profiles of total chloride were measured after 2 years of exposure. The procedure for analysis of chloride- and binder profiles is described in /23,24/.

6.4.1.8 Calculation of chloride threshold

The location of the corrosion pit was used to measure the exact distance from the exposed concrete surface to the steel surface at the pit. The measured profiles of total chloride at various exposure ages were then used to extrapolate the total chloride content at the depth of the corrosion pit at the time of corrosion initiation.

*6.4.2 Types of binder and concrete mix designs tested in concrete corrosion cells*

Three different binder types, sulfate resisting Portland cement (SRPC), sulfate resisting Portland cement with 5 % silica fume, and slag cement with 50 % slag interground with Portland cement, were used as specified in Table 6.1.

Details of the concrete or mortar mixes are shown in Table 6.4.

Table 6.4. Details of concrete/mortar mixes used in corrosion cell tests

| Mix No. | Material | Cover mm | SRPC kg/m$^3$ | Slag cem. kg/m$^3$ | Silica fume kg/m$^3$ | Sand 0-2 mm kg/m$^3$ | Sand 0-4 mm kg/m$^3$ | Aggr. 0-8 mm kg/m$^3$ | Aggr. 8-16 mm kg/m$^3$ | w/c ratio * | Air cont. vol % |
|---|---|---|---|---|---|---|---|---|---|---|---|
| 1 | Concrete | 10 | 330 | 0 | 0 | - | 645 | 189 | 1058 | 0.50 | 1.0 |
| 2 | Concrete | 10 | 435 | 0 | 0 | 760 | - | 970 | - | 0.41 | 2.1 |
| 3 | Concrete | 10 | 420 | 0 | 16 | 750 | - | 970 | - | 0.42 | 1.9 |
| 4 | Concrete | 10 | 0 | 435 | 0 | 755 | - | 965 | - | 0.40 | 1.4 |
| 5 | Mortar | 4-14 | 555 | 0 | 29 | 1440 | - | 0 | - | 0.40 | - |

*w/c ratio defined as w/(C+SF). w = water, C = cement

*6.4.3 Exposure regimes for corrosion cells*

6.4.3.1 General

Corrosion cells with plain sulfate resisting portland cement (SRPC), sulfate resisting portland cement with 5 % silica fume, or slag cement were exposed to 3 different exposure regimes, Table 6.5 and Figure 6.5. A varying number of steel electrodes were kept under potentiostatic control, Table 6.5, at different potentials as shown by the voltages in Tables 6.6-6.8. "Free pot." denotes that no potential control was applied. "Defects" denotes whether previously described artificial filter paper defects, Figure 6.6, were introduced or not.

6.4.3.2 Laboratory submerged exposure tests of corrosion cells

A total of 6 corrosion cells with concrete or mortar mix designs according to Table 6.4, Mix No. 1-5, were configured with steel electrodes at various potentiostatically controlled potentials and labelled according to Table 6.6. Some electrodes were left at their natural potentials as indicated in the column labelled "free pot.". Artificially produced filter paper defects were introduced at the steel-concrete interface of some electrodes according to Table 6.6.

Table 6.5. Variables tested or inspected in exposure tests of corrosion cells

| Variable | Laboratory exposure | | Field exposure*** | |
|---|---|---|---|---|
| | Submerged* | Wetting and drying** | Submerged | Splash zone |
| Potentiostatic control | SRPC w/c 0.50<br>1 cell with<br>18 electrodes of 20<br><br>All binders w/c 0.4<br>3 cells with<br>16 electrodes of 20 | All binders w/c 0.4<br>3 cells with<br>1 electrode of 20 | All binders w/c 0.4<br>3 cells with<br>4 electrodes of 20 | All binders w/c 0.4<br>3 cells with<br>4 electrodes of 20 |
| Filter paper defects | SRPC w/c 0.50<br>No electrodes<br><br>All binders w/c 0.4<br>3 cells with<br>10 electrodes of 20 | All binders w/c 0.4<br>3 cells with<br>10 electrodes of 20 | All binders w/c 0.4<br>3 cells with<br>10 electrodes of 20 | All binders w/c 0.4<br>3 cells with<br>10 electrodes of 20 |
| Exposure temperature | SRPC w/c 0.50<br>Room temperature<br><br>SRPC w/c 0.4<br>Room temperature<br><br>All binders w/c 0.4<br>+ 5 °C | All binders w/c 0.4<br>Room temperature | All binders w/c 0.4<br>Variable, between approx. +4 °C and +25 °C | All binders w/c 0.4<br>Variable, between approx. -5 °C and +30 °C |
| Inspected for visible voids at steel – concrete interface | SRPC w/c 0.50<br>All electrodes<br><br>All binders w/c 0.4<br>All electrodes | All binders w/c 0.4<br>3 cells with<br>10 electrodes of 20 | All binders w/c 0.4<br>3 cells with<br>all electrodes | SRPC 5% SF and slag cement, w/c 0.4<br>2 cells with<br>all electrodes |

* Submerged exposure in a circulating 16 % NaCl solution

**Cycles of 2 hrs wetting in a 16 % NaCl solution and 22 or 166 hours drying

***1.4 % Cl in sea water at Träslövsläge Marine Field station

Table 6.6. Configuration of steel electrodes in concrete or mortar corrosion cells exposed submerged in a circulating 16 % NaCl solution at room temperature or at + 5 °C.

| | | Steel potentials (mV rel. $MnO_2$) | | | | | | | | | | | |
|---|---|---|---|---|---|---|---|---|---|---|---|---|---|
| **Cell Label** | **Mix No.** | **free pot.** | **-450 mV** | **-350 mV** | **-250 mV** | **-200 mV** | **-150 mV** | **-100 mV** | **-50 mV** | **0 mV** | **+50 mV** | **Defects** | **Exp. temp.** |
| **A-PC0.50** | **1** | 2* | 2 | 2 | 2 | 2 | 2 | 2 | 2 | 2 | 2 | none | + 20 °C |
| **B-PC0.41** | **2** | 4 | 4 | 4 | none | none | none | 4 | none | none | 4 | yes** | + 20 °C |
| **C-PC0.41** | **2** | 4 | 4 | 4 | none | none | none | 4 | none | none | 4 | yes** | + 5 °C |
| **D-SF0.42** | **3** | 4 | 4 | 4 | none | none | none | 4 | none | none | 4 | yes** | + 5 °C |
| **E-SL0.40** | **4** | 4 | 4 | 4 | none | none | none | 4 | none | none | 4 | yes** | + 5 °C |
| **F-mortPC** | **5** | 10 | none | 10 | none | none | none | none | none | none | none | none | + 5 °C |

* Figure denotes number of electrodes.

** 2 electrodes with filter paper on the steel surface tested at each potential.

The corrosion cells in Table 6.6 were exposed fully submerged in a circulating 16 % NaCl solution for 2 years, except for Cell A-PC0.50 which was exposed for 4 years. The exposure temperature was fixed at +5 °C except for 2 corrosion cells which were exposed at room temperature (+20 °C) according to Table 6.6. These tests were carried out at LTH, Table 1.1.

6.4.3.3 Laboratory wetting and drying exposure tests of concrete corrosion cells

These exposure tests started very late in the research program and have therefore only been carried out for 8 months. 3 corrosion cells with concrete mix designs according to Table 6.4, Mix No. 2-4, were configured with steel electrodes left at their natural (free) potential according to Table 6.7. One electrode was kept under potentiostatic control at -350 mV ($MnO_2$). Artificially produced filter paper defects were introduced on the steel surface on 50 % of the electrodes. The corrosion cells were exposed at room temperature (here +23 °C) to cycles of 2 hours wetting in a circulating 16 % NaCl solution and 22 or 166 hours drying, Figure 6.5. Thus 245 and 35 cycles were completed within the 8 months of testing. The tests were performed at AEC, Table 1.1.

Table 6.7. Configuration of steel electrodes in concrete corrosion cells exposed to a 16 % NaCl solution and subjected to cyclic wetting and drying in the laboratory at room temperature.

| | | **Steel potentials (mV rel $MnO_2$)** | | | | | | | |
|---|---|---|---|---|---|---|---|---|---|
| | | **2 hrs weekly wetting** | | | | **2 hrs daily wetting** | | | |
| | | **Free potential** | | **-350 mV** | | **Free potential** | | **-350 mV** | |
| **Cell Label** | **Mix No.** | **Filter paper defects** | | **Filter paper defects** | | **Filter paper defects** | | **Filter paper defects** | |
| | | **Yes** | **No** | **Yes** | **No** | **Yes** | **No** | **Yes** | **No** |
| **K-PC0.41** | **2** | 4* | 4 | 0 | 0 | 6 | 5 | 0 | 1 |
| **L-SF0.42** | **3** | 4 | 4 | 0 | 0 | 6 | 5 | 0 | 1 |
| **M-SL0.40** | **4** | 4 | 4 | 0 | 0 | 6 | 5 | 0 | 1 |

* Figure denotes number of electrodes

6.4.3.4 Marine field exposure tests of concrete corrosion cells

A total of 6 corrosion cells with 3 different concrete mix designs according to Table 6.4, Mix No. 2-4, were configured with steel electrodes at natural and potentiostatically controlled potentials and labelled according to Table 6.8. Artificially produced filter paper defects were introduced at the steel-concrete interface on 50 % of the steel electrodes.

For each mix design, one corrosion cell was mounted submerged and one in the splash zone of a floating pontoon at the Träslövsläge Marine Field Station on the Swedish west coast, Table 6.8 and Figure 3.3. Each concrete mix was exposed for 2 years.

Table 6.8. Configuration of steel electrodes in concrete corrosion cells field exposed at the Träslövsläge Marine field Station.

| | | Steel potentials (mV rel $MnO_2$) | | | | | | | |
|---|---|---|---|---|---|---|---|---|---|
| | | Submerged | | | | Splash zone | | | |
| | | Free potential | | -350 mV | | Free potential | | -350 mV | |
| Cell Label | Mix No. | Filter paper defects | | Filter paper defects | | Filter paper defects | | Filter paper defects | |
| | | Yes | No | Yes | No | Yes | No | Yes | No |
| O-subPC0.41 | 2 | 8* | 8 | 2 | 2 | - | - | - | - |
| P-splaPC0.41 | 2 | - | - | - | - | 8 | 8 | 2 | 2 |
| R-subSF0.42 | 3 | 8 | 8 | 2 | 2 | - | - | - | - |
| S-splaSF0.42 | 3 | - | - | - | - | 8 | 8 | 2 | 2 |
| T-subSL0.40 | 4 | 8 | 8 | 2 | 2 | - | - | - | - |
| U-splaSL0.40 | 4 | - | - | - | - | 8 | 8 | 2 | 2 |

* Figure denotes number of electrodes

*6.4.4 Results on chloride thresholds in concrete corrosion cells exposed submerged at a constant temperature in the laboratory*

6.4.4.1 General

Several of the steel electrodes did not start to corrode before the end of the test period. The chloride threshold for such electrodes has been evaluated as > x % total Cl by weight of binder. The variable x denotes the measured chloride content at the depth of the electrode after the indicated exposure time (2 years or 8 months).

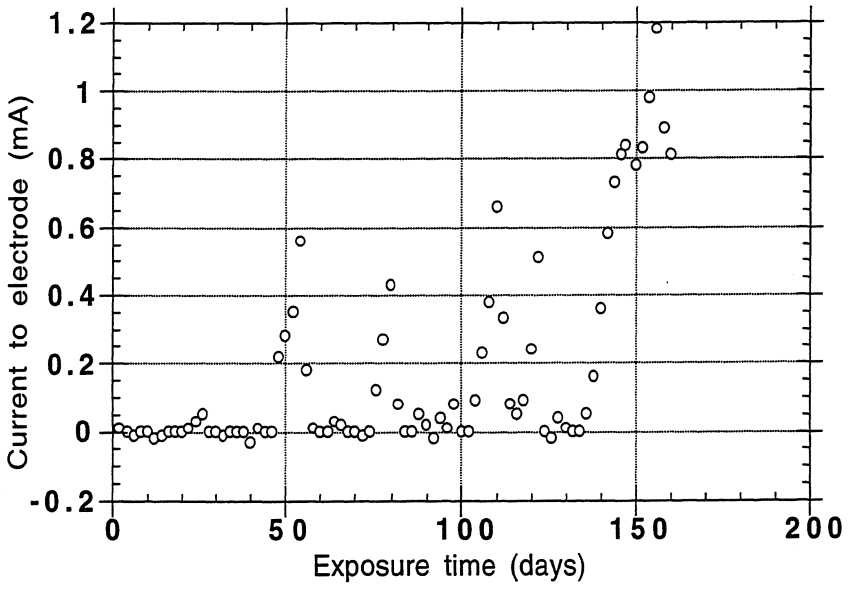


Figure 6.9. Cycles of activation and repassivation of a steel electrode under potentiostatic control in the passive state.

Chloride thresholds measured on smooth mild steel electrodes exposed in fully submerged concrete or mortar corrosion cells are shown in Table 6.9. A typical graph of the corrosion activity, measured as the current needed to maintain the steel potential under potentiostatic control, is shown in Figure 6.9 for a steel electrode kept at - 100 mV ($MnO_2$) in SRPC concrete w/c 0.50 exposed at + 20 °C, no filter paper defect applied. The measured electrical current indicated activation-repassivation cycles for more than 4 months until stable active corrosion was indicated and thus the threshold was reached as described in Chapter 6.4.1.4.

Table 6.9. Chloride thresholds expressed as % total Cl by weight of binder, for steel electrodes in corrosion cells exposed for 2 years submerged in a 16 % NaCl solution.

| | | | | Steel potentials (mV rel $MnO_2$) | | | | | | | | | |
|---|---|---|---|---|---|---|---|---|---|---|---|---|---|
| **Cell Label** | **Mix No.** | **Defects** | **Exp. temp. °C** | **free pot.** | **-450 mV** | **-350 mV** | **-250 mV** | **-200 mV** | **-150 mV** | **-100 mV** | **-50 mV** | **0 mV** | **+50 mV** |
| **A-PC0.50** | **1** | no | + 20 | 1.2<br>2.1 | >3.0<br>>3.0 | >3.0<br>>3.0 | >3.0<br>>3.0 | 2.5<br>3.0 | 2.0<br>1.7 | 2.3<br>1.7 | 1.8<br>1.2 | 1.6<br>1.9 | 1.5<br>1.8 |

| | | | | Steel potentials (mV rel $MnO_2$) | | | | |
|---|---|---|---|---|---|---|---|---|
| **Cell Label** | **Mix No.** | **Defects** | **Exp. temp. °C** | **free potential** | **-450 mV** | **-350 mV** | **-100 mV** | **+50 mV** |
| **B-PC0.41** | **2** | no | + 20 | 2.2 1.9 | >3.0<br>>3.0 | >3.3 >3.3 | >3.0<br>>3.0 | 1.7<br>>3.0 |
| **B-PC0.41** | **2** | yes | + 20 | 0.5 >3.3 | >3.0<br>>3.0 | >3.3 >3.3 | >3.0<br>>3.0 | 1.9<br>>3.0 |
| **C-PC0.41** | **2** | no | + 5 | >2.0 >2.0 | >2.0<br>>2.0 | >2.0 >2.0 | 1.8<br>>2.0 | >2.0<br>>2.0 |
| **C-PC0.41** | **2** | yes | + 5 | >2.0 >2.0 | >2.0<br>>2.0 | >2.0 >2.0 | >2.0<br>>2.0 | >2.0<br>>2.0 |
| **D-SF0.42** | **3** | no | + 5 | >1.2 >1.2 | >1.2<br>>1.2 | >1.2 >1.2 | >1.2<br>>1.2 | >1.2<br>>1.2 |
| **D-SF0.42** | **3** | yes | + 5 | >1.2 >1.2 | >1.2<br>>1.2 | >1.2 >1.2 | >1.2<br>>1.2 | >1.2<br>>1.2 |
| **E-SL0.40** | **4** | no | + 5 | >1.0 >1.0 | >1.0<br>>1.0 | >1.0 >1.0 | >1.0<br>>1.0 | >1.0<br>>1.0 |
| **E-SL0.40** | **4** | yes | + 5 | >1.0 >1.0 | >1.0<br>>1.0 | >1.0 >1.0 | >1.0<br>>1.0 | >1.0<br>>1.0 |
| **F-mortPC** | **5** | no | + 5 | >1.7 >0.9 N.A.<br>>1.5 >0.7 N.A.<br>>1.3 >0.5 N.A.<br>>1.1 | - | >1.7 >0.9 N.A.<br>>1.5 >0.7 N.A.<br>>1.3 >0.5 N.A.<br>>1.1 | - | - |

">" indicates that no corrosion was seen within the test period. The figure indicates the total chloride content at the depth of the steel electrode at the end of the exposure test.
N.A. = Not analysed.

6.4.4.2 The effect of steel potential on the chloride threshold

The effect of applied constant steel potentials on the measured chloride threshold for a concrete (SRPC w/c 0.50) corrosion cell exposed submerged at + 20 °C is shown in Figure 6.10. Steel electrodes with no potentiostatic control had a varying potential in the range of -150 to - 300 mV ($MnO_2$) during the exposure test. No filter paper defects were introduced.

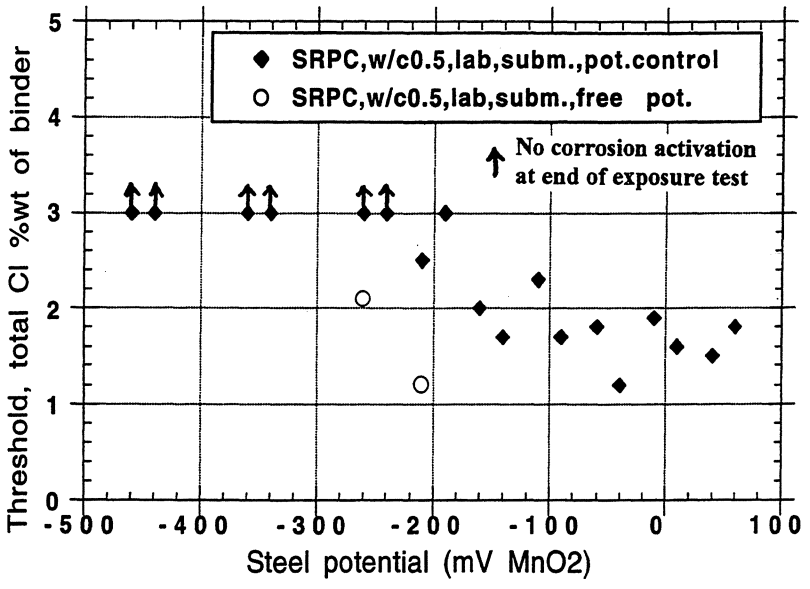


Figure 6.10. The effect of steel potential on the chloride threshold measured on smooth steel electrodes in submerged concrete (SRPC, w/c 0.50) exposed for 2 years at + 20 °C.

6.4.4.3 The effect of exposure temperature on the chloride threshold

The results from laboratory exposure for 2 years of corrosion cells submerged in 16 % NaCl solution gave some vague indications on a relationship between exposure temperature and the measured chloride threshold, Table 6.9. At +5 °C active corrosion was only initiated in 1 of 80 electrodes in mortar or concrete, at 1.8 % total Cl by weight of binder. At room temperature active corrosion was initiated in 19 of 40 electrodes in concrete, at concentrations as low as 0.5 % total Cl by weight of binder. However, it should be noted that the total chloride concentration at the depth of the steel electrodes after 2 years of exposure were also much lower in corrosion cells exposed at +5 °C as compared to corrosion cells exposed at room temperature.

*6.4.5 Results on chloride thresholds in concrete corrosion cells exposed for wetting and drying at a constant temperature in the laboratory*

Chloride thresholds for smooth mild steel electrodes exposed to wetting and drying at room temperature in concrete corrosion cells are shown in Table 6.10. Note that only 1 electrode in each corrosion cell was kept under potentiostatic control. The remaining 19 electrodes in each corrosion cell were exposed at their natural free potential, which varied in the range of -200 to -350 mV ($MnO_2$) according to the wetting and drying exposure cycles. Electrodes in slag cement concrete exhibited substantially lower chloride thresholds as compared to electrodes in SRPC concrete with or without silica fume, as indicated in Table 6.10.

Table 6.10. Chloride thresholds expressed as % total Cl by weight of binder, for steel electrodes in corrosion cells exposed for 8 months to cycles of 2 hours wetting and 22 or 166 hours drying in a 16 % NaCl solution in the laboratory at room temperature.

| | | **Steel potentials (mV rel $MnO_2$)** | | | | | | | |
|---|---|---|---|---|---|---|---|---|---|
| | | **2 hrs weekly wetting** | | | | **2 hrs daily wetting** | | | |
| | | **Free potential** | | **-350 mV** | | **Free potential** | | **-350 mV** | |
| **Cell Label** | **Mix No.** | **Filter paper defects** | | **Filter paper defects** | | **Filter paper defects** | | **Filter paper defects** | |
| | | **Yes** | **No** | **Yes** | **No** | **Yes** | **No** | **Yes** | **No** |
| **K-PC0.41** | 2 | >0.6 >0.6<br>>0.6 >0.6 | >0.6 >0.6<br>>0.6 >0.6 | - | - | 0.4 >0.6<br>>0.6 >0.6<br>>0.6 >0.6 | >0.6 >0.6<br>>0.6 >0.6<br>>0.6 | - | >0.6 |
| **L-SF0.42** | 3 | >0.6 >0.6<br>>0.6 >0.6 | >0.6 >0.6<br>>0.6 >0.6 | - | - | 0.5 >0.7<br>>0.7 >0.7<br>>0.7 >0.7 | >0.7 >0.7<br>>0.7 >0.7<br>>0.7 | - | >0.7 |
| **M-SL0.40** | 4 | nil nil<br>nil >1.0 | nil nil<br>nil >1.0 | - | - | nil nil<br>nil nil<br>nil >0.8 | nil nil<br>nil >0.8<br>nil | - | >0.8 |

">" indicates that no corrosion was seen within the test period. The figure indicates the total chloride content at the depth of the steel electrode at the end of the exposure test.
"nil" indicates that corrosion was initiated within a week after the start of chloride exposure.

*6.4.6 Results on chloride thresholds in concrete corrosion cells exposed submerged or in the splash zone at the Träslövsläge Marine Field Station*

Chloride thresholds for smooth mild steel electrodes in concrete corrosion cells exposed submerged or in the splash zone at the Träslövsläge Marine Field Station are shown in Figure 6.11 and in Table 6.11.

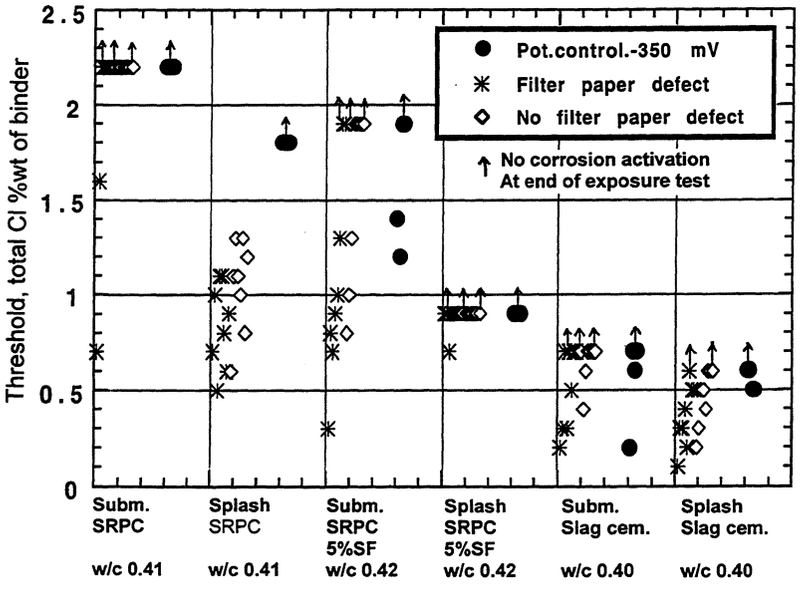


Figure 6.11. Chloride thresholds for steel electrodes in concrete corrosion cells exposed submerged and in the splash zone for 2 years at the Träslövsläge Marine Field Station.

Table 6.11. Chloride thresholds expressed as % total Cl by weight of binder, for steel electrodes in corrosion cells exposed for 2 years at the Träslövsläge Marine Field Station.

| | | Steel potentials (mV rel $MnO_2$) | | | | | | | | | | | |
|---|---|---|---|---|---|---|---|---|---|---|---|---|---|
| | | Submerged | | | | | | Splash zone | | | | | |
| | | Free potential | | | | -350 mV | | Free potential | | | | -350 mV | |
| Cell Label | Mix No. | Filter paper defects | | | | Filter paper defects | | Filter paper defects | | | | Filter paper defects | |
| | | Yes | | No | | Yes | No | Yes | | No | | Yes | No |
| O-subPC0.41 | 2 | 0.7 | >2.2 | >2.2 | >2.2 | >2.2 | >2.2 | - | - | - | - | - | - |
| | | 1.6 | >2.2 | >2.2 | >2.2 | >2.2 | >2.2 | | | | | | |
| | | >2.2 | >2.2 | >2.2 | >2.2 | | | | | | | | |
| | | >2.2 | >2.2 | >2.2 | >2.2 | | | | | | | | |
| P-splaPC0.41 | 2 | - | - | - | - | - | - | 0.7 | 1.1 | 0.6 | 1.0 | >1.8 | >1.8 |
| | | | | | | | | 1.0 | 0.8 | 1.1 | 1.3 | >1.8 | >1.8 |
| | | | | | | | | 0.5 | 0.6 | 1.3 | 0.8 | | |
| | | | | | | | | 1.1 | 0.9 | 1.1 | 1.2 | | |
| R-subSF0.42 | 3 | 0.3 | >1.9 | >1.9 | 0.8 | 1.4 | >1.9 | - | - | - | - | - | - |
| | | 0.8 | 1.0 | >1.9 | >1.9 | 1.2 | >1.9 | | | | | | |
| | | 0.7 | 0.9 | 1.3 | 1.0 | | | | | | | | |
| | | >1.9 | 1.3 | >1.9 | >1.9 | | | | | | | | |
| S-splaSF0.42 | 3 | - | - | - | - | - | - | >0.9 | >0.9 | >0.9 | >0.9 | >0.9 | >0.9 |
| | | | | | | | | 0.9 | >0.9 | >0.9 | >0.9 | >0.9 | >0.9 |
| | | | | | | | | 0.7 | >0.9 | >0.9 | >0.9 | | |
| | | | | | | | | >0.9 | >0.9 | >0.9 | >0.9 | | |
| T-subSL0.40 | 4 | 0.2 | >0.7 | >0.7 | >0.7 | 0.2 | >0.7 | - | - | - | - | - | - |
| | | 0.3 | 0.5 | >0.7 | >0.7 | 0.6 | >0.7 | | | | | | |
| | | >0.7 | >0.7 | 0.4 | >0.7 | | | | | | | | |
| | | 0.3 | >0.7 | 0.6 | >0.7 | | | | | | | | |
| U-splaSL0.40 | 4 | - | - | - | - | - | - | 0.1 | 0.2 | 0.2 | 0.4 | 0.5 | >0.6 |
| | | | | | | | | 0.3 | >0.6 | 0.3 | >0.6 | 0.5 | >0.6 |
| | | | | | | | | 0.3 | 0.5 | 0.5 | >0.6 | | |
| | | | | | | | | 0.4 | 0.5 | 0.5 | >0.6 | | |

">" indicates that no corrosion was seen within the test period. The figure indicates the total chloride content at the depth of the steel electrode.

Note that 4 electrodes in each corrosion cell were kept under potentiostatic control. The remaining 16 electrodes in each corrosion cell were exposed at their natural free potential, which varied in the range of -200 to -350 mV ($MnO_2$) according to the exposure conditions. Cell P-splaPC0.41 was lost in the sea after 17 months of exposure. Therefore the corresponding calculated chloride thresholds have not been confirmed by a visual examination of corrosion pits.

*6.4.7 Results on the effect of exposure regime on pitting corrosion in concrete corrosion cells*

Results of the effect of the exposure regime on pitting corrosion in concrete corrosion cells are presented in Figure 6.12. Corrosion cells with a w/c ratio of 0.4 were exposed submerged in the laboratory at constant temperature, for cycles of wetting and drying in the laboratory at constant temperature, and submerged or in the splash zone at the Träslövsläge Marine Field Station. Figure 6.12 shows the percentage of electrodes corroding with pitting on the inside of electrodes, on the outside of electrodes, or with pitting on both the inside and the outside of electrodes. Note that the exposure time was only 8 months in the laboratory wetting and drying exposure test as compared to 2 years exposure in all other tests.

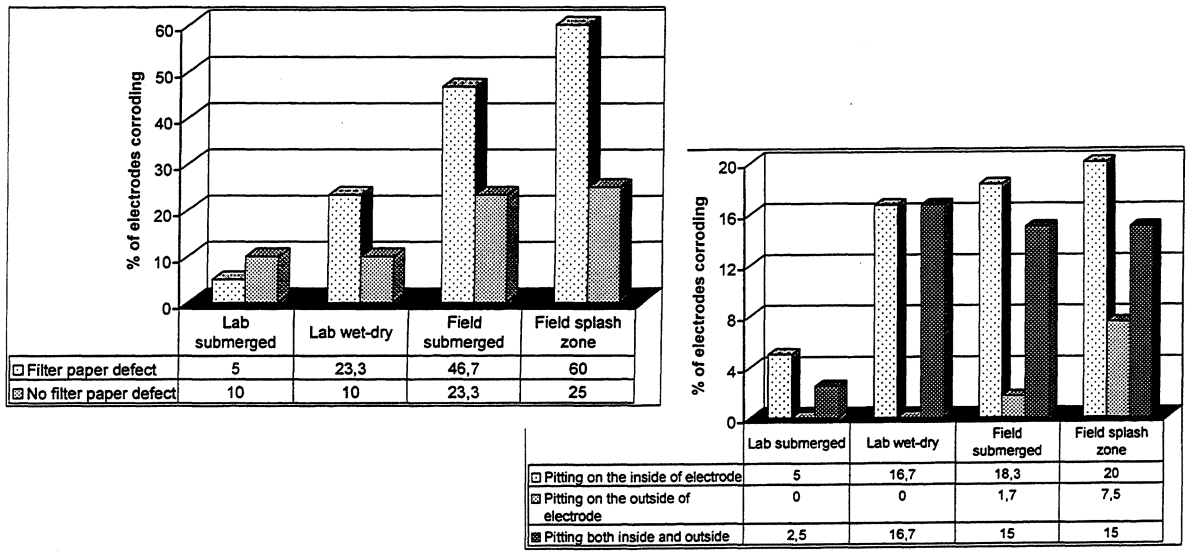


Figure 6.12. The effect of exposure regime on the corrosion activity in all concrete corrosion cells with w/c 0.40. Figures denotes percentage of electrodes.

*6.4.8 Results on the effect of artificial filter paper defects and compaction voids on pitting corrosion in concrete corrosion cells*

The incorporation of artificial filter paper defects at the steel – concrete interface had a strong negative effect on the resistance to corrosion, except for electrodes in concrete exposed submerged in the laboratory, as shown in Figure 6.12.

In all, 35 of a total of 210 examined electrodes in all concrete mixes exposed, exhibited evidence on visible compaction voids at the steel surface. 17 electrodes or approximately 50 % of the electrodes with visible compaction voids at the steel surface also experienced pitting corrosion. However, only approximately 25 % of the electrodes with visible compaction voids at the steel surface corroded in concrete exposed submerged in the laboratory.

*6.4.9 Results on the effect of bending of steel on pitting corrosion in concrete corrosion cells*

In all exposure tests, corrosion was initiated at the deformed U-bend parts at the inside of the electrodes in approximately 70 % of the corroding electrodes. The bending of hot rolled black steel is likely to cause cracking of the scale and roughening of the steel surface in the deformed zone, and especially so at the inside of the U-bent steel electrodes.

*6.4.10 Results on the effect of binder on pitting corrosion in concrete corrosion cells*

The use of slag cement had a strong negative effect on the resistance to pitting corrosion, except for slag cement concrete exposed submerged in the laboratory at + 5 °C, as compared to the use of SRPC with 0 or 5 % silica fume. The net effect considering all exposure regimes is illustrated in Figure 6.13. However, it should be noted that the slag cement concrete also exhibited more visible voids at the steel – concrete interface, as illustrated in Figure 6.14. The results nevertheless indicate that slag cement concrete is more sensitive to the formation of voids, and that the effect of voids on the resistance to pitting corrosion is more negative for slag cement as compared to SRPC with 0 or 5 % silica fume.

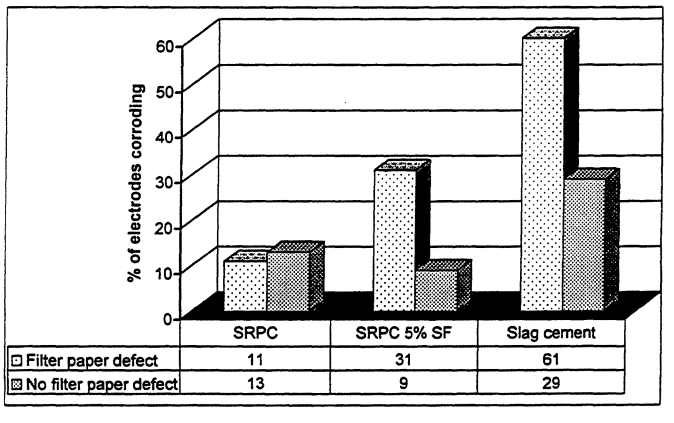


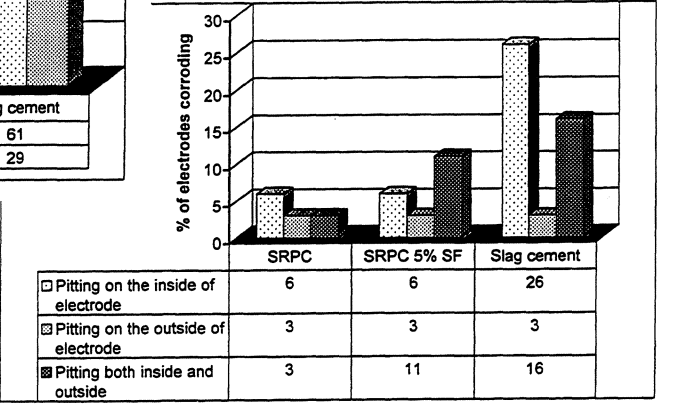


Figure 6.13. The effect of binder composition on the resistance to pitting corrosion in concrete corrosion cells. All exposure regimes considered. 2 years exposure time generally, except for 8 months for laboratory wetting and drying exposure tests.

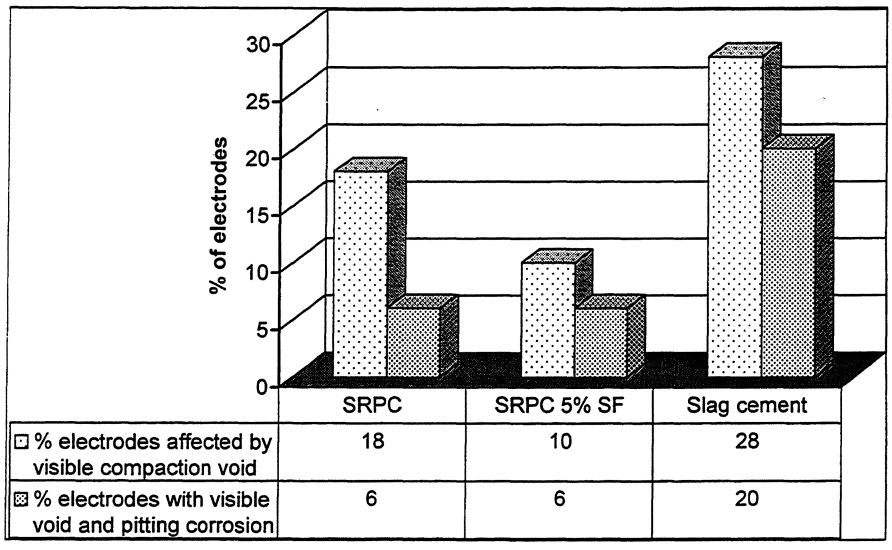


Figure 6.14. The effect of binder composition and compaction voids 0.1-2 mm wide at the steel – concrete interface on the resistance to pitting corrosion in concrete corrosion cells. All exposure regimes considered. 2 years exposure time generally, except for 8 months for laboratory wetting and drying exposure tests.

## 6.5 Evaluation of chloride thresholds for service life prediction

### *6.5.1 General*

If one would only evaluate the results from laboratory submerged exposure tests of concrete corrosion cells, one would get the impression that chloride thresholds are very high. On the other hand, the results from laboratory wetting and drying exposure tests indicates very low chloride thresholds, especially so for slag cement concrete. It is therefore most important to evaluate all results together and to compare them with the results from field exposed reinforced concrete.

The results from exposure tests of concrete corrosion cells are useful for the identification of factors affecting the chloride threshold. However, chloride thresholds for service life prediction of reinforced concrete should preferably be derived from field exposure tests on reinforced concrete, as the surface and size of the steel electrodes in corrosion cells are not representative for reinforced concrete.

Mean values and standard deviations have been calculated and used as a tool for evaluation of data available. Calculations of standard deviations with less than 6 data points, sometimes with only 2 data points, were calculated with the sole purpose to illustrated the spread in data. The number of data points used in the calculations has been printed together with the standard deviations.

The evaluation procedure in this thesis has been carried out in the following steps.

A. Evaluation of the relative effect of voids 0.1-2 mm wide in the concrete at the steel – concrete interface on the chloride threshold, as compared to concrete with no voids 0.1-2 mm wide. Results from exposure tests of concrete corrosion cells were used.

B. Evaluation of the relative effect of defects at the steel surface on the chloride threshold. Results from exposure tests of concrete corrosion cells were used.

C. Evaluation of the effect of exposure regime and binder on the chloride threshold. Results from exposure tests of concrete corrosion cells were compared with results from the field exposure tests of reinforced concrete slabs.

D. Evaluation of the effect of cover thickness and w/c ratio on the chloride threshold. Results from field exposure tests of reinforced concrete slabs were compared with simulations of the moisture variations in concrete at various exposure regimes, Arfvidsson and Hedenblad /27/.

E. A synthesis of chloride thresholds for service life prediction was carried out using the results from the evaluations in steps A-D.

### *6.5.2 Evaluation of the relative effect of voids 0.1-2 mm wide on the chloride threshold*

#### 6.5.2.1 Corrosion cells exposed submerged in the laboratory at +5°C and at room temperature

The relative effect of voids 0.1-2 mm wide on the chloride threshold in corrosion cells exposed submerged in the laboratory at +5°C and at room temperature is shown in Table 6.12. None of 4 electrodes affected with a void 0.1-2 mm wide were corroding after 2 years of exposure at +5°C. At room temperature 3 out of 7 electrodes with voids 0.1-2 mm wide at the steel surface were corroding.

The relative effect of voids 0.1-2 mm wide on the chloride threshold was evaluated as small for corrosion cells exposed submerged in the laboratory, as only approximately 25 % of the electrode affected started to corrode within 2 years. However, if the voids initiated active corrosion, the chloride threshold was reduced with 40 to 75 %.

Table 6.12. The effect of voids 0.1-2 mm wide on the chloride threshold in corrosion cells exposed for 2 years submerged in the laboratory at +5°C and at room temperature. Total chloride thresholds, % total Cl by weight of binder.

| 1 | 2 | 3 | 4 | 5 | 6 | 7 | 8 |
|---|---|---|---|---|---|---|---|
| **Cell Label** | **Mix No.** | **Exp. temp °C** | **No. of electro-des investi-gated** | **Number of electrodes affected by void 0.1-2 mm wide** | **Chloride threshold for electrodes in column 5** | **Chloride thresholds for electrodes unaffected by void 0.1-2 mm wide** | |
| | | | | | | **Filter paper defects** | |
| | | | | | | **Yes** | **No** |
| **A-PC0.50** | **1** | +20 | 20 | 4 | 1.2 1.2<br>No corrosion<br>No corrosion | -<br>No electrodes with filter paper defects in this cell | 1.5 1.6 1.7<br>1.7 1.8 1.8<br>1.9 2.0 2.1<br>2.3 2.5 3.0<br>4 electrodes with no corrosion |
| **B-PC0.41** | **2** | +20 | 20 | 3 | 0.5<br>No corrosion<br>No corrosion | 1.9<br>7 electrodes with no corrosion | 1.7 1.9 2.2<br>6 electrodes with no corrosion |
| **C-PC0.41** | **2** | +5 | 20 | N.A. | N.A. | 10 electrodes with no corrosion | 1.8<br>9 electrodes with no corrosion |
| **D-SF0.42** | **3** | +5 | 20 | 1 | No corrosion | 9 electrodes with no corrosion | 10 electrodes with no corrosion |
| **E-SL0.40** | **4** | +5 | 20 | 3 | 3 electrodes with no corrosion | 8 electrodes with no corrosion | 9 electrodes with no corrosion |
| **F-mortPC** | **5** | +5 | 20 | N.A. | N.A. | 10 electrodes with no corrosion | 10 electrodes with no corrosion |

N.A. = Not analysed.

6.5.2.2 Corrosion cells exposed for wetting in 16% NaCl and drying at room temperature

The relative effect of voids 0.1-2 mm wide on the chloride threshold in corrosion cells exposed for wetting in 16% NaCl and drying at room temperature is shown in Table 6.13.

As indicated in Table 6.13, 1 of 4, or 25 %, of the electrodes affected by a void 0.1-2 mm wide were corroding in SRPC concrete with 0 or 5 % silica fume after 8 months of exposure. In slag cement concrete the corresponding figures were 5 corroding electrodes of 7 affected, or 70%.

Table 6.13. The effect of voids 0.1-2 mm wide on the chloride threshold in concrete corrosion cells exposed to wetting in 16% NaCl and drying at room temperature for 8 months. Total chloride thresholds, % total Cl by weight of binder.

| 1 | 2 | 3 | 4 | 5 | 6 | 7 |
|---|---|---|---|---|---|---|
| **Cell Label** | **Mix No.** | **Number of electrodes investigated *** | **Number of electrodes affected by void 0.1-2 mm wide** | **Chloride threshold for electrodes in column 4** | **Chloride thresholds for electrodes unaffected by void 0.1-2 mm wide** | |
| | | | | | **Filter paper defects** | |
| | | | | | **Yes** | **No** |
| **K-PC0.41** | **2** | 10 | 3 | 0.4<br>No corrosion<br>No corrosion | 3 electrodes with no corrosion | 4 electrodes with no corrosion |
| **L-SF0.42** | **3** | 10 | 1 | No corrosion | 0.5<br>3 electrodes with no corrosion | 5 electrodes with no corrosion |
| **M-SL0.40** | **4** | 10 | 7 | 0 0 0<br>0 0 >1.0<br>>1.0 | 0 | 0 0 |

*Only 10 out of 20 electrodes in each corrosion cell have been visually examined for voids in concrete close to the electrode. The remaining electrodes were left for further exposure tests.

6.5.2.3 Corrosion cells exposed at Träslövsläge field station

The relative effect of voids 0.1-2 mm wide on the chloride threshold in corrosion cells exposed at Träslövsläge field station is shown in Table 6.14.

None of the 2 electrodes affected with a void 0.1-2 mm wide were corroding in SRPC concrete after 2 years of exposure. In SRPC concrete with 5 % silica fume, 3 of the 4 electrodes affected with a void 0.1-2 mm wide were corroding. For slag cement concrete, 5 electrodes of 7 affected with a void 0.1-2 mm wide were corroding.

The average reduction in the chloride threshold for electrodes affected by a void 0.1-2 mm wide was 40 % for both SRPC concrete with 5 % silica fume and slag cement concrete, as compared to electrodes without visible defects.

Table 6.14. The effect of voids 0.1-2 mm wide on the chloride threshold in concrete corrosion cells field exposed at Träslövsläge Field Station. Total chloride thresholds, % total Cl by weight of binder.

| 1 | 2 | 3 | 4 | 5 | 6 | 7 |
|---|---|---|---|---|---|---|
| **Cell Label** | **Mix No.** | **Number of electrodes investigated** | **Number of electrodes affected by void 0.1-2 mm wide** | **Chloride threshold for electrodes in column 4** | **Chloride thresholds for electrodes unaffected by void 0.1-2 mm wide** | |
| | | | | | **Filter paper defects** | |
| | | | | | **Yes** | **No** |
| **O-PC0.41** | **2** | 20 | 2 | No corrosion<br>No corrosion | 0.7 1.6<br>7 electrodes with no corrosion | 9 electrodes with no corrosion |
| **R-SF0.42**<br>**S-SF0.42** | **3** | 20 | 4 | 0.3 0.7 0.8<br>No corrosion | 0.7 0.8 0.9<br>0.9 1.0 1.2<br>1.3 1.4<br>10 electrodes with no corrosion | 1.0 1.3<br>16 electrodes with no corrosion |
| **T-SL0.40**<br>**U-SL0.40** | **4** | 20 | 7 | 0.1 0.2<br>0.2<br>0.3 0.4<br>No corrosion<br>No corrosion | 0..2 0.3 0.3<br>0.3 0.4 0.5<br>0.5 0.5 0.5<br>0.5 0.6<br>4 electrodes with no corrosion | 0.2 0.3 0.4<br>0.5 0.5 0.6<br>12 electrodes with no corrosion |

Note that corrosion cell P-PC0.41 was lost in the sea and has not been examined visually.

*6.5.3 Evaluation of the relative effect of other defects than artificially produced filter paper defects on the chloride threshold*

The relative effect of filter paper defects on the steel surface on the chloride threshold was shown in Tables 6.12 – 6.14. No effect of filter paper defects was found for corrosion cells submerged in the laboratory.

The effect of filter paper defects on the chloride threshold are summarised in Table 6.15, with all values from electrodes affected by voids 0.1-2 mm wide at the steel surface removed. It was assumed that no electrodes in the lost corrosion cell P-PC0.41 was affected by such voids. Only data from field exposure tests was considered, as too little thresholds were available from the laboratory exposure tests.

Table 6.15. The effect of filter paper defects on the chloride threshold in concrete corrosion cells exposed at the Träslövsläge Marine Field Station. Electrodes affected by voids > 0.1 mm wide are excluded.

| Concrete mix | Chloride threshold, tot Cl % by weight of binder. | | | |
|---|---|---|---|---|
| | Filter paper defect | | | |
| | Yes | | No | |
| | Mean value and standard deviation (in brackets) | Number of data | Mean value and standard deviation (in brackets) | Number of data |
| **SRPC w/c 0.41** | 0.90 (0.32) | 10 | 1.0 (0.24) | 8 |
| **SRPC 5 % SF w/c 0.42** | 1.0 (0.25) | 8 | 1.1 (0.21) | 2 |
| **Slag cement w/c 0.40** | 0.42 (0.13) | 11 | 0.42 (0.15) | 6 |

As indicated in Table 6.15, the effect of filter paper defects at the steel surface on the chloride threshold was insignificant. However, it should be noted that electrodes with filter paper defects exhibited almost double the amount of corroding electrodes as compared to electrodes without filter paper defects, as illustrated in Figure 6.12. If the exposure test would have been continued, a larger number of higher thresholds would be anticipated for electrodes without filter paper defects, as more electrodes are still passive as compared to electrodes with filter paper defects.

The effect of deforming or cracking of the scale on electrodes by means of bending of electrodes was illustrated by the fact that 70 % of the actively corroding steel in all exposure tests had initiation of pitting corrosion at the inside of the U-bend steel.

### *6.5.4 Evaluation of the effects of exposure regime and binder on the chloride threshold*

The effects of the exposure regime and binder on the chloride threshold can be evaluated by comparing the data in Tables 6.12 – 6.15. Alternatively, it can be done by comparing the data in Figure 6.10, for corrosion cells exposed submerged at the laboratory at room temperature, with data in Figure 6.11, for corrosion cells exposed at Träslövsläge Marine Field Station.

According to the data in Table 6.15, the chloride threshold for slag cement concrete exposed in the splash zone is approximately 40 – 50 % of the threshold for SRPC concrete with 0 or 5 % silica fume in the binder.

According to the data in Tables 6.9-6.11, 6.15 and Figures 6.10 – 6.11, the chloride threshold is generally much higher in fully submerged concrete corrosion cells, as compared to cells subjected to variations in moisture and temperature. The effect seems especially pronounced for slag cement concrete. By comparing the chloride thresholds in Tables 6.9 and 6.15, it was found that the chloride thresholds for laboratory submerged cells with plain SRPC, SRPC

with 5 % silica fume in the binder, and slag cement, were at least a factor 2.0, 1.2, and 2.6 times higher, respectively, as compared to the corresponding chloride thresholds for field exposed concrete corrosion cells. Probably the "true" mean chloride thresholds are even higher for the laboratory submerged concrete, as most electrodes had not yet started to corrode at the total chloride concentrations listed as "> x" % total chloride by weight of binder in Table 6.9. The factor 2.0 as found for plain SRPC concrete was considered as the most relevant one, as a relatively large number (20) of electrodes had started to corrode in SRPC concrete submerged in the laboratory. No electrodes had started to corrode in cells with SRPC and 5 % silica fume in the binder or with slag cement.

The effect of the binder on the chloride threshold in the splash zone can also be evaluated from chloride thresholds for field exposed reinforced concrete slabs in Figure 6.4. According to the results in Figure 6.4, the mean chloride threshold for slag cement concrete exposed in the splash zone, with w/c ratio 0.40 and 10 mm cover, is 0.6 % total chloride by weight of binder (standard deviation 0.22, 4 values). The corresponding mean chloride thresholds for SRPC concrete with 0 and 5 % silica fume in the binder are both 0.95 % total chloride by weight of binder (standard deviation 0.07 and 0.21, respectively, but only 2 values available for both concrete mixes). Looking at 15 mm cover with 4 values available for the SRPC mixes but no thresholds available for slag cement concrete, the mean chloride thresholds for SRPC concrete with 0 and 5 % silica fume in the binder are both 1.1 % total chloride by weight of binder (standard deviation 0.10 and 0.22, respectively). Thus the data in Figure 6.4 indicates that the chloride threshold for slag cement concrete exposed in the splash zone is approximately 60 % of the threshold for SRPC concrete with 0 or 5 % silica fume in the binder.

It was calculated from the data in Figure 6.4 that the mean chloride threshold for concrete with 10-20 % fly ash in the binder exposed in the splash zone is 70 to 85 % of the corresponding chloride threshold for SRPC concrete with 5 % silica fume. As discussed in Chapter 6.4.10, slag cement concrete is more sensitive to the formation of voids, and the effect of voids on the resistance to pitting corrosion is more negative for slag cement as compared to SRPC with 0 or 5 % silica fume. It is speculated that this is valid also for fly ash concrete. The slower strength development in slag cement or fly ash concrete makes it more vulnerable for drying shrinkage cracking and also for separation as compared to SRPC concrete with 0 or 5 % silica fume. Furthermore, concrete with slag cement or high amounts of fly ash or combinations of fly ash and silica fume contains less calcium hydroxide as compared to SRPC concrete with 0 or 5 % silica fume. It was observed in /16/ that calcium hydroxide at the steel concrete interface acts as a reservoir of hydroxides and prevents the formation of local acid corrosion pits on the steel surface, thereby having a positive effect on the chloride threshold.

According to the evaluations above, no significant difference in the chloride threshold can be found between SRPC concrete with 0 and 5 % silica fume in the binder. The spread in chloride thresholds for field exposed reinforced slabs however were larger for SRPC concrete with 5 % silica fume than for plain SRPC concrete, as seen by the standard deviations.

*6.5.5 Evaluation of the effect of cover thickness and w/c ratio on the chloride threshold*

6.5.5.1 Evaluation of chloride thresholds for reinforced concrete slabs

The effect of cover thickness and w/c ratio on the chloride threshold for reinforced concrete slabs exposed in the splash zone can be evaluated from the results in Figure 6.3, with linear trend lines incorporated as shown in Figure 6.15.

The effect of increasing the cover from 10 to 20 mm is clear as shown in Figure 6.15. However, the linear trend lines for 15 mm cover do not agree with the trend lines for 10 and 20 mm cover. A closer look at the data behind the 15 mm trend lines reveals that 1 or 2 individual data points at w/c ratio 0.75 are causing the disagreement between the trend lines. On the other hand, for higher w/c ratios the difference in moisture condition at the reinforcement with different covers is more pronounced than at low w/c ration, see Figure 6.16 /27/. Therefore one would expect that the effect of cover thickness would be larger at high w/c ratios as compared to low w/c ratios, as a result of a lower moisture permeability at lower w/c ratios.

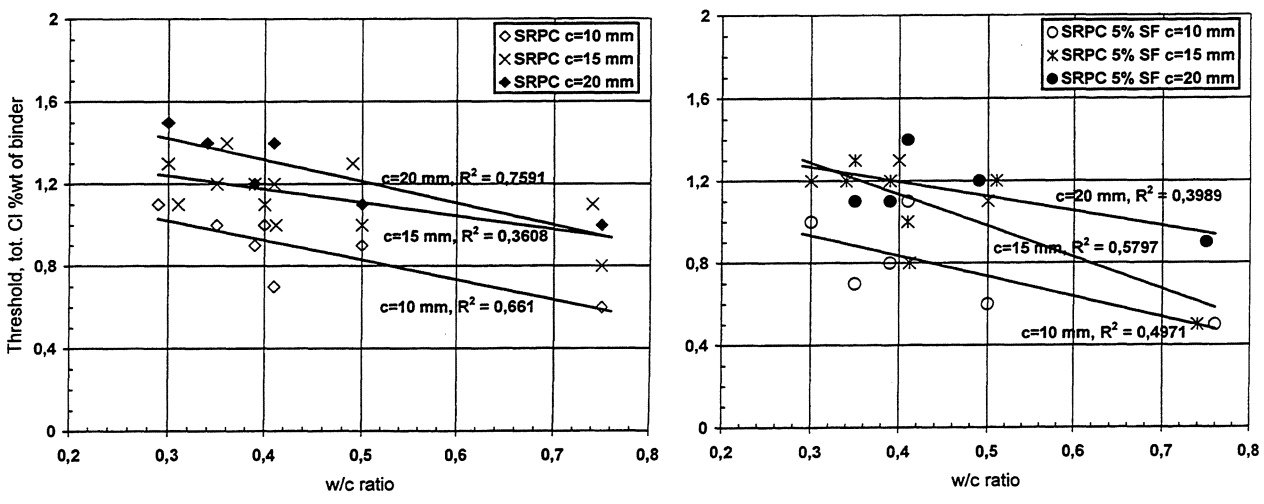


Figure 6.15 Evaluation of the effect of the cover thickness on the chloride threshold for reinforced concrete slabs exposed in the splash zone. A) Plain SRPC concrete, B) SRPC concrete with 5 % silica fume in the binder

6.5.5.2 Evaluation of the effect of cover and w/c ratio on moisture variations and chloride thresholds

Chloride thresholds for reinforced concrete slabs exposed in the splash zone at the Träslövsläge Marine Field Station have so far only been available for 10, 15 and 20 mm covers. No corrosion has yet started in concrete slabs with w/c ratio 0.35 and 0.40 with 30-55 mm cover. The effect of covers thicker than 20 mm on the chloride threshold was evaluated by simulations of the moisture variations in a concrete cover carried out by Arfvidsson and Hedenblad, Figure 6.16 /27/.

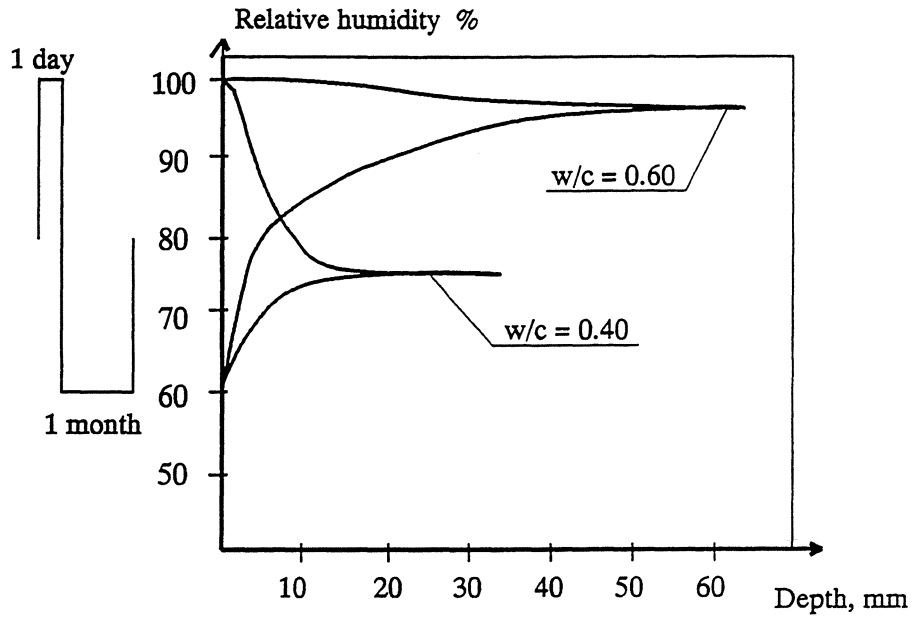


Figure 6.16 Simulations of the moisture variations in concrete w/c 0.40 and 0.60, exposed to 1 day of wetting (capillary suction) and 1 month of drying at RH 60 % /27/.

It is known that the moisture state affects the oxygen permeability in concrete /4/ and the chloride threshold in mortar, Figure 5.1 /20/. At RH < 80 % the chloride threshold increases with a lower RH because of a lack of electrolyte. At RH > 90 % the chloride threshold increases with a higher RH because of a lack of oxygen /20/. The relationship between the exposure regime and the chloride threshold was discussed in Chapter 6.5.4. It was found that the chloride threshold can be substantially higher for a corrosion cell exposed submerged at a constant temperature as compared to when exposed to wetting and drying or when field exposed submerged close to the water line.

The difference between the chloride threshold for steel in SRPC mortar conditioned at 100 and 90 % RH was a factor of 7 in /20/, Figure 5.1, with the lowest threshold at 90 % RH. On the other hand, the chloride threshold for concrete slabs field exposed partly submerged was found to be higher for w/c ratio 0.3 as compared to w/c ratio 0.5, Figure 6.3, although the RH at the depth of the reinforcement at the time and place of corrosion initiation was in the range of 80-90 % for w/c ratio 0.30 and > 95 % for w/c ratio 0.50 /43/. The corrosion initiation in most cases took place in submerged parts of the concrete slabs, probably because of the higher total chloride concentration at the depth of the reinforcement in submerged parts. Submerged concrete with w/c ratio 0.30 may have a lower RH at the depth of the reinforcement as a result of self desiccation and a lower moisture permeability, as compared to a concrete with w/c ratio 0.50.

The positive effect of a thicker cover and a lower w/c ratio on the chloride threshold, Figure 6.3, therefore indicate that it is variations in the moisture state and temperature at the depth of the reinforcement rather than the absolute levels which affects the chloride threshold for steel in concrete. A thicker cover and a lower w/c ratio would lead to less variations in moisture and temperature at the depth of the reinforcement. A further discussion is available in (paper XI).

It can be evaluated from Figure 6.16 that external moisture variations are not likely to affect reinforcement with a minimum cover of 20 mm in concrete with a w/c ratio of 0.40. The

corresponding cover for reinforcement in concrete with a w/c ratio of 0.60 is seen to be about 55 mm. As a consequence, the chloride threshold is not likely to increase if the cover is increased from 20 mm in concrete with a w/c ratio of 0.40 or lower. For a concrete with w/c ratio 0.60, the chloride threshold will probably increase with an increased cover up to 55 mm, as a result of the reduced moisture variations as shown in Figure 6.16. If the cover is thick enough to eliminate all moisture variations at the depth of the reinforcement, it is possible that the apparent effect of w/c ratio on the chloride threshold, Figure 6.15, will be greatly reduced. It is then assumed that the observed relationship between w/c ratio and chloride threshold is in fact based on a relationship between w/c ratio and moisture variations at a given depth from the exposed surface, as indicated in Figure 6.16. The results from the laboratory submerged exposure tests of corrosion cells, Chapter 6.4.4 and Table 6.9, did not indicate a clear relationship between w/c ratio and chloride thresholds. This can be interpreted as indicating that the effect of the w/c ratio on the chloride threshold is not significant for exposure conditions with no moisture variations at the depth of the reinforcement.

It must be noted, however, that the calculations behind Figure 6.16 are very approximate. Other variations in the external moisture state than showed in Figure 6.16 will also give other moisture variations in the cover. On the other hand, the drying period of 1 month at 60 % RH used can be considered as extreme for a marine concrete, at least in Scandinavia. A shorter drying period and a higher RH leads to less moisture variations at a given depth from the concrete surface. Therefore is assumed that the moisture variations in marine concrete in most cases are less extensive than indicated in Figure 6.16.

It should also be noted that temperature variations in the cover can also be expected to induce moisture variations as the relative humidity depends on the temperature.

#### 6.5.5.3 Evaluation of the effect of hydroxide leaching on chloride thresholds

The effect of cover thickness and w/c ratio on the leaching of hydroxide ions may also affect the chloride threshold. It is known that a reduced concentration of hydroxide ions in the pore solution has a negative effect on the chloride threshold /17/ as discussed in (paper XI).

Studies of free chloride and hydroxide ion concentration profiles in the laboratory /31/ and in the field (paper IV) have indicated that the penetration rate of free chlorides and the leaching rate of free hydroxides are approximately the same in submerged concrete, see Figures 7.1-7.2. Data from the splash zone is lacking as the pore solution expression method used in the field study (paper IV) is considered as reliable only for water saturated concrete /30/.

Based on the results in /31/ and (paper IV) it is assumed that the penetration rate of free chlorides and the leaching rate of free hydroxides are approximately the same in submerged concrete. It is also assumed that the leaching rate of free hydroxides in the splash zone is not higher than the chloride penetration rate, provided that the carbonation depth is less than 1/5 of the cover thickness. These assumptions lead to the conclusion that the effect of hydroxide leaching is accounted for in the field exposure tests. A thicker cover will not affect the relative shape of the free chloride and hydroxide ion concentration profiles, and therefore neither the free chloride ion concentration and nor the Cl/OH ratio in the pore solution, at the depth of the reinforcement at the corrosion initiation.

The net result from the discussions in Chapter 6.5.5 is that it is assumed that the effects of cover and w/c ratio on the chloride threshold are mainly controlled by the effects on the moisture variations at the depth of the reinforcement.

### *6.5.6 Synthesis of chloride thresholds for service life prediction*

The following information can be extracted from the evaluations in 6.5.2-6.5.5

1) Normal ribbed reinforcement is assumed to exhibit defects in the scale which affect the corrosion initiation in a similar way as for U-bend steel electrodes. Therefore no extra consideration is given to the observed effect of bending of steel.

2) The observed effect of voids 0.1-2 mm wide can be assumed to be accounted for in field exposure tests of reinforced concrete slabs, as such voids are frequently found in conventional concrete and therefore also in the test concrete. On the other hand, the effect of voids indicates that the chloride threshold can be improved by 40 to 75 %, if reinforced concrete can be produced without voids > 0.1 mm wide at the steel surface.

3) The chloride threshold in uncracked concrete is generally 2 times higher in fully submerged concrete as compared to concrete exposed in the splash zone. The term fully submerged denotes that the distance between the potential anode in fully submerged concrete and a potential cathode in concrete exposed to the atmosphere is large enough to prevent the formation of a macrocell. The distance depends on the resistivity of the concrete between the potential anode and cathode, which in turn depends on the w/c ratio and the amount and type of pozzolan in the binder /42/. This distance has not been evaluated in this thesis, but is often assumed to be 1.0 m in concrete with a w/c ratio less than 0.40 /44/.

4) No significant difference in the chloride threshold for binder combinations of the types tested can be anticipated for concrete exposed fully submerged.

5) The chloride threshold for slag cement concrete exposed in the splash zone can be assumed to be 60 % of the chloride threshold for SRPC concrete with 5 % silica fume. The corresponding chloride threshold for concrete with 10-20 % fly ash in the binder can be assumed to be 80 % of the threshold for SRPC concrete with 5 % silica fume.

6) No significant difference in the mean chloride threshold can be found for concrete with plain SRPC and SRPC with 5 % silica fume, when exposed in the splash zone. However, if the spread in the data is considered and chloride thresholds are selected with 95 % confidence assuming a normal frequency distribution of data, the solid lines in Figure 6.17 B could be used for service life prediction. Figure 6.17 A shows the linear trend lines for the chloride threshold for SRPC concrete with 0 or 5 % silica fume in the binder, exposed in the splash zone in the field with a 20 mm cover. Figure 6.17 B shows the corresponding lower trend lines when a normal frequency distribution with 95 % confidence is assumed.

7) It is assumed that the effects of cover and w/c ratio on the chloride threshold are mainly controlled by the effects on the moisture variations at the depth of the reinforcement.

8) The chloride threshold for concrete exposed in the splash zone is assumed to increase with an increased cover up to approximately 20 mm cover thickness for concrete with w/c 0.40, and 55 mm thickness for w/c 0.60. Beyond these depths the effect of moisture variations is supposed to be negligible and therefore not affecting the chloride threshold. This assumption is conservative and should not overpredict the chloride threshold in concrete at thicker covers. Thus chloride thresholds measured in field exposed concrete with 20 mm cover can be used for prediction of the initiation time in concrete with thicker cover if the w/c ratio is $\leq 0.40$.

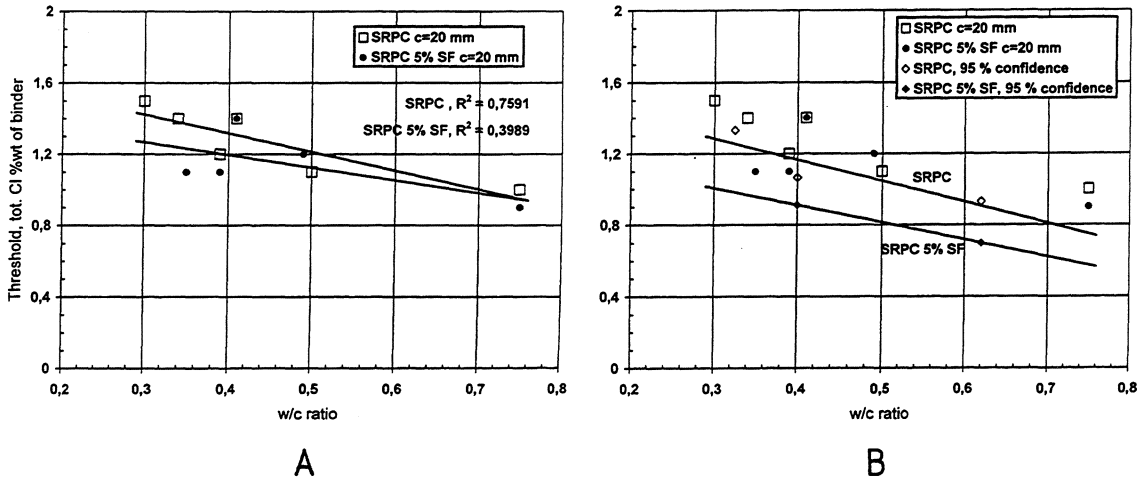


Figure 6.17 A) Linear trend lines for the chloride threshold for SRPC concrete with 0 or 5 % silica fume in the binder, field exposed in the splash zone with a 20 mm cover.
B) The corresponding trend lines when a normal frequency distribution is assumed with 95 % confidence.

## 6.6 Analysis of sensitivity

### *6.6.1 General*

The following is a discussion of possible errors affecting the analysis and evaluations carried out regarding the chloride threshold.

### *6.6.2 Errors associated with chloride profiles*

Chloride ingress in concrete is not evenly distributed as shown in Photo 5 in the Appendix. However, the data in the chloride profiles used in determining the threshold represents a mean value in the area analysed. Considering that drilled cylinders with diameter 75 – 100 mm were used, the spread in the chloride profiles can be assumed to be relatively small as illustrated in

Figure 6.18, provided that no voids are large enough to alter the chloride distribution locally. The mean chloride threshold at a depth of 10 mm was 0.98 % total chloride by weight of binder, with a standard deviation of 0.10 % total chloride by weight of binder for these 3 profiles. An example of slag cement concrete with large voids can be seen in Photo 6 in the Appendix.

Any errors associated with the analysis of the binder content should be small, as no aggregates containing acid soluble calcium were used.

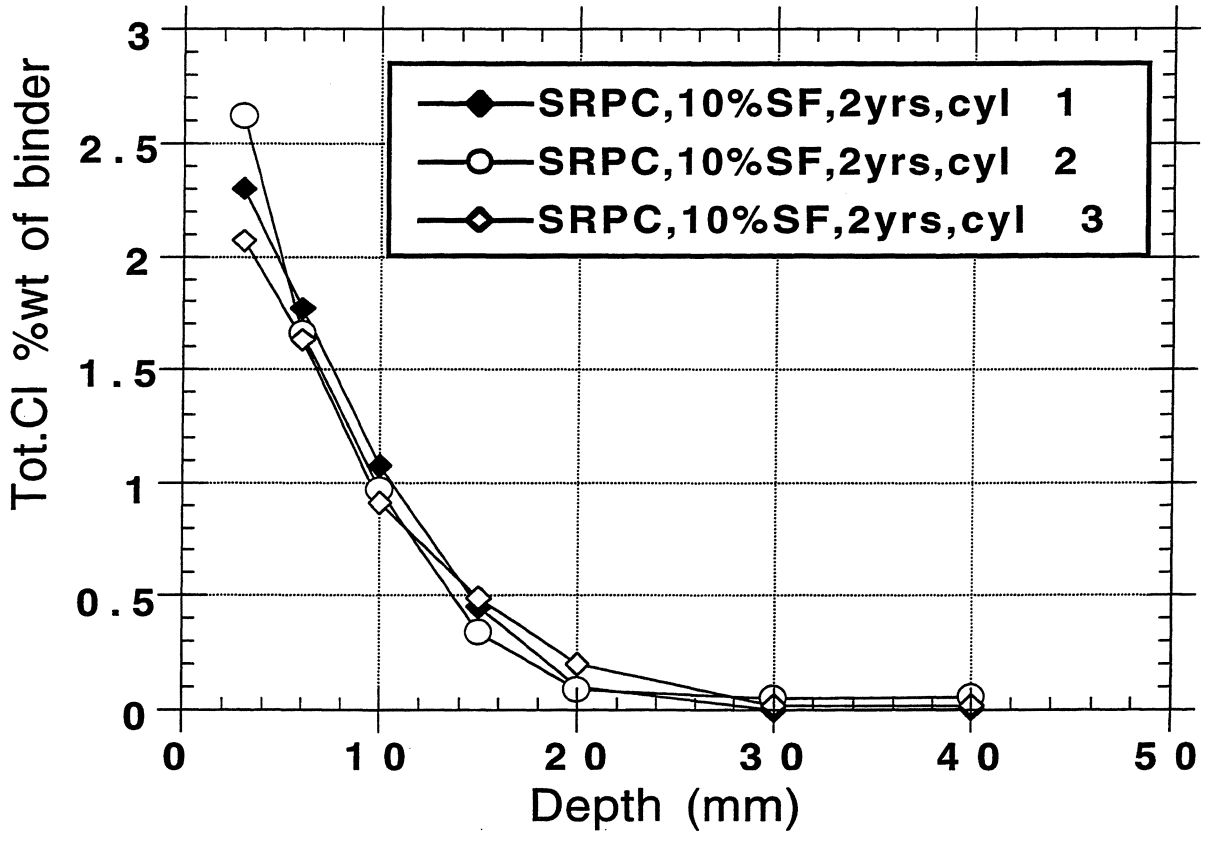


Figure 6.18 Illustration of the spread in chloride profiles, for 3 concrete cylinders drilled next to each other in concrete with SRPC and 10 % silica fume, exposed submerged at the Träslövsläge Field Station.

### *6.6.3 Errors associated with the detection of corrosion initiation*

In the laboratory exposure tests a distinct indication of the corrosion state was available as exemplified in Figures 6.7 and 6.9. In the field exposure tests, however, the indications were less clear as the passive potentials and currents were shifting to a greater extent. In fact, the distinction between active and passive corrosion is probably less clear in the field exposure tests as compared to the laboratory exposure tests, because of the varying exposure conditions resulting in a series of activation and repassivation. As a consequence, field exposed specimens were not opened up for a visual examination of the corrosion pit until measurements of both corrosion potential and corrosion rate indicated active corrosion during

2 consecutive weeks. Therefore the threshold might be somewhat exaggerated. However, the difference in total chloride concentration at the depth of reinforcement, at the time when the chloride threshold is reached and at the time of analysis, is negligible as the changes in the total chloride profile is too small to be measured after 2 weeks of exposure.

However, it should be noted that according to the definition of the chloride threshold used in this thesis, Chapter 4.4, series of activation lasting less than 2 weeks followed by repassivation were not considered as affecting the chloride threshold. Short cycles of activation and repassivation are defined as electrochemical noise and occur normally in passive steel in concrete. A lower chloride threshold would be achieved if the electrochemical noise was considered as being a state of active corrosion.

### *6.6.4 Errors associated with the handling and evaluation of data*

As shown in Figures 6.3-6.4 and Tables 6.3, 6.12-6.15, relatively few data stand behind the evaluation of chloride thresholds in Chapter 6.5. In some cases only 2 datapoints were available for calculation of the standard deviation. The chloride thresholds for SRPC concrete with 0 and 5 % silica fume are based on a total of 24 and 22 datapoints, respectively, from field exposure tests of reinforced concrete slabs. Therefore this data is considered as quantitative with the data in Figure 6.17 extracted for prediction of the initiation time in concrete with a minimum cover of 20 mm. The chloride thresholds for concrete mixes with fly ash or slag cement are based on 11 and 4 datapoints, respectively, for concrete with w/c ratio 0.3-0.4. The mean values were lower and the standard deviations higher as compared to SRPC concrete with 0 and 5 % silica fume in the binder, especially so for slag cement concrete, see Chapter 6.5.4. Therefore this data is considered as somewhat less quantitative. The main reasons for the increased standard deviation in the chloride thresholds for concrete with slag cement or fly ash in the binder was considered to be the increased tendency for the formation of micro structural defects in the concrete and an increased sensitivity for defects on the initiation of corrosion, as compared to SRPC concrete with 0 or 5 % silica fume.

# 7. EXPERIMENTAL WORK ON CHLORIDE BINDING IN FIELD EXPOSED CONCRETE

## 7.1 General

Relationships between total, free and bound chloride ions in concrete are important for the development of models for service life predictions of reinforced concrete with respect to reinforcement corrosion. The binding of chlorides in hydrated cement paste affects both the transport rate of chlorides into concrete, and the amount of total chlorides necessary to initiate active corrosion.

## 7.2 Literature data on equilibrium laboratory studies of chloride binding in hydrated cement paste

Equilibrium laboratory studies of chloride binding in hydrated cement paste normally results in a non-linear relationship between free and total (or bound) chloride as reported in /28,29/. Tang and Nilsson /28/ studied the adsorption of chloride ions in crushed cement paste and mortar from a NaCl solution saturated with calcium hydroxide, see Figure 7.1 (A). The total acid soluble chloride content and the available pore volume, defined as the dry porosity at 11 % RH, were analysed while the free chloride concentration was assumed to be equal to that in the equilibrium solution.

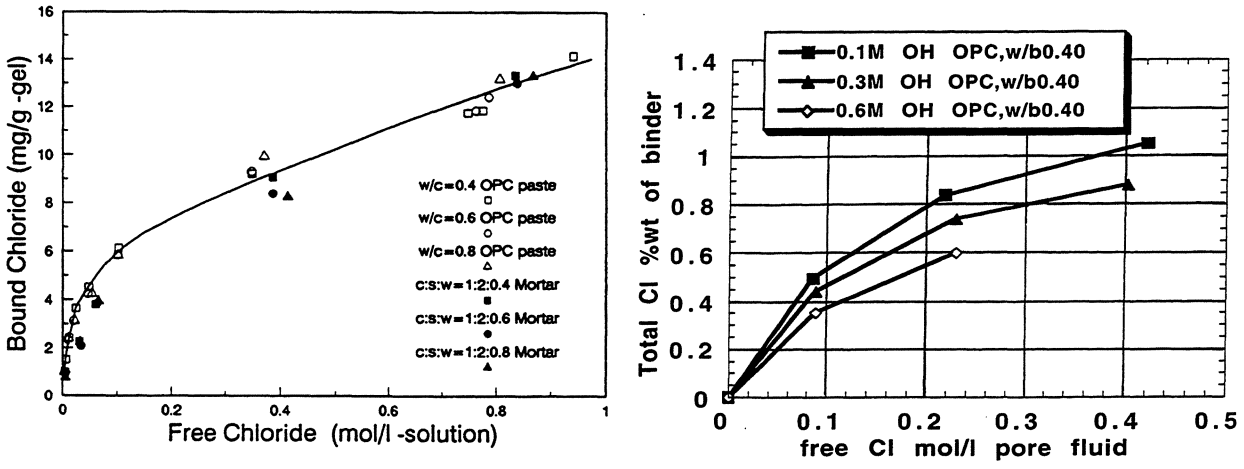


A B

Figure 7.1. A) Chloride adsorption isotherms of OPC pastes and mortars (per unit weight of CSH gel) /28/. B) Influence of the hydroxide ion concentration on the chloride adsorption /29/. w/b = water-cement ratio.

Sandberg and Larsson used a similar approach to study the effect of hydroxide ion concentration on the chloride binding in cement paste discs exposed for 6 months in simulated pore solutions reflecting the composition of the pore solution in concrete, see Figure 7.1 (B). The total acid soluble chloride content was analysed according to AASHTO T 260-A, as

described in Chapter 6.3.4, and the available pore volume was analysed as the dry porosity at 11 % RH. The free chloride- and hydroxide ion concentrations in the cement paste were analysed in extracted pore solution by means of the pore solution expression method /30/ and also in the surrounding solution at the end of the exposure. It was found that the difference in free chloride- and hydroxide ion concentrations measured in the surrounding simulated pore solution and in the extracted pore solution was less than 5%, indicating that equilibrium had actually been reached.

## 7.3 Literature data on laboratory studies of the combined transport of chloride and hydroxide ions in cement paste

Laboratory studies of the transport of chloride and hydroxide ions in cement paste immersed in a saline solution have indicated that the transport rates for chloride (ingress) and hydroxide (leaching) are about the same /31/, see Figure 7.2. The corresponding diffusivities for chloride and hydroxide ions was calculated to 15 E-12 $m^2/s$ and 19 E-12 $m^2/s$, respectively, by fitting the measured profiles to a solution to Fick's second law of diffusion assuming a constant diffusion coefficient.

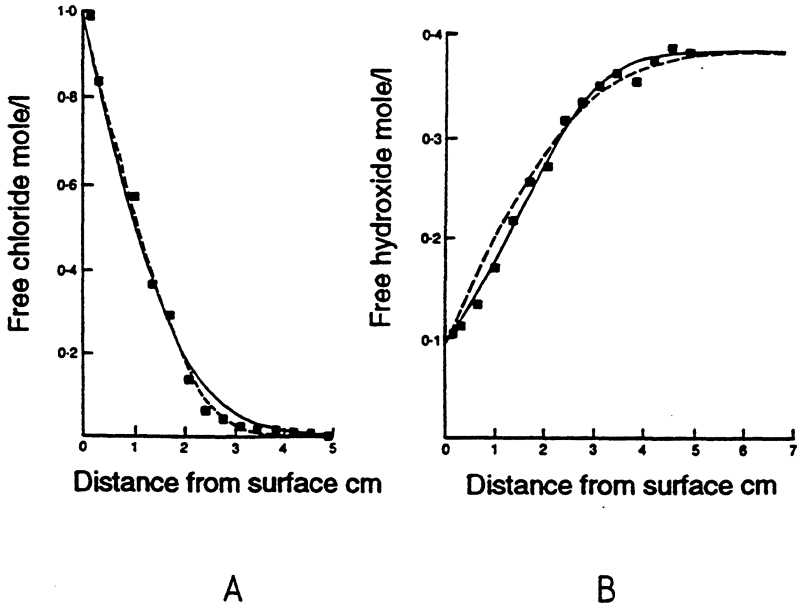


Figure 7.2 Concentration profiles of A) chloride ion, B) hydroxide ion, in expressed pore solution from a Portland cement paste, w/c 0.50, immersed for 100 days in a 1.0 M NaCl solution saturated with calcium hydroxide /31/.

## 7.4 The relationship between free and bound chlorides in field exposed concrete

The relationship between free and bound chlorides shown in Figure 7.1 is derived from equilibrium studies of thin cement paste or mortar specimens in saline solutions. Field exposed concrete on the other hand is not at equilibrium. In submerged concrete the chloride concentration gradient is accompanied by a hydroxide concentration gradient as indicated in

Figure 7.2. It can therefore be anticipated that the effect of hydroxide ion concentration on the chloride binding, Figure 7.1 (B), and the effect of the hydroxide gradient, Figure 7.2 (B), would increase the amount of bound chlorides in the surface of submerged field exposed concrete. As a consequence the relationship between free and bound chlorides would become more linear in field exposed concrete with a hydroxide gradient, as compared to the relationships shown in Figure 7.1. This was also confirmed as shown in Figure 7.4.

## 7.5 Field exposure tests

Concrete slabs, height 100 cm, width 70 cm, thickness 10 cm, were cast according to Tables 7.1 – 7.2 and moist cured for 10 days prior to marine exposure at the Träslövsläge Marine Field Station. The bottom half of each slab was submerged into the sea, Figures 3.3-3.4.

Concrete with high w/c ratios was studied for the following reasons:

1) The pore solution expression method is relatively easy to perform on concrete with w/c ratio > 0.45. The amount of expressible pore solution is high which improves the accuracy of the method.

2) The chloride penetration, the hydroxide leaching and the cement hydration proceeds faster the higher the w/c ratio. A shorter field exposure time for concrete with a high w/c ratio may therefore simulate the situation in concrete with a low w/c ratio after a much longer field exposure time. However, it must then be assumed that the ratio between the chloride diffusion rate and the hydroxide counter diffusion rate remains approximately the same.

After 7, 14 and 24 months of field exposure, cores with diameter 100 mm were drilled from the submerged- and the splash zone parts of the slabs. Immediately after drilling, the cores were split parallel to the exposed surface into 10-15 mm thick discs. Each disc was immediately sealed into an airtight plastic bag prior to the transport to the laboratory. At the laboratory the outermost 10 mm close to the sawn surface of each disc was removed. The remaining part of each disc was analysed for total acid soluble chloride content by weight of binder, and for the concentration of free chloride and hydroxide ions in expressed pore solution. The total acid soluble chloride content and the binder content was analysed as described in /23,24/ while the free chloride and hydroxide ions in expressed pore solution were analysed as described in /29,32/.

Table 7.1. Details of binders used

| | | Sulfate resisting Portland cement (SRPC) | Ordinary Portland Cement (OPC) | Silica fume (SF) |
|---|---|---|---|---|
| Fineness - % passing | 45 microns | 85.9 | 97.4 | 100 |
| | 20 microns | 51.3 | 64.0 | |
| | 10 microns | 33.1 | 41.7 | |
| | 5 microns | 19.5 | 26.0 | |
| | 1 micron | 3.8 | 5.4 | |
| Specific surface $m^2/kg$ | Blaine | 300 | 360 | |
| | BET | | | 23 000 |
| Specific gravity | | 3.15 | 3.11 | 2.22 |
| Compressive Strength | 1 day | 10.1 | 18.9 | |
| of standard 40 mm | 7 days | 35.6 | 45.2 | |
| mortar cubes, MPa | 28 days | 56.2 | 55.2 | |
| Chemical analysis % | CaO | 63.8 | 62.5 | 0.4 |
| | $SiO_2$ | 22.8 | 19.6 | 94.2* |
| | $Al_2O_3$ | 3.48 | 4.17 | 0.62 |
| | $Fe_2O_3$ | 4.74 | 2.17 | 0.95 |
| | MgO | 0.80 | 3.45 | 0.65 |
| | $SO_3$ | 1.88 | 3.29 | 0.33 |
| | $K_2O$ | 0.55 | 1.29 | 0.5 |
| | $Na_2O$ | 0.06 | 0.26 | 0.2 |
| | Loss of ignition | 0.55 | 2.65 | 1.79 |
| Bogue potential compounds -% | $C_3S$ | 51.5 | 61.4 | |
| | $C_2S$ | 25.5 | 9.9 | |
| | $C_3A$ | 1.3 | 7.6 | |
| | $C_4AF$ | 14.3 | 6.6 | |

*amorphous silica content

Table 7.2. Concrete mix designs

| | | SRPC w/c 0.45 | SRPC w/c 0.50 | OPC w/c 0.50 | SRPC 5% SF w/c 0.50 | SRPC w/c 0.75 | SRPC 5% SF w/c 0.75 |
|---|---|---|---|---|---|---|---|
| **Materials** dry $kg/m^3$ | Cement | 400 | 370 | 390 | 351 | 240 | 233 |
| | Silica fume | - | - | - | 19 | - | 12 |
| | Sand 0-8 mm | 850 | 876 | 853 | 840 | 1013 | 966 |
| | Gravel 8-16 mm | 788 | 808 | 787 | 840 | 796 | 823 |
| | Air content (%) | 6 | 6 | 6 | 6 | 6 | 6 |
| | f'c 28d (MPa) | 47 | 41 | 43 | 45 | 21 | 21 |

## 7.6 Results

A typical set of concentration profiles of hydroxide and chloride ions measured in expressed concrete pore solution is shown in Figure 7.3, w/c ratio 0.50, 14 months exposure. The relationship between measured total chloride content by weight of binder and the measured concentration of chloride ions in expressed pore solution is shown for all discs analysed in Figure 7.4.

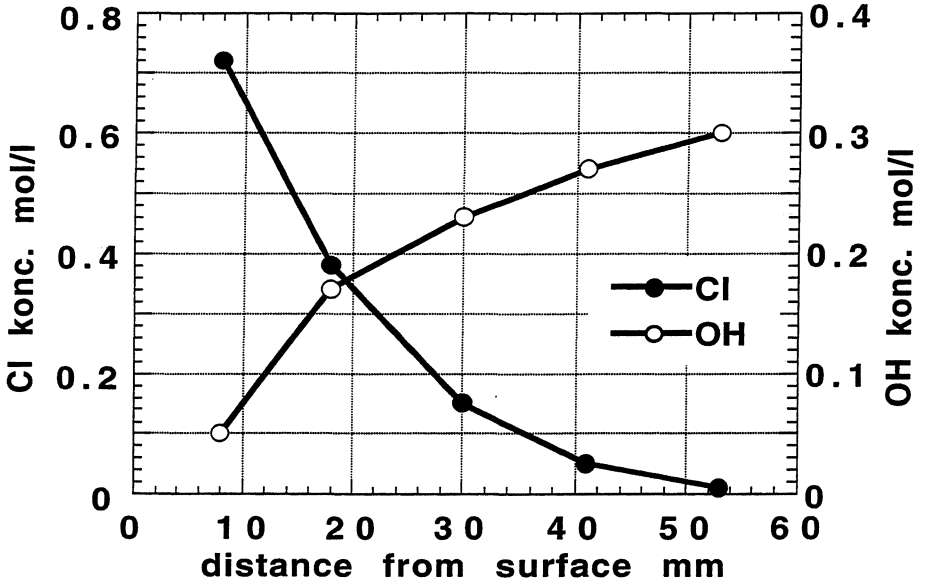


Figure 7.3. Concentration profiles of hydroxide and chloride ions measured in expressed concrete pore solution, concrete w/c 0.50, 14 months exposure.

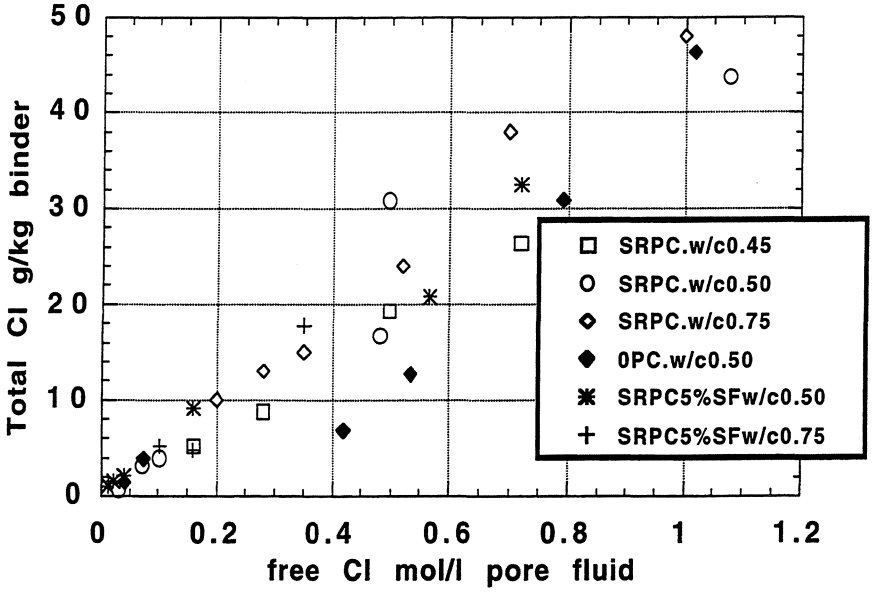


Figure 7.4 The relationship between free and total chlorides in expressed pore solution from concrete exposed submerged in seawater or in the splash zone.

## 7.7 Discussion

### *7.7.1 General*

The relationship between free and total chlorides measured in field exposed concrete was found to be more linear as compared to the corresponding relationship measured in equilibrium experiments without gradients of free chloride and hydroxide ions in the sample. The increased chloride binding at lower free hydroxide concentrations found in laboratory equilibrium experiments seems to, at least partly, explain the more linear relationship found in field exposed concrete with concentration gradients of free chloride and hydroxide in the concrete pore solution.

The results from this field study suggest that the non-linear chloride binding relationship observed in laboratory equilibrium tests is not relevant for submerged concrete with diffusion gradients of chloride and hydroxide. It is suggested that most, if not all, chloride penetration in concrete prior to corrosion initiation in ordinary steel reinforcement takes place in concrete with a hydroxide concentration gradient as indicated in Figures 7.2 and 7.3.

The transport rate of hydroxide ions appears very similar to the transport rate of chloride ions in concrete. However, the source of chloride ions in submerged concrete is unlimited while the amount of alkali hydroxide depends on the cement type and -content, and is limited as compared to the source of chloride ions. The chloride ion diffusion rate in a thick concrete member would be affected by a continuous counter diffusion of hydroxide ions from the alkali hydroxide in the interior concrete for a relatively long time. But in a thin concrete member the reservoir of alkali hydroxides would be more quickly removed. As the hydroxide ion concentration drops, the chloride binding and the solubility of calcium hydroxide increases. It is possible that the net effect would be a chloride penetration rate which is dependent on the thickness of the concrete member.

### *7.7.2 Errors in the experimental method*

The pore solution expression method is known to be more inaccurate when used on concrete as compared to cement paste. The scatter of the results in Figure 7.4 however indicates that the error is small enough to validate the use of the pore solution expression method on concrete. The data points at higher chloride concentrations correspond to measurements in concrete close to the exposed surface, e.g. concrete with low hydroxide ion concentrations in the expressed pore solution.

It would be anticipated that a difference in the exposure temperature and the laboratory temperature at which the pore solution expression is carried out would affect the chloride binding. The concrete temperature when sampled at the field station was approximately + 15 °C, + 7 °C and + 4 °C after 7, 14 and 24 months of exposure respectively. The concrete temperature was measured by thermal electrodes at relevant positions on parallel concrete slabs. The disc temperature was approximately + 20 °C when subjected to the pore solution expression in the laboratory. The difference in chloride binding at such small temperature differences is probably not very large, as shown by Tritthart /33/ for laboratory exposed cement paste. Furthermore, any temperature "error" should have the same relative size at low

and high chloride concentrations, and therefore the degree of linearity in Figure 7.3 should not change.

## 7.8 Conclusions with respect to service life prediction

The almost linear relationship found between free and total chlorides in field exposed concrete implies that solutions to Fick´s second law of diffusion based on linear chloride binding and a constant diffusivity can be used for simple prediction of chloride ingress in concrete. However, as the diffusivity is not a constant but varies with time and moisture content, the prediction has to be carried out either in a series of short time spans with a constant diffusivity in each time span, or with an average (constant) mean effective (representative) diffusivity over the entire exposure time considered.

# 8. EXPERIMENTAL WORK ON CHLORIDE TRANSPORT RATES IN CONCRETE

## 8.1 General

Traditionally, chloride penetration into concrete has been modelled by the use of Fick's second law of diffusion, assuming constant diffusivity and linear chloride binding /34/. On the other hand combined laboratory and field exposure tests of concrete have indicated that the traditional use of Fick's second law of diffusion was not applicable for long term chloride transport into concrete /3,9-11,13/. When fitting a solution to Fick's second law of diffusion to measured profiles of total chloride from field exposed concrete, the calculated "effective chloride diffusivity" was found to vary with the exposure time and -conditions. Besides, if binding is non-linear then a calculation of an effective chloride diffusivity is not correct since the profile will not follow the solutions to Fick's law. Thus the value of the effective chloride diffusivity depends on which point in the profile is used for the calculation, unless a mean value is calculated by considering the best fit of several data points in a measured profile.

Nevertheless solutions to Fick's second law of diffusion are still widely used as a tool to evaluate and predict chloride transport rate in concrete /37/. The "effective chloride diffusivity" calculated from profiles of total chloride in concrete represents an indication of the average chloride transport rate in the concrete at the exposure time and –condition considered.

## 8.2 Experimental work on chloride penetration into a concrete bridge column

The effect of elevation on the chloride ingress was studied in the Swedish bridge "Nya Ölandsbron" which is a repair of the existing bridge "Ölandsbron", SRPC concrete, w/c 0.38, after 4 years of exposure (paper VIII). The concrete was exposed to sea water after a pre-curing of a minimum of 14 days. Profiles of total chloride were measured as described in Chapter 6.3.4. A summary of the results regarding chloride penetration is given in Figure 8.1.

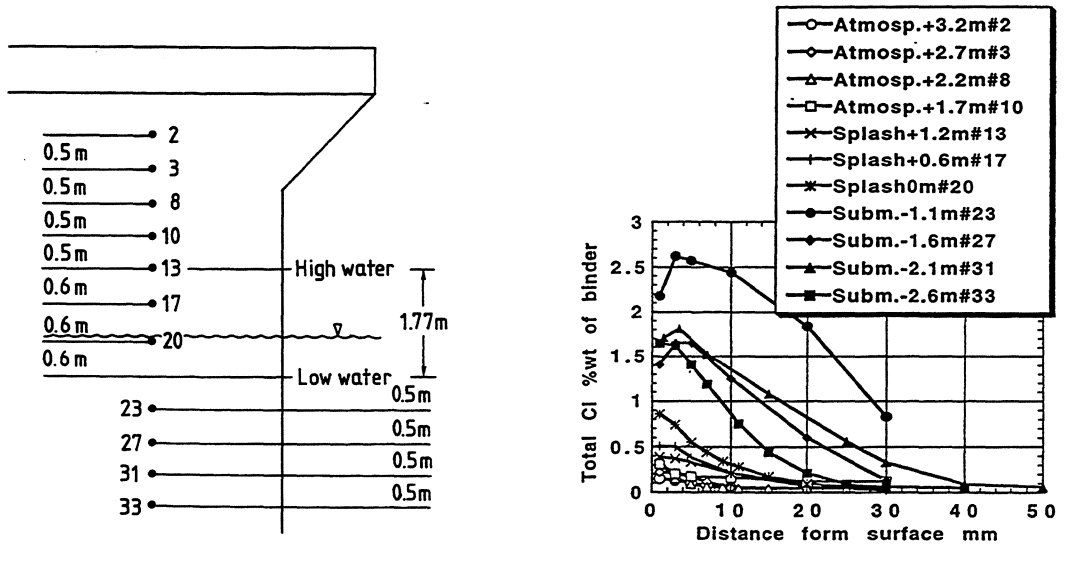


Figure 8.1. Profiles of total chloride measured at various height from the mean water level after 4 years of exposure.

It was concluded that the micro climate, here the amount of sea water splashing, has a large influence on the amount and rate of chloride penetration.

## 8.3 Experimental work on chloride penetration in field exposed concrete slabs

### *8.3.1 General*

Reinforced concrete slabs, height 100 cm, width 70 cm, thickness 10 cm, were cast according to Table 8.1 and moist cured for 10 days prior to marine exposure at the Träslövsläge Marine Field Station in 1992, Figures 3.3-3.4. The concrete slabs were subject to recurrent studies of chloride ingress in uncracked marine concrete, as described more in detail in (papers V-VIII).

Sulfate resisting portland cement, silica fume and fly ash were used according to Table 6.1. Ordinary portland cement was used according to Table 7.1. A more detailed description of the experimental procedure was given in (paper V).

Table 8.1 Details of concrete mixes

| **Mix No.** | **ID** | **w/c ratio *** | **SRPC or OPC kg/m³** | **Silica fume ** kg/m³** | **Fly ash kg/m³** | **Aggr. 0-8 mm kg/m³** | **Aggr. 8-16 mm kg/m³** | **fc 28d *** MPa** | **Air cont. vol %** |
|---|---|---|---|---|---|---|---|---|---|
| **1** | OPC 0.40 | 0.40 | - | - | - | 871 | 804 | 54 | 6 |
| **2** | SRPC 0.50 | 0.50 | 370 | - | - | 876 | 808 | 41 | 6 |
| **3** | SRPC 0.40 | 0.40 | 420 | - | - | 873 | 806 | 58 | 6 |
| **4** | SRPC 0.30 | 0.30 | 492 | - | - | 791 | 892 | 96 | 4 |
| **5** | SRPC 5%SF 0.50 | 0.50 | 351 | 19 dry | - | 840 | 840 | 45 | 6 |
| **6** | SRPC 5%SF 0.40 | 0.40 | 399 | 21 dry | - | 835 | 835 | 61 | 6 |
| **7** | SRPC 5%SF 0.40 | 0.40 | 399 | 21 slu | - | 840 | 840 | 62 | 6 |
| **8** | SRPC 5%SF 0.30 | 0.30 | 475 | 25 slu | - | 836 | 942 | 112 | 1 |
| **9** | SRPC 5%SF 0.25 | 0.25 | 525 | 26 slu | - | 806 | 946 | 125 | 1 |
| **10** | SRPC 10%SF 0.30 | 0.30 | 450 | 50 slu | - | 820 | 963 | 117 | 1 |
| **11** | SRPC 5%SF 10%FA 0.35 | 0.35 | 382 | 23 slu | 45 | 781 | 917 | 84 | 6 |
| **12** | SRPC 5%SF 17%FA 0.40 | 0.40 | 345 | 21 slu | 75 | 770 | 905 | 69 | 6 |
| **13** | SRPC 20%FA 0.30 | 0.30 | 493 | - | 123 | 680 | 865 | 98 | 3 |

*w/c ratio defined as w/(C+SF+0.3FA). w = water, C = cement (SRPC = sulfate resisting portland cement, OPC = ordinary portland cement), SF = silica fume, FA = fly ash.
** Silica fume added "dry" = compacted, or "slu" = as a 50 % slurry. Figure denotes amount of solid.
*** fc 28d = compressive cube strength (MPa) after 28 days of standard curing.

Profiles of total chloride were analysed after 7 or 12 months, 2 years, and 5 years exposure by the method described in Chapter 6.3.4. The analyses were carried out by Chalmers, LTH, AEC, CBI and SP, see Table 1.1.

*8.3.2Evaluation of profiles of total chloride*

Acid soluble chloride profiles, expressed as % total Cl by weight of binder, were evaluated by fitting the measured chloride data to a theoretical profile calculated from a solution to Fick's second law of diffusion /36/, as shown in Figure 8.2. Linear binding was assumed. The fitting procedure was started at the maximum total chloride concentration which was sometimes several datapoints below the concrete surface. The theoretical total chloride profile was defined by the chloride transport coefficient, "effective chloride diffusivity", and the calculated or apparent surface total chloride concentration, "Cs, calc.". As seen in Figure 8.2, a drop in the total chloride concentration close to the exposed surface was found in nearly all concrete samples. The area affected by the surface drop in the total chloride concentration was bigger for concrete exposed in the splash zone as compared to submerged concrete. Parallel studies of profiles of total chloride and calcium carbonate in (paper 8) revealed that the drop in the total chloride concentration was mainly affected by the carbonation depth, as carbonation reduces the chloride binding capacity /4/.

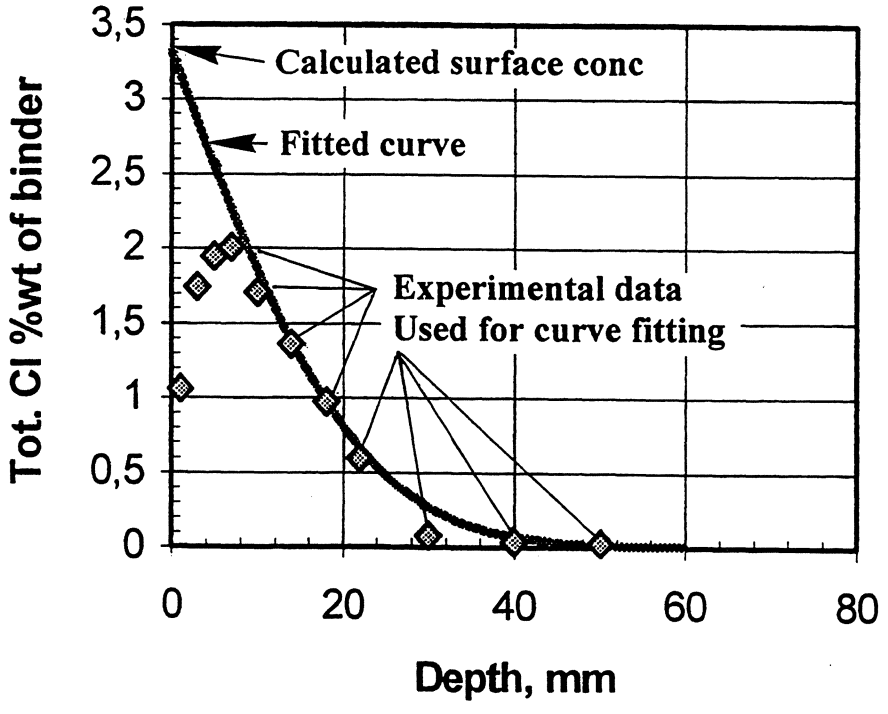


Figure 8.2. Curve fitting procedure for estimation of the "effective chloride diffusivity".

*8.3.3 Results*

8.3.3.1 General

The calculated effective chloride diffusivity, DeCl (xE-12m$^2$/s), and the calculated apparent surface chloride concentration, Cscalc. (total Cl % by weight of binder), from fitting profiles of total chloride to a solution to Fick's second law of diffusion, assuming constant diffusivity and linear chloride binding, are presented for submerged concrete in Table 8.2 and for concrete exposed in the splash zone in Table 8.3.

Table 8.2. Curve fitting results at various exposure times for concrete exposed submerged at the Träslövsläge Marine Field Station

| **Concrete exposed in the submerged zone** | | | **DeCl** xE-12m$^2$/s and **Cscalc.** Total Cl % by weight of binder | | | | | | | |
|---|---|---|---|---|---|---|---|---|---|---|
| **Mix** | **Exposure time** | | **0.6-0.8 years** | | **1.0-1.3 years** | | **2.0-2.3 years** | | **5.1-5.4 years** | |
| **No.** | **ID** | **w/c** | **DeCl** | Cscalc | **DeCl** | Cscalc | **DeCl** | Cscalc | **DeCl** | Cscalc |
| **1** | OPC 0.40 | 0.40 | - | - | **2.1** | 2.7 | **2.4** | 3.2 | **1.9** | 4.2 |
| **2** | SRPC 0.50 | 0.50 | **4.7** | 2.5 | - | - | **5.1** | 2.9 | **2.3** | 4.5 |
| **3** | SRPC 0.40 | 0.40 | **4.5** | 2.8 | **3.6** | 3.1 | **2.8** | 3.1 | **1.4** | 4.4 |
| **4** | SRPC 0.30 | 0.30 | - | - | **1.8** | 2.7 | **2.4** | 2.6 | **1.5** | 3.8 |
| **5** | SRPC 5%SFdry 0.50 | 0.50 | **4.8** | 2.4 | - | - | **2.6** | 3.9 | **1.2** | 4.2 |
| **6** | SRPC 5%SFdry 0.40 | 0.40 | **3.4** | 3.2 | - | - | **1.4** | 3.4 | **1.3** | 4.9 |
| **7** | SRPC 5%SF 0.40 | 0.40 | **2.0** | 3.5 | - | - | **0.8** | 4.3 | **0.8** | 4.9 |
| **8** | SRPC 5%SF 0.30 | 0.30 | - | - | **0.9** | 2.7 | **0.7** | 3.9 | **0.5** | 4.7 |
| **9** | SRPC 5%SF 0.25 | 0.25 | - | - | **0.4** | 1.6 | **0.5** | 2.9 | **0.2** | 4.4 |
| **10** | SRPC 10%SF 0.30 | 0.30 | - | - | **0.6** | 1.6 | **0.5** | 2.5 | **0.2** | 4.9 |
| **11** | SRPC 5%SF 10%FA 0.35 | 0.35 | **1.0** | 1.3 | - | - | **0.9** | 3.5 | **0.8** | 5.2 |
| **12** | SRPC 5%SF 17%FA 0.40 | 0.40 | **1.6** | 2.3 | - | - | **0.8** | 3.4 | **0.8** | 7.4 |
| **13** | SRPC 20%FA 0.30 | 0.30 | - | - | **1.4** | 2.8 | **1.1** | 2.9 | **0.5** | 5.3 |

Table 8.3. Curve fitting results at various exposure times for concrete exposed in the splash zone at the Träslövsläge Marine Field Station

| **Concrete exposed in the splash zone** | | | **DeCl** xE-12m$^2$/s and **Cscalc.** Total Cl % by weight of binder | | | | | | | |
|---|---|---|---|---|---|---|---|---|---|---|
| **Mix** | **Exposure time** | | **0.6-0.8 years** | | **1.0-1.3 years** | | **2.0-2.3 years** | | **5.1-5.4 years** | |
| **No.** | **ID** | **w/c** | **DeCl** | Cscalc | **DeCl** | Cscalc | **DeCl** | Cscalc | **DeCl** | Cscalc |
| **1** | OPC 0.40 | 0.40 | - | - | **0.6** | 2.7 | **1.6** | 3.1 | **0.9** | 3.3 |
| **2** | SRPC 0.50 | 0.50 | **4.8** | 3.5 | - | - | **2.6** | 2.7 | **1.9** | 3.8 |
| **3** | SRPC 0.40 | 0.40 | **2.3** | 1.3 | - | - | **2.6** | 3.1 | **1.4** | 1.9 |
| **4** | SRPC 0.30 | 0.30 | - | - | **0.5** | 1.3 | **1.4** | 2.5 | **1.2** | 3.8 |
| **5** | SRPC 5%SFdry 0.50 | 0.50 | **2.0** | 1.4 | - | - | **2.3** | 3.3 | **1.5** | 5.7 |
| **6** | SRPC 5%SFdry 0.40 | 0.40 | **1.4** | 1.5 | - | - | **0.7** | 2.9 | **0.4** | 2.4 |
| **7** | SRPC 5%SF 0.40 | 0.40 | **1.2** | 1.9 | - | - | **0.8** | 2.0 | **0.5** | 2.6 |
| **8** | SRPC 5%SF 0.30 | 0.30 | - | - | **0.4** | 1.6 | **0.2** | 1.6 | **0.2** | 1.3 |
| **9** | SRPC 5%SF 0.25 | 0.25 | - | - | **0.3** | 1.3 | **0.2** | 2.0 | **0.2** | 4.8 |
| **10** | SRPC 10%SF 0.30 | 0.30 | - | - | **0.4** | 1.2 | **0.4** | 3.3 | **0.2** | 2.8 |
| **11** | SRPC 5%SF 10%FA 0.35 | 0.35 | **0.9** | 1.0 | - | - | **0.8** | 3.2 | **0.3** | 1.6 |
| **12** | SRPC 5%SF 17%FA 0.40 | 0.40 | **0.5** | 1.4 | - | - | **0.4** | 2.5 | **0.3** | 2.9 |
| **13** | SRPC 20%FA 0.30 | 0.30 | - | - | **0.7** | 2.5 | **0.5** | 2.3 | **0.4** | 3.1 |

Most of the results presented in the following relates to the chloride penetration in concrete exposed in the submerged- and the splash zone. The splash zone is the most critical zone in practice, but the exposure condition is more well defined in the submerged zone. The chloride

penetration rate may be higher in submerged concrete, but then the chloride threshold is also higher and it is relatively easy to prevent corrosion by the use of inexpensive protection systems (paper XI).

Small differences in the sampling height from the water level may have large impact on the salt- and moisture load, and thus on the chloride penetration profile in the splash zone. In addition, concrete itself is an inhomogeneous material with local variations in the porosity and therefore local variations in the chloride diffusivity. As a consequence the spread in measured profiles of total chloride may be relatively high, and it should be higher in the splash zone compared to the submerged zone as the exposure conditions vary less in the submerged zone.

An indication on the spread which can be expected in the submerged- and in the splash zone was given in Figure 8.3, which shows more chloride penetration in the splash zone for a concrete with w/c 0.30 than with w/c 0.40. One should therefore be careful no to use individual profiles for service life prediction, but rather extract information from trends observed from several profiles. The reason for the unexpectedly high chloride penetration in the concrete with w/c 0.30 is not clear, as no examination of the micro structure was carried out. It is possible, however, that the existence of cracks has accelerated the chloride penetration in the concrete with w/c 0.30. High performance concrete, w/c $\leq$ 0.40, is considered as being more sensitive to the formation of cracks as compared to normal concrete /42/. A similar high but unexpected chloride penetration was found for concrete with w/c 0.25 exposed in the splash zone, Figure 8.4 (B). It was found in (paper VIII) that cracks > 0.1 mm wide and open to the surface may have a strong influence on the measured profile of total chloride, see Chapter 8.4.

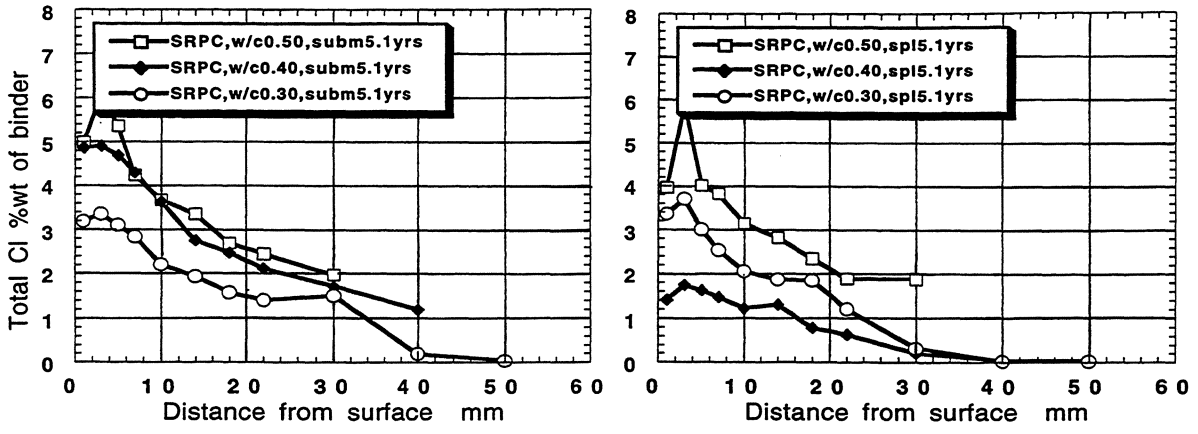


Figure 8.3. Profiles of total chloride in SRPC concrete exposed for 5 years, A) submerged, and B) in the splash zone.

8.3.3.2 The effect of w/c ratio

The effect of w/c ratio on the chloride penetration profiles in concrete exposed submerged and in the splash zone for 5 years is shown for plain SRPC concrete in Figure 8.3 and for SRPC

concrete with 5 % silica fume in the binder in Figure 8.4. As expected, the effect of w/c ratio on chloride penetration in concrete is significant.

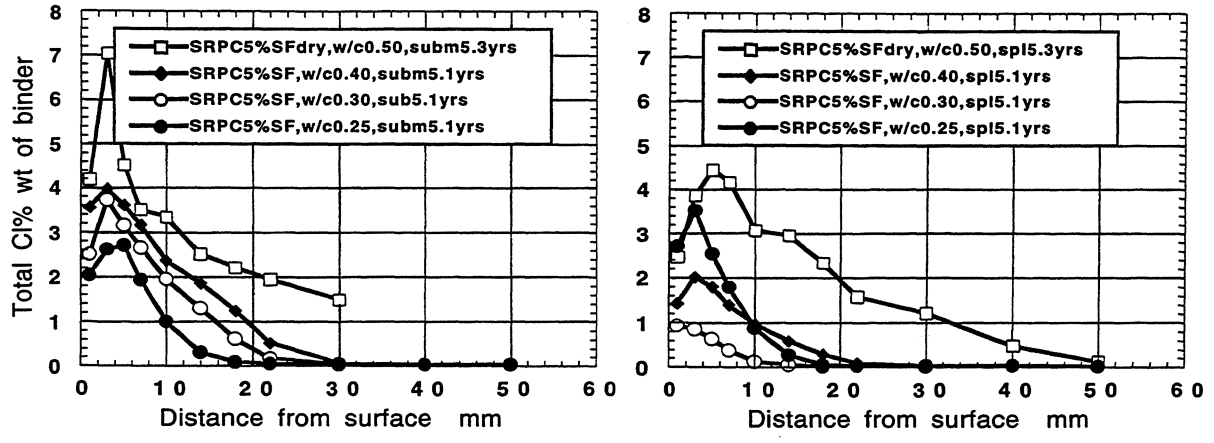


A B

Figure 8.4. Profiles of total chloride in SRPC concrete with 5 % silica fume in the binder fraction, exposed for 5 years submerged (A) and in the splash zone (B).

8.3.3.3 The effect of pozzolan in the binder

The effect silica fume and/or fly ash in the binder on the chloride penetration profiles in concrete exposed submerged and in the splash zone for 5 years is shown for w/c 0.40 in Figure 8.5 and for w/c 0.30 in Figure 8.6. The relative efficiency of silica fume seems far higher than that of fly ash.

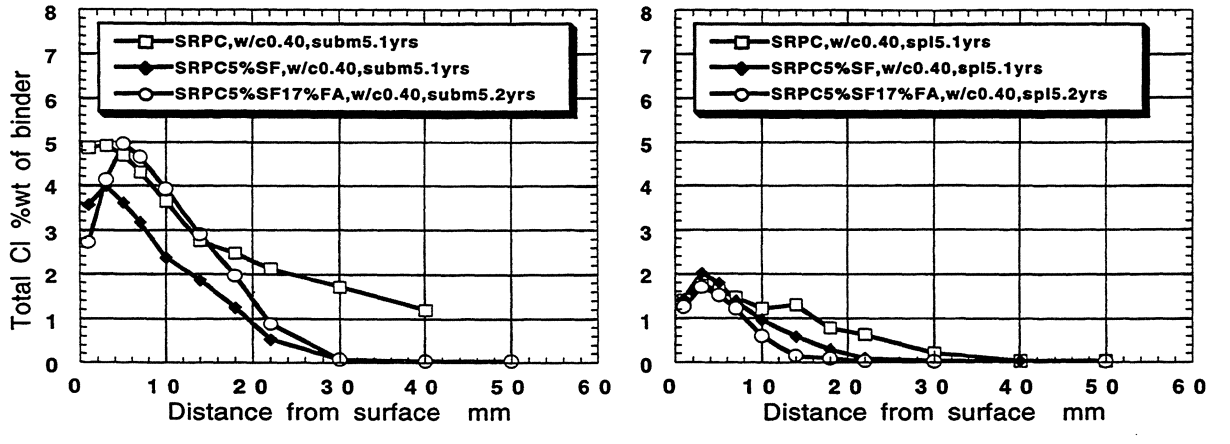


A B

Figure 8.5. Profiles of total chloride in plain concrete and in concrete with silica fume and/or fly ash in the binder fraction, w/c ratio 0.40, exposed for 5 years submerged (A) and in the splash zone (B).

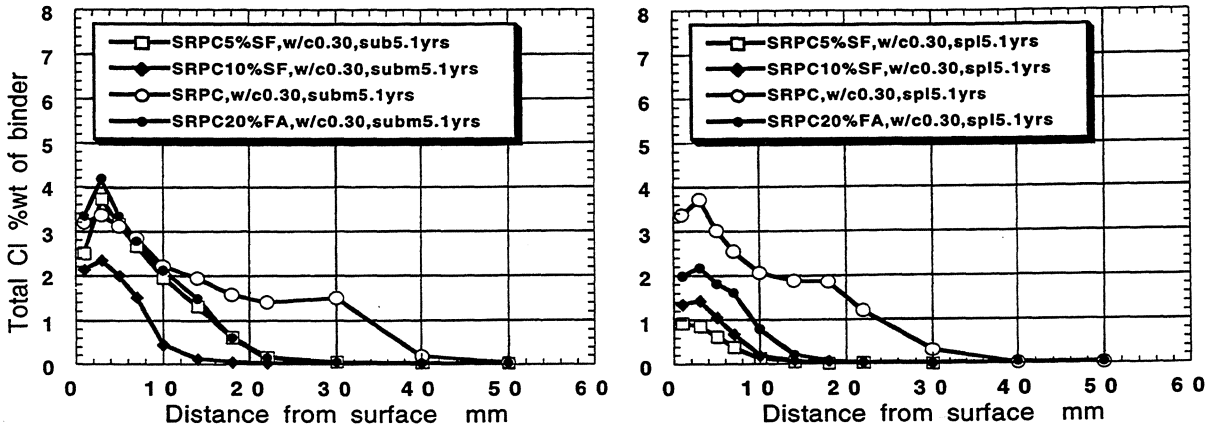


A B

Figure 8.6. Profiles of total chloride in plain concrete and in concrete with silica fume and/or fly ash in the binder fraction, w/c ratio 0.30, exposed for 5 years submerged (A) and in the splash zone (B).

8.3.3.4 The effect of the type of silica fume in the binder

The effect the type of silica fume in the binder on the chloride penetration profiles in concrete exposed submerged and in the splash zone for 5 years was shown for w/c 0.40 in Figure 8.7. The relative efficiency of silica fume when added as a 50 % slurry seems to be higher than when the same amount of solid silica fume is added as a compacted powder.

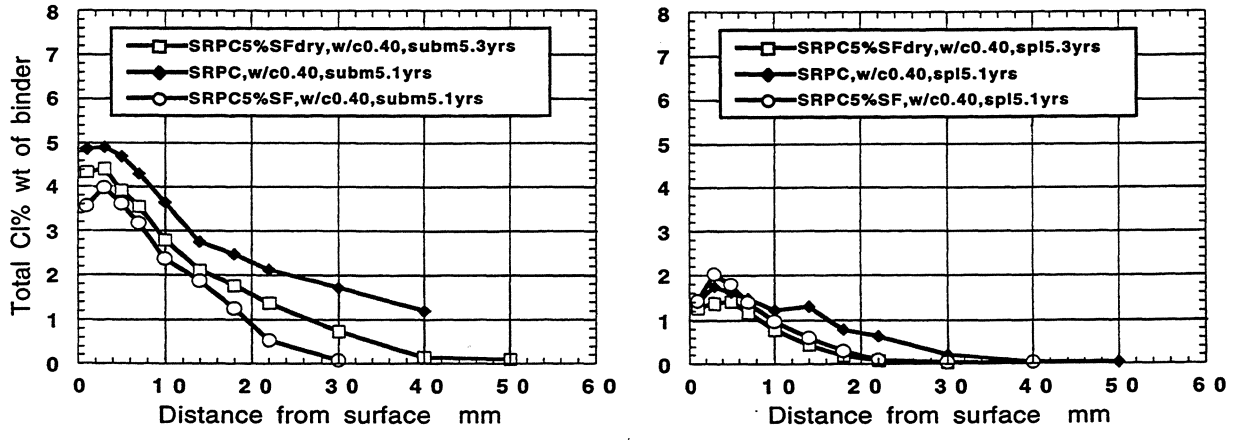


A B

Figure 8.7. Profiles of total chloride in plain concrete and in concrete with silica fume added as a 50 % slurry or as a compacted powder, w/c ratio 0.40, exposed for 5 years submerged (A) and in the splash zone (B).

8.3.3.5 The combined effect of w/c ratio and of pozzolan in the binder

The combined effect of w/c ratio and of silica fume in the binder on the calculated effective chloride diffusivity is shown in Figure 8.8, for concrete exposed in the splash zone and for concrete tested in a standard laboratory immersion test according to NT Build 443 /23/. In general, the effective chloride diffusivity was found to decrease with a lower w/c ratio, and to be lower in the field exposure tests as compared to the laboratory exposure tests. However, the effective chloride diffusivity calculated for SRPC concrete with w/c ratio 0.30 was unexpectedly high, possibly as a consequence of cracks as discussed in Chapter 8.3.3.1.

The results in Figure 8.8 indicate that for a w/c ratio of 0.40, which is the maximum w/c ratio recommended for marine concrete in several codes of practice, the effective chloride diffusivity can be reduced by a factor of 3-5 by using 5 % silica fume in the form of a well dispersed slurry in the binder fraction of the concrete. If on the other hand the w/c ratio is reduced from 0.40 to 0.30 besides the introduction of 5 % silica fume in the binder, it seems that the effective chloride diffusivity can be reduced by a factor of 8-10.

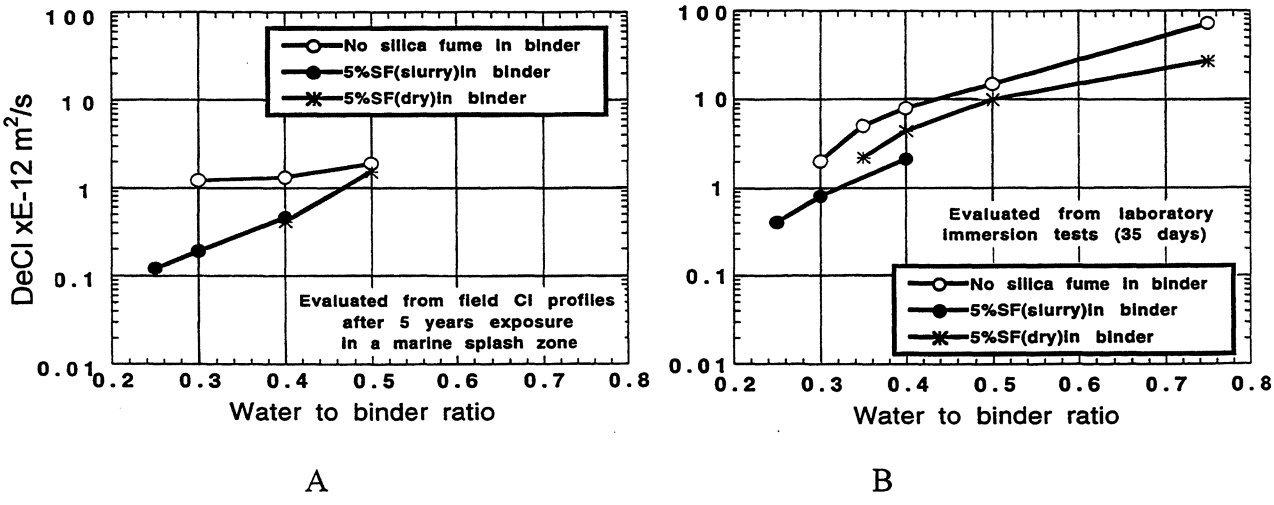


Figure 8.8. Calculated effective chloride diffusivity in plain concrete and in concrete with silica fume and/or fly ash in the binder fraction. A) Exposed in the splash zone for 5 years. B) Exposed in a standard laboratory immersion test in 16 % NaCl.

## 8.4 Analysis of sensitivity

The sensitivity analysis of profiles of total chloride made in Chapter 6.6.2 applies also here. The effect of a visible crack (0.1-2 mm wide) in the concrete cylinder analysed, on the total chloride profile was illustrated for cylinder # 23 as compared to the uncracked cylinders # 27, 31 and 33 in Figure 8.1.

Note that all cylinders # 23, 27, 31 and 33 were taken in the submerged zone, below the lowest water level registered. Thus the exposure condition was regarded as similar for these 4 concrete cylinder. The differences between the profiles of total chloride measured in the 3 uncracked cylinders # 27, 31 and 33 illustrate the effect of local differences in the concrete quality.

## 8.5 Conclusions from field exposure tests of chloride penetration in concrete

1. After 5 years of field exposure, most profiles of total chloride measured (with the exemption of the outermost millimetres) fits well to a theoretical profile calculated by Fick´s second law of diffusion assuming linear chloride binding and constant diffusivity, as illustrated in Figure 8.2.

2. The effective chloride diffusivity, calculated as described above, decreases over time in field exposed concrete, see Figures 3.2 and 9.1- 9.2.

3. The effective chloride diffusivity can be reduced by a factor of 3-5 by using 5 % silica fume in the form of a well dispersed slurry in the binder fraction of the concrete, as compared to a plain SRPC concrete of the same w/c ratio. If on the other hand the w/c ratio is reduced from 0.40 to 0.30 besides the introduction of 5 % silica fume in the binder, it seems that the effective chloride diffusivity can be reduced by a factor of 8-10. The service life would theoretically increase by the same factor provided that all other factors determining the service life are unchanged.

## 9. SIMPLE PREDICTIONS OF CHLORIDE INGRESS IN MARINE CONCRETE

Simple predictions of the profiles of total chloride are undertaken in 3 different ways for all profiles of total chloride measured in the splash- and in the submerged zone (paper V). Procedure C) is developed by the author and is compared with 2 commonly used procedures A) and B). The purpose of the comparisons is to get an idea of the spread in predicted chloride ingress and in the required cover, Chapter 10, which can be expected when different procedures are used to predict the chloride ingress in marine concrete structures. The procedures A) – C) are carried out according to the following alternative assumptions:

A) 100 years exposure time. The effective chloride diffusivity and apparent surface concentration calculated for the exposure period 0-5 years remain constant onwards. This assumption is considered unrealistic as shown in Figure 9.1, but nevertheless commonly used for service life prediction on the safe side /45/.

B) 100 years exposure time. The effective chloride diffusivity calculated for the exposure period 0-5 years is reduced to 50% of its value and then considered as representative for the exposure period 0-100 years. The reduction factor was chosen from extrapolations of the calculated effective chloride diffusivity as presented in Figures 9.1-9.2. The extrapolated general trend lines indicated a reduction of the effective chloride diffusivity in the range of 50-75 % from 5 to 100 years of exposure, Figures 9.1-9.2. A 50 % reduction of the effective chloride diffusivity was considered as conservative. The calculated apparent surface concentration was fixed as 10 % total chloride by weight of binder, as being the highest value extrapolated from the data in Figures 9.3-9.4 using the general trend lines indicated. This value is considered as an upper extreme and should be on the safe side. The highest measured total chloride concentrations the author is aware of are in the range of 7-8 % total chloride by weight of binder, in marine concrete exposed for 10-40 years /10,11,35/. 10 % total chloride by weight of binder was calculated as the highest chloride concentration measured in a mortar in Japan after 96 years marine field exposure /37/.

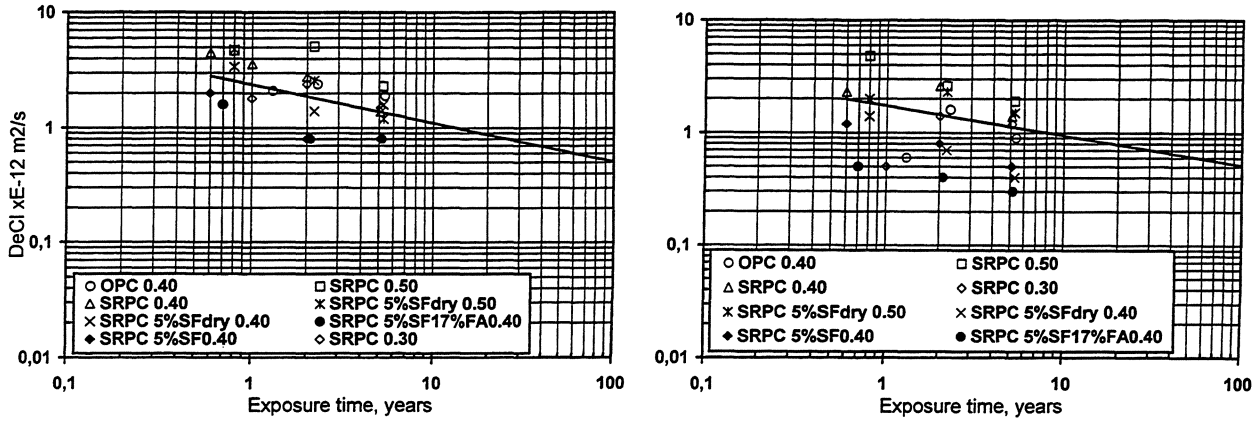


Figure 9.1. Calculated effective chloride diffusivity for concrete mixes with w/c ≥ 0.40 and for plain SRPC concrete with w/c 0.30, exposed submerged (A) and in the splash zone (B). Solid power trend lines extrapolated by regression analysis. The data can be compared with data calculated in a similar way from existing marine structures, Figure 52 in (paper XI).

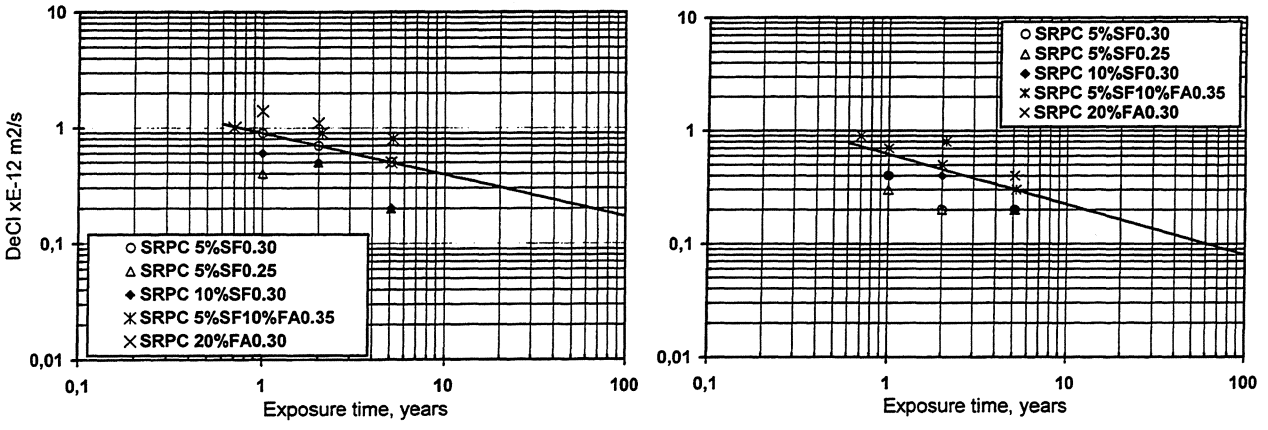


A B

Figure 9.2. Calculated effective chloride diffusivity for concrete mixes with pozzolan in the binder and w/c ≤0.35, exposed submerged (A) and in the splash zone (B). Solid power trend lines extrapolated by regression analysis.

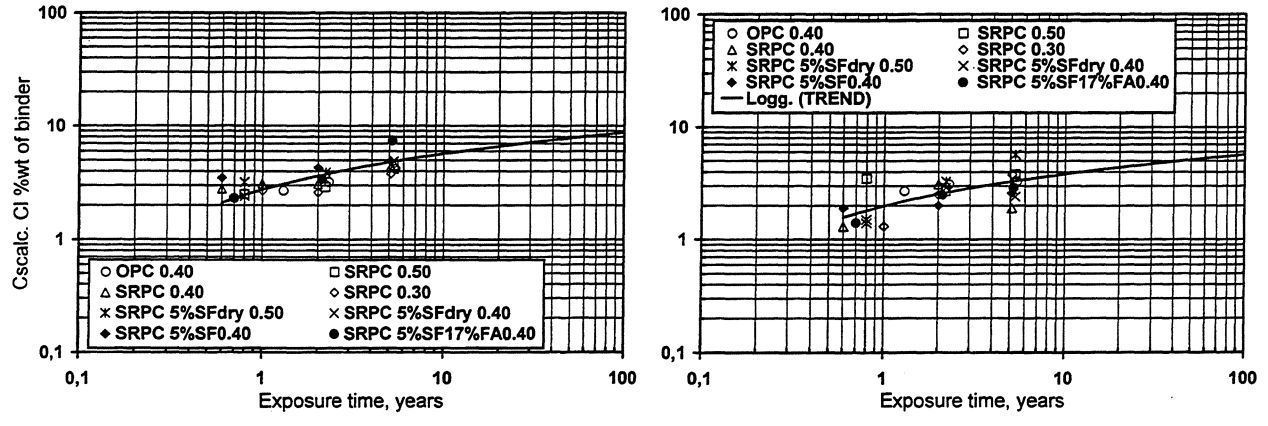


A B

Figure 9.3. Calculated apparent surface chloride concentration for concrete mixes with w/c ≥ 0.40 and for plain SRPC concrete with w/c 0.30, exposed submerged (A) and in the splash zone (B). Solid logarithmic trend lines extrapolated by regression analysis.

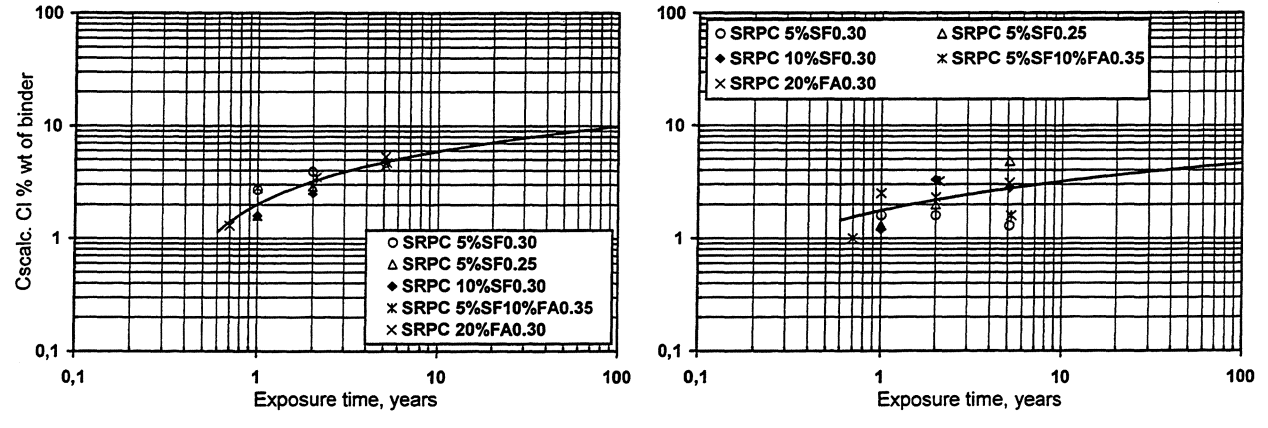


A B

Figure 9.4. Calculated apparent surface chloride concentration for concrete mixes with pozzolan in the binder and w/c ≤0.35, exposed submerged (A) and in the splash zone (B). Solid logarithmic trend lines extrapolated by regression analysis.

C) The concrete cover is divided into a "convection zone" and a "diffusion zone" as shown in Figure 9.5 /38/. The "convection zone" is strongly affected by leaching of hydroxide ions, penetration of carbonate and sulfate ions, and also by wetting and drying for concrete exposed above water. The "diffusion zone has a relatively constant moisture state and the chloride diffusion is mainly affected by the moisture state inside the concrete, e.g. self desiccation and the counter-diffusion of hydroxide ions. The border between the "convection zone" and the "diffusion zone" is defined as the depth of the maximum measured total chloride concentration. For the sake of simplicity, the depth of the maximum total chloride concentration was assumed to be controlled by the depth of carbonation. It can be calculated from data in /4/ that the depth of carbonation in a marine concrete not sheltered from rain, with w/c ratio $\leq 0.40$, is less than 7 mm after 100 years of exposure. Therefore it is assumed that the depth of the maximum total chloride concentration is unchanged from 5 years of exposure and onwards in the predictions.

The simulation is carried out in the "diffusion zone" only, thus with the calculated apparent surface concentration equal to the maximum measured total chloride concentration, labelled Cmax, and located at the depth of the maximum measured total chloride concentration after 5 years of exposure, Figure 9.5. The values on the effective chloride diffusivity and the maximum total chloride concentration (Cmax) are extrapolated from the corresponding data in Figures 9.1-9.2 and 9.6-9.7 respectively, using the slope of the general trend lines for the extrapolation of individual data series.

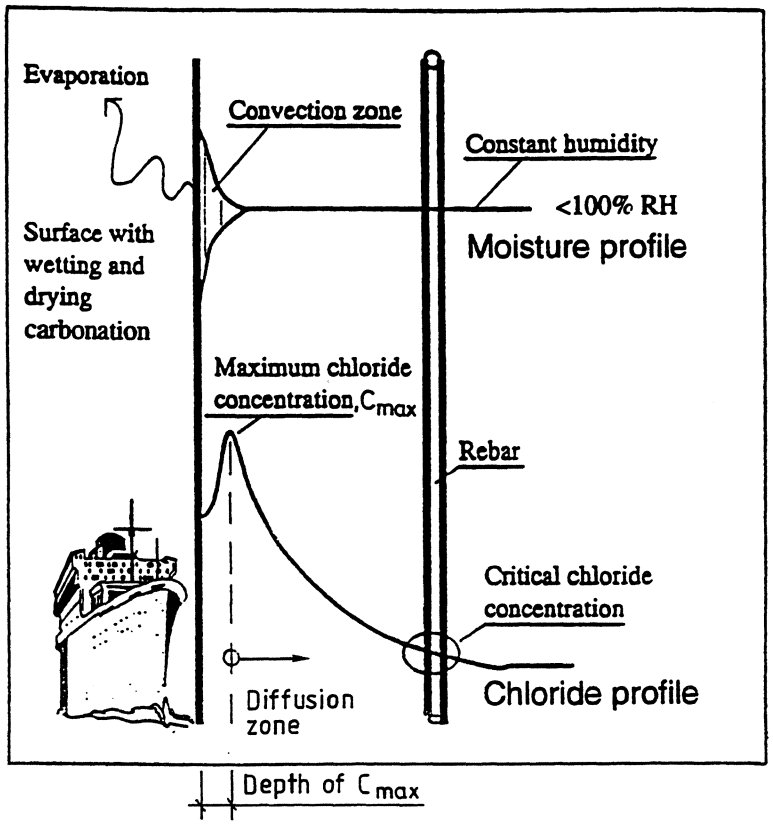


Figure 9.5 Illustration of the proposed "convection zone" and the "diffusion zone" in concrete.

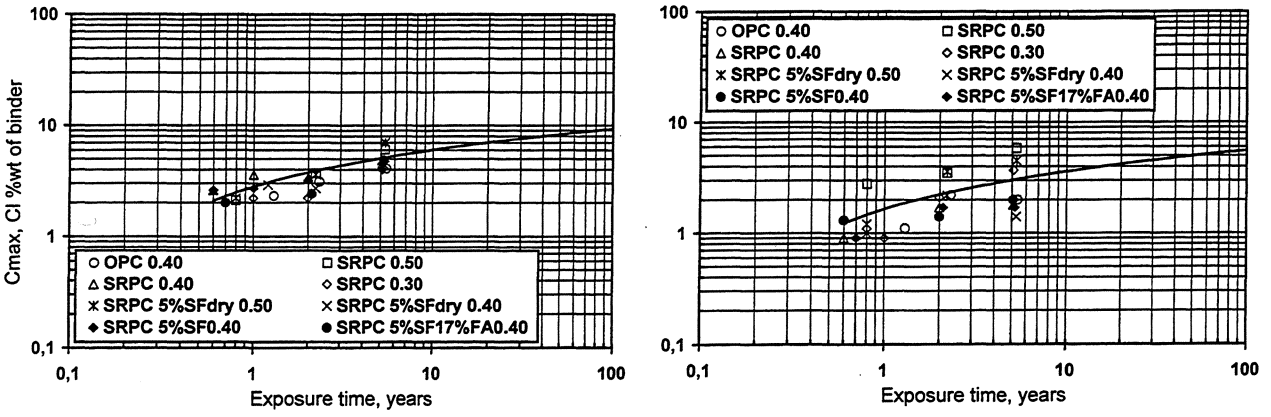


Figure 9.6. Maximum total chloride concentrations measured in concrete mixes with w/c ≥ 0.40 and for plain SRPC concrete with w/c 0.30, exposed submerged (A) and in the splash zone (B). Solid logarithmic trend lines extrapolated by regression analysis.

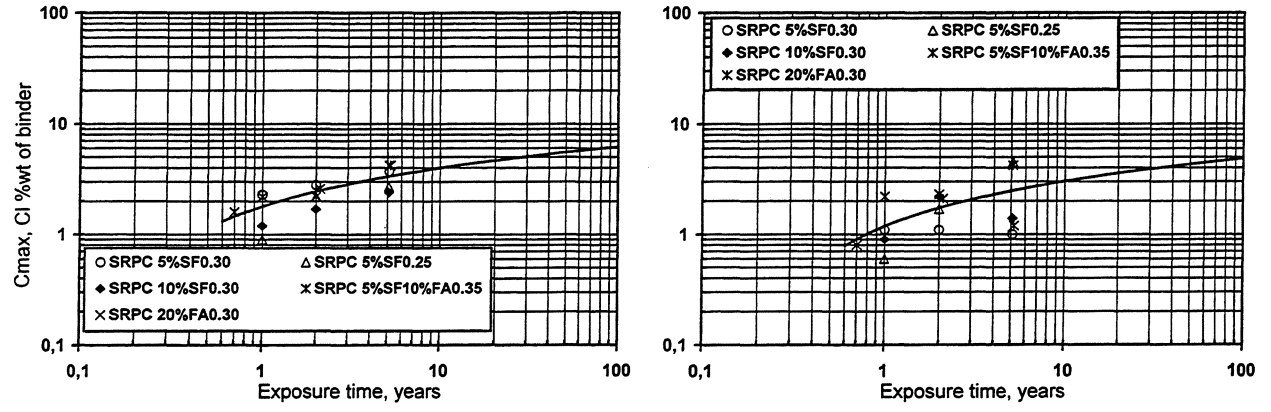


Figure 9.7. Maximum total chloride concentrations for concrete mixes with pozzolan in the binder and w/c ≤ 0.35, exposed submerged (A) and in the splash zone (B). Solid logarithmic trend lines extrapolated by regression analysis.

The maximum total chloride concentration, Cmax, measured after 5 years of exposure was found to be generally higher in submerged concrete than in concrete exposed in the splash zone, Figures 9.6 and 9.7. This is somewhat surprising, as enrichment of chlorides in concrete exposed to wetting and drying can be thought to cause the opposite effect /35/. On the other hand, most of the datapoints shown in Figures 9.6 and 9.7 relate to high quality concrete, with a w/c ratio ≤ 0.40 and therefore a very low capillary porosity. Thus it can be argued that the effect of chloride enrichment, caused by cycles of capillary suction and drying, on the chloride penetration in well cured concrete with a w/c ratio ≤ 0.40 should be insignificant.

The results from the prediction of the total chloride profile after 100 years of exposure time, based on the assumptions in A) – C), are presented for all concrete mixes considering exposure submerged and in the splash zone, in (paper V). On example is shown in Figure 9.8, for SRPC concrete with 5 % silica fume in the binder, w/c 0.40.

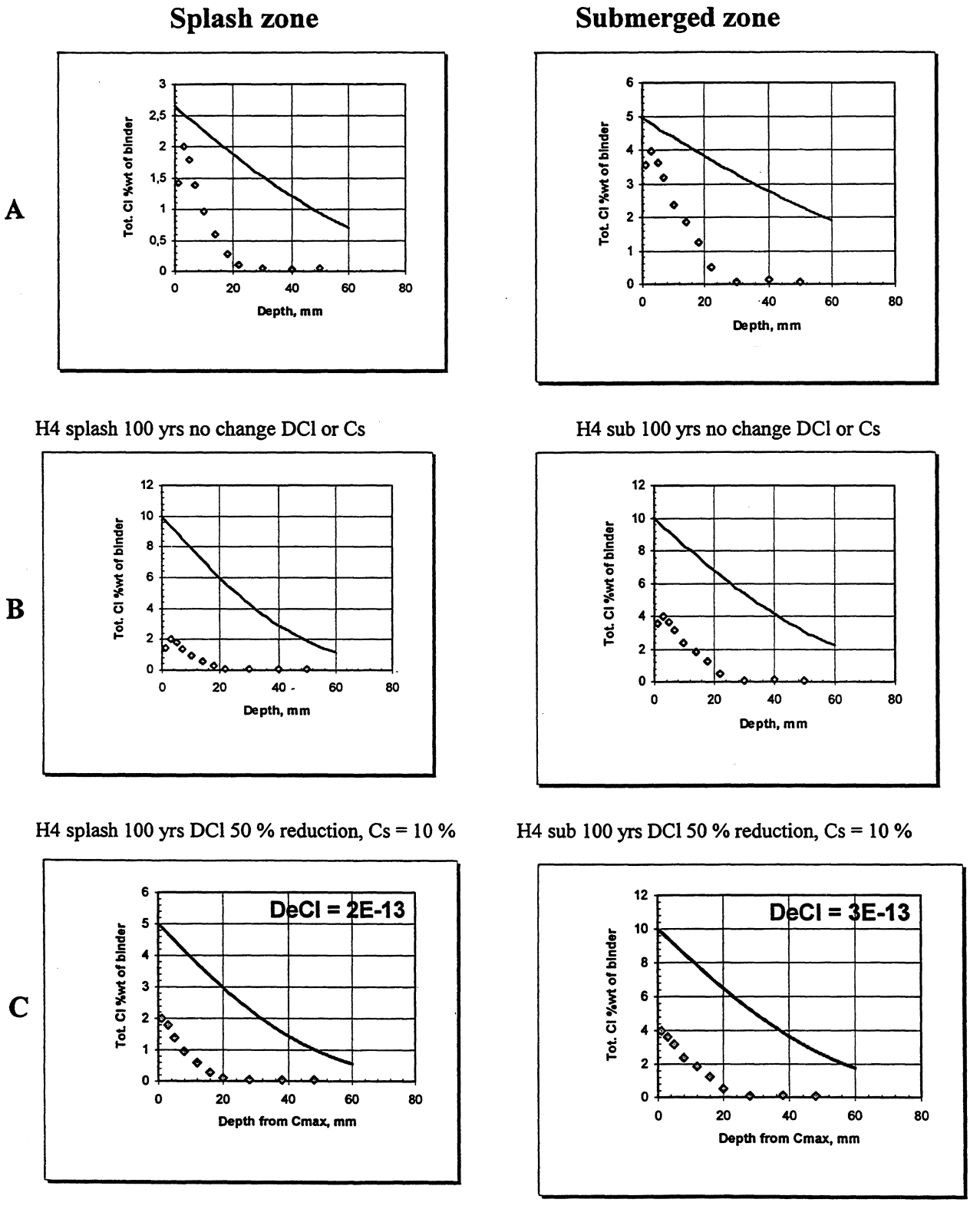


Figure 9.8. Prediction of total chloride profiles after 100 years of marine exposure. SRPC concrete with 5 % silica fume in the binder, w/c 0.40.

# 10. SERVICE LIFE PREDICTION

## 10.1 General

Two different approaches to a service life prediction with respect to reinforcement corrosion in concrete exposed in a marine environment are outlined:

1. A prediction of the required cover to achieve an initiation time of 100 years in uncracked concrete exposed in a marine splash zone. The chloride thresholds presented in Chapter 6.5.6 and the simulations of the profiles of total chloride after 100 years of exposure, according to procedures A-C as described in Chapter 9.1 and presented in (paper V), are used.

2. A prediction of the "permissible propagation time" for corrosion pits in cracks wider than 0.2 mm affecting the reinforcement. The service life is assumed to be the shortest of the initiation time in uncracked concrete and the "permissible propagation time" at cracks.

## 10.2 Prediction of the required cover for 100 years initiation time in uncracked concrete

Simple service life predictions with respect to the required cover for a 100 years initiation time for reinforcement corrosion are undertaken. The simulations presented in (paper V) and chloride thresholds assuming a normal frequency distribution and 95 % confidence for chloride thresholds for SRPC concrete with 0 and 5 % silica fume and > 20 mm cover, were used as presented in Chapter 6.5.6. The chloride threshold for SRPC concrete with 10 % silica fume and with a combination of silica fume fly ash are assumed to be 20 % lower than the chloride threshold for SRPC with 5 % silica fume, as was indicated in Figure 6.4. The predictions are carried out for concrete exposed in the splash zone, as this exposure zone is regarded as most critical with respect to reinforcement corrosion. The predicted minimum covers required are shown in Table 10.1, considering concrete with w/c ratio $\leq 0.40$.

As seen in Table 10.1, for most concrete mixes the calculated required cover vary considerably depending on the simulation procedure chosen. In order to compare the results for the different mixes, a mean value of procedures A, B and C is calculated.

The calculations of the required cover thickness indicate that the use of 5% silica fume and a reduction of the w/c ratio from 0.40 to 0.30 would reduce the required cover with approximately 50 % as compared to a typical Swedish bridge concrete of w/c 0.40 with no pozzolan. It is however important to point out that other durability issues such as the durability to freezing and thawing may completely alter the overall judgement of the most durable concrete mix. In general, the addition of pozzolans, especially fly ash and ground granulated blast furnace slag, to the concrete binder has a marked negative effect on the durability to freezing and thawing /39/. Considering the durability to both reinforcement corrosion and freezing and thawing, the optimum binder is probably a mix with SRPC and 5% silica fume, as this relatively small amount of pozzolan has a strong positive effect on the resistance to chloride penetration, but only a small negative effect on the chloride threshold and on the resistance to freezing and thawing /40/. OPC would be an alternative to SRPC, if the negative effects of a higher $C_3A$ content in OPC on the resistance to thermal cracking, freezing and thawing and sulfate attack can be overcome.

Table 10.1. Concrete mixes, threshold levels and calculated required cover thickness in the splash zone

| Binder composition | w/c ratio | OPC or SRPC kg/m$^3$ | Silica fume kg/m$^3$ | Fly ash kg/m$^3$ | Chloride threshold %Cl of binder | Required cover mm Procedure A/B/C | Required cover mm Mean value of A, B & C |
|---|---|---|---|---|---|---|---|
| SRPC | 0.40 | 420 | - | - | 1.15 | 48/90/78 | 72 |
| SRPC | 0.30 | 492 | - | - | 1.3 | 78/82/75** | 78** |
| SRPC 5%SF | 0.40 | 399 | 21 dry | - | 0.9 | 43/62/49 | 51 |
| SRPC 5%SF | 0.40 | 399 | 21 slu | - | 0.9 | 50/63/53 | 55 |
| SRPC 5%SF | 0.30 | 475 | 25 slu | - | 1.0 | */40/26 | 33 |
| SRPC 5%SF | 0.25 | 525 | 26 slu | - | 1.05 | 44/41/30 | 38 |
| SRPC 10%SF | 0.30 | 450 | 50 slu | - | 0.8 | 30/34/32 | 32 |
| SRPC 5%SF 10%FA | 0.35 | 382 | 23 slu | 45 | 0.75 | 31/55/33 | 40 |
| SRPC 5%SF 17%FA | 0.40 | 345 | 21 slu | 75 | 0.7 | 45/47/51 | 48 |
| SRPC 20%FA 0 | 0.30 | 493 | - | 123 | 0.8 | 49/55/45 | 50 |

* The predicted value was less than 20 mm and not considered relevant, see Chapter 6.5.5.
**The profile of total chloride concentration measured in the concrete slab with SRPC, w/c 0.30, exposed in the splash zone, did not fit the general pattern with a decreasing chloride penetration at decreasing w/c ratios. See Figure 8.3 and the corresponding calculated effected chloride diffusivity in Figure 9.1. As a consequence the predicted required cover is higher than expected for a concrete with such a low w/c ratio as compared to the other mixes. As speculated in Chapter 8.3.3.1, the formation of cracks is a possible explanation to the observed poor performance.

Potentially it would be of great interest to consider the use of high performance concrete with 5-10 % silica fume in the binder and a maximum w/b ratio of 0.30. As indicated in Table 10.1 the required cover would be relatively thin. Furthermore, research on the durability of high performance concrete with respect to freezing and thawing indicates that concrete with such low w/c ratios are potentially very durable to freezing and thawing as a consequence of self desiccation /39/. Another strong benefit from using high performance concrete with silica fume is the very high resistivity of such concrete, which may depress active corrosion rates to insignificant levels also in cracked concrete /41/.

Alternatively, it is suggested in (papers IX and XI) that ordinary black steel reinforcement can be replaced with stainless steel reinforcement in the most aggressive exposure zones. It is speculated that the higher initial cost for stainless steel reinforcement can be counteracted by savings on reinforcement for crack control and on the required cover thickness, as a consequence of very high chloride thresholds for stainless steel. The amount of normal reinforcement which would need to be replaced would be less than 10 % of the total amount of reinforcement in a marine concrete bridge. A more comprehensive discussion on the use of stainless steel reinforcement in concrete structures is available in (papers IX and XI).

## 10.3 Prediction of the propagation stage for corrosion in cracks

### *10.3.1 General*

A general system for service life prediction of reinforced concrete structures with respect to chloride initiated reinforcement corrosion is outlined. The system involves

1) The prediction of the initiation time in uncracked concrete; see Chapter 10.2 above.
2) The prediction of the permissible time of active corrosion - the propagation time - in cracks < 0.4 mm wide.

The predicted service life is suggested as the shortest of the two predicted times. Examples on the use of the model are given in (paper X).

### *10.3.2 Prediction of the permissible time of active chloride initiated corrosion in cracks*

Little or no experimental data exists on the permissible reduction of cross section of corroding reinforcement subjected to chloride initiated pitting corrosion for various types of concrete structural parts. At this stage it has therefore been generally hypothesised that the service life is over when a maximum of 20 % of the reinforcement cross section area has been lost in a crack. The maximum permissible loss of cross section area should be calculated for various structural parts by relevant experts in construction and design, and then experimentally verified in large scale corrosion tests on concrete structural parts under relevant loads.

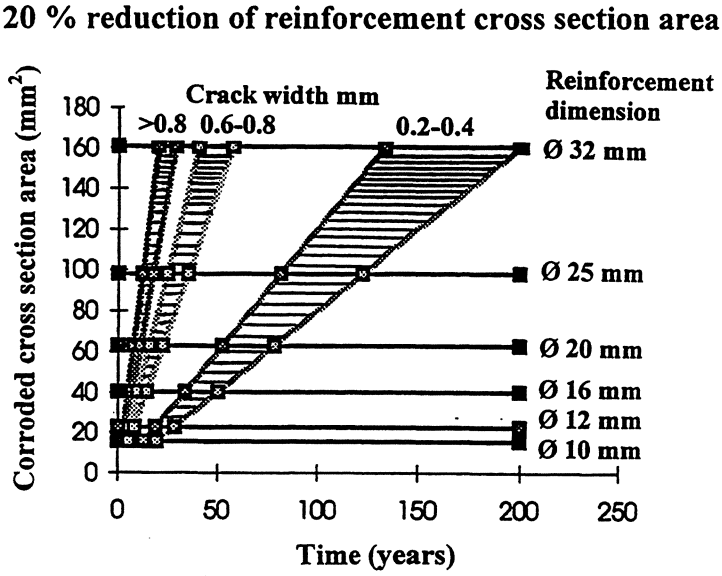


Figure 10.1. Calculated propagation times in marine exposed high performance concrete with a maximum of 20% loss of the reinforcement cross section area within the service life. Corrosion rate based on 2 years field exposure tests at Kristiansand /42/.

Experimental studies of the propagation rate in high performance concrete with cracks wider than 0.1 mm exposed to seawater have been carried out within the Swedish project on High Performance Concrete Structures /41,42/. The results on loss of reinforcement cross section

area at corrosion pits in cracked concrete have been used by Pettersson in /42/ to calculate the time to reach a 20 % loss of cross section area for ordinary reinforcement, Figure 10.1. The figure is hypothetical and based on the assumption that the loss of cross section area is linear over time. This is an oversimplification as the loss of cross section area depends on the geometry of the corrosion pit, which in turn depends on further cracking and spalling, precipitation of corrosion products in the crack, etc. However, in this thesis the figure is only used to schematically describe the propagation stage in a crack.

### *10.3.3 Combination of predicted initiation- and propagation time to a service life model*

#### 10.3.3.1 General

Suggested principles are outlined for the development of a service life model for reinforced concrete with respect to reinforcement corrosion both in cracks wider than 0.2 mm and in uncracked parts.

Most concrete structures have crack widths > 0.2 mm as a result of shrinkage, structural load, etc. A model for service life prediction of reinforced concrete should therefore require a prediction of the corrosion status in both uncracked concrete and at neighbouring cracks wider than 0.2 mm.

The following assumptions have been made for the sake of simplicity:

A) Concrete with crack widths ≤ 0.2 mm are regarded as crack free if the cover is thicker than 25 mm. Field exposure tests of cracked concrete with w/c ratio ≤ 0.40 and 30 mm cover did not experience any corrosion initiation within 2 years of exposure submerged or in the splash zone /42/.

B) The service life is ended if corrosion is initiated in uncracked concrete, Figure 10.2, or if more than 20 % of the reinforcement cross section area is lost in cracked concrete, Figure 10.3.

C) The concrete cover should always be a minimum of 25 mm in saline environment. Experimental studies in marine environment have indicated that

   i) The chloride threshold level in uncracked concrete is significantly lower in concrete with 10 mm cover as compared to 20 mm cover, Figure 6.15.

   ii) The corrosion rate in cracked concrete is significantly lower in a concrete with 30 mm cover as compared to 15 mm cover and thinner /41,42/.

D) The propagation time for uncracked concrete exposed to the atmosphere with a minimum of 25 mm cover is very small as compared to the initiation time, because

   i) Active corrosion in normal concrete, w/c > 0.40, is relatively fast and may lead to spalling of the cover within a few years of active corrosion.

ii) Active corrosion in high performance concrete, w/c ≤ 0.40, may be very slow due to the very high resistivity of the concrete, but the very low porosity and the high brittleness and low ductility of high performance concrete may still result in spalling of the cover within a few years of active corrosion.

E) The chloride threshold level in uncracked high performance concrete would not be significantly affected by an active corrosion in nearby cracks, because of the high resistivity of high performance concrete.

F) In uncracked normal concrete the chloride threshold level would be affected (increased) by the localised cathodic protection provided by rapid corrosion in nearby cracks.

G) Spalling of concrete cover does not occur in underwater concrete because of the lack of oxygen at the anode for the formation of expansive rust.

H) Macrocell corrosion in submerged concrete > 1 m below the water level can be prevented by the use of high performance concrete, with w/c ≤ 0.40 and ≥ 5 % silica fume in the binder. This assumption is based on the assumption that the resistivity in such concrete is high enough to reduce the distance between possible anode and cathode sites to less than 1 m. The resistivity in well cured high performance concrete is typically 100-150 kΩcm as compared to 4-30 kΩcm for normal concrete exposed in the splash zone /42/.

10.3.3.2 Classification of corrosion modes

A small number of corrosion modes would describe in principle the service life of most reinforced concrete with the aid of the assumptions made above:

***Mode 1. Corrosion in uncracked concrete exposed to the atmosphere***

The service life of uncracked concrete in a saline and oxygen rich environment is defined as the initiation time, Figure 10.2. The chloride threshold level is low as the availability of oxygen is high. Once active corrosion is initiated, expansive corrosion products are formed and the remaining time until spalling occurs is very short compared to the initiation time.

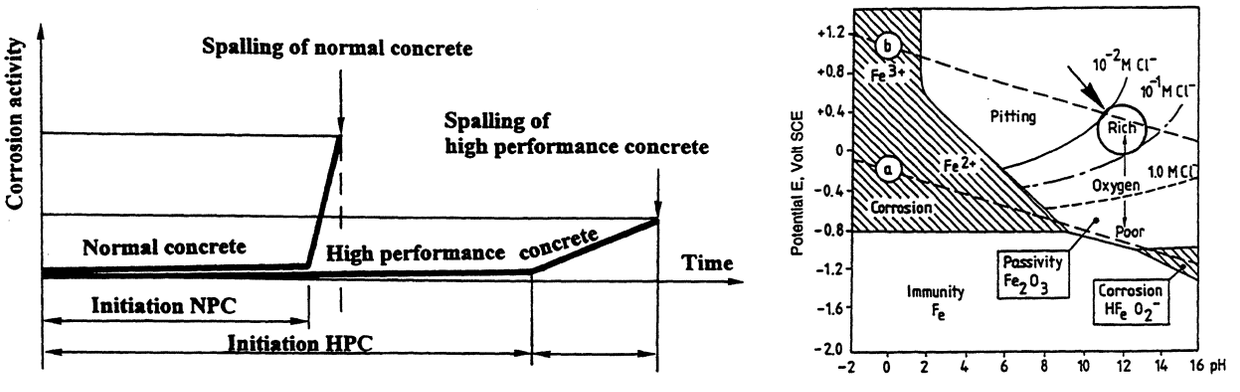


Figure 10.2. Service life (initiation time) of uncracked concrete exposed in the atmosphere.

This corrosion mode applies to normal (NPC) and high performance (HPC) concrete. In normal concrete active corrosion is relatively fast. In high performance concrete active corrosion may be very slow, but the very low porosity and the high brittleness and low ductility allow for very little amounts of expansive rust to form without spalling.

However it is important to recognise the very slow chloride transport rate in high performance concrete. An uncracked high performance concrete would require substantially less cover thickness than an normal concrete for a given initiation time.

| Assumption:<br>Service life ≈ initiation time for uncracked parts of concrete with cracks ≤ 0.2 mm wide, exposed to the atmosphere. |
|---|

*Mode 2. Corrosion in cracked concrete exposed to the atmosphere*

The service life of cracked concrete in a saline and oxygen rich environment is illustrated in Figure 10.3 for cracks > 0.2 mm wide. The initiation time is often close to zero if the crack reaches the reinforcement. The availability of oxygen is very high and the corrosion rate is anodically controlled by the clogging by corrosion products in the crack. The corrosion products clogging the crack do not cause spalling of the cover.

The uncracked parts of the structure follows mode 1. The service life of the combined cracked and uncracked concrete will be determined by the shortest of the initiation time in the uncracked part according to mode 1 and the propagation time to reach a maximum reduction of the reinforcement cross section area in the crack according to mode 2. Once active general corrosion is initiated in uncracked concrete, the corrosion products formed are expansive and the remaining propagation time until spalling occurs is very short.

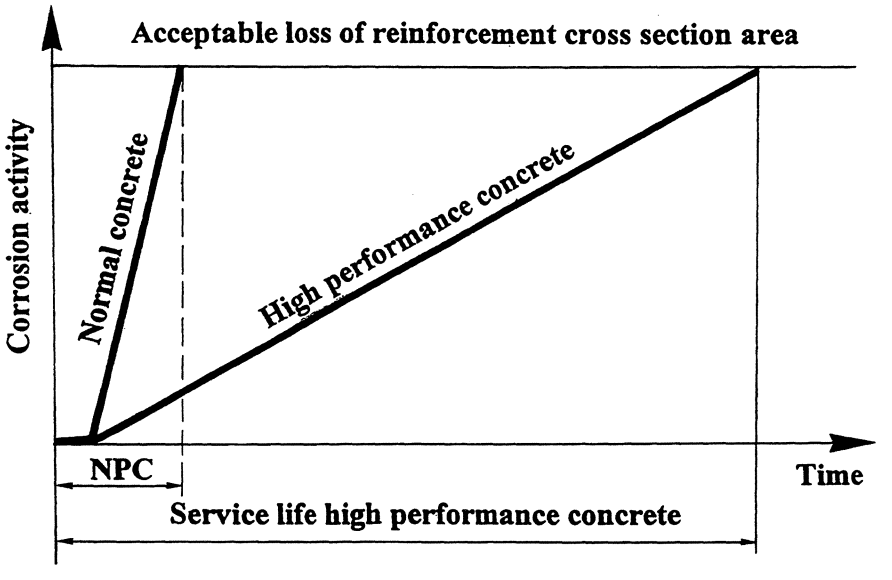


Figure 10.3. The service life of cracked concrete exposed in the atmosphere. The initiation time is close to zero in cracks wider than 0.2 mm, but the propagation time to reach the acceptable reduction of reinforcement cross section is longer for high performance concrete.

This corrosion mode applies to normal and high performance concrete. In normal concrete active corrosion once initiated in cracks is fast. In high performance concrete the active corrosion in cracks is relatively slow /42/, which may lead to a long service life provided that the effects of a high resistivity and/or clogging of the anode by corrosion products are strong enough to maintain relatively low corrosion rates. If spalling occurs the total corrosion activity may increase as a result of an increased conductivity in delaminated concrete. On the other hand the loss of reinforcement cross section area in a given corrosion pit may decrease as a result of an increased anodic area.

| Assumption for normal and high performance concrete with cracks > 0.2 mm wide exposed to the atmosphere:<br>Service life ≈ the shortest time of the initiation time in uncracked concrete and the propagation time to reach the acceptable loss of reinforcement cross section area at cracks. |
|---|

*Mode 3. Corrosion in uncracked concrete fully exposed under water*

The service life of uncracked concrete in a saline and oxygen free environment (More than 1 m below the sea level) is illustrated in Figure 10.4, provided that the concrete resistivity is high enough to prevent the formation of a macrocell with the cathode in oxygen rich concrete. The chloride threshold can be very low as the amount of oxygen available may be insufficient to maintain passivity of steel. Thus active general corrosion may be initiated also in the absence of chlorides. However, in the absence of oxygen, pitting corrosion cannot initiate /8/. Besides, the corrosion products are non-expansive and the corrosion rate is extremely slow. The propagation time is therefore so long that a prediction is unnecessary.

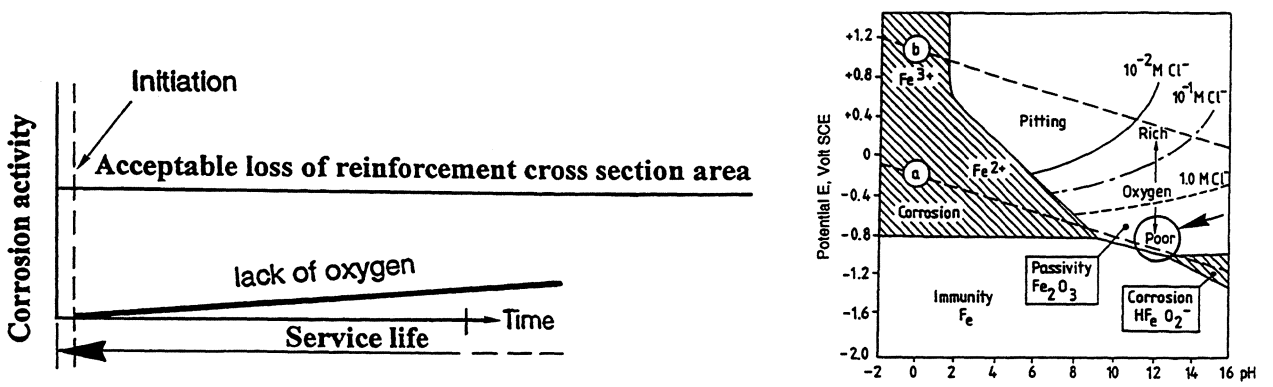


Figure 10.4. The service life of uncracked concrete fully exposed under water. The initiation time can be short as the amount of oxygen available may be insufficient to maintain passivity of steel. The propagation rate is very slow provided that the resistivity of the concrete is high enough to prevent the formation of a macrocell with the cathode in oxygen rich concrete.

This corrosion mode applies to normal and high performance concrete. However, the required depth below the water level in order to prevent macro cell corrosion is much bigger for normal concrete than for high performance concrete. It does not apply if parts of the reinforcement system can act as a cathode in concrete exposed to the atmosphere, as rapid macro cell corrosion may develop. Macrocell corrosion is represented by mode 2, with the difference that less corrosion products will precipitate and block the crack. As a consequence the corrosion rate may remain very high throughout the propagation stage. Macrocell corrosion is considerably less rapid in high performance concrete as the high resistivity reduces the corrosion rate.

Corrosion mode 3 also applies to cracked normal and high performance concrete if the concrete is submerged several meters below the sea level and the resistivity of the concrete is high enough to prevent macrocell corrosion with the cathode present in oxygen rich concrete.

Alternatively, corrosion mode 3 also applies if the entire concrete structure is submerged several meters below the water level, with no access to enough oxygen for any cathodic process to take place at a significant rate.

| Assumption:<br>The service life for submerged concrete is extremely long provided that either the depth from the water level and the resistivity of the concrete is high enough to prevent the formation of a cathode in oxygen rich concrete, or the entire structure is exposed in an oxygen free environment. |
|---|

## 10.4 Analysis of sensitivity

### *10.4.1 Errors associated with the measured profiles of total chloride*

The error analyses of profiles of total chloride in Chapters 6.6.2 and 8.4 apply also here. The consequence of visible cracks on the measured profile of total chloride is illustrated in Figure 8.1. Cracks are likely to have affected the measured profile of total chloride and the predicted minimum cover required for concrete with SRPC, w/c 0.30, exposed in the splash zone, as discussed in Chapter 10.2.

It is possible to identify deviations and estimate their size by examining series of profiles of total chloride, Figures 8.1 and 8.3, and series of predicted minimum covers required, Table 10.1. By comparing the profiles of total chloride in Figures 8.1 and 8.3, and the predicted minimum covers required in Table 10.1, the observed deviation in the SRPC concrete exposed in the splash zone, w/c 0.30, can be estimated to be in the range of 30 mm of the predicted minimum cover required.

### *10.4.2 Errors associated with the chloride thresholds*

The evaluations in Chapter 6.5 indicated that the spread in chloride threshold is relatively large, as affected by normal defects at the interface between the concrete and the reinforcement. The effect of the spread in chloride thresholds on the predicted covers can be evaluated by comparing the covers predicted in Table 10.1 with the covers predicted in (paper

V), using the mean values in Table 6.3 without considering the standard deviation. It was found that the predicted mean values for required covers were generally about 5 mm thinner if the standard deviation is not considered.

### *10.4.3 Errors associated with the prediction of chloride ingress*

The possible errors in the prediction of the chloride ingress can be evaluated by comparing the results on the required cover for the 3 different predictions A-C, as presented for 10 different concrete mixes in Table 10.1. It can be seen that the difference between the smallest and the thickest predicted cover for a given concrete quality can be as high as 42 mm. The mean difference between the smallest and the thickest predicted cover was 15 mm with a standard deviation of 11 mm.

## 10.5 Conclusions

1. The predicted cover is much more sensitive to predicted variations in parameters affecting the chloride transport rate than to variations in the chloride threshold.

2. The calculations of the required cover thickness indicate that the use of 5% silica fume and a reduction of the w/c ratio from 0.40 to 0.30 would reduce the minimum cover required with approximately 50 % as compared to a typical Swedish bridge concrete with w/c 0.40 and no pozzolan.

2. Service life prediction based on both prediction of the initiation time in uncracked concrete and prediction of the permissible time of active corrosion in cracks appears to be more useful than predictions based on the initiation time only, as the effect of cracks can be accounted for. However, data on the permissible cross section loss at a corrosion pit appears to be lacking.

# 11. RESEARCH NEEDS

## 11.1 General

Some most important research needs with respect to reinforcement corrosion and service life prediction of concrete structures exposed in a saline environment was listed.

## 11.2 The initiation phase

A) Chloride transport rates and chloride thresholds from recurrent studies of chloride ingress in concrete exposed to de-icing salt. Field and laboratory exposure tests for identification of mechanisms, quantification of relevant parameters and modelling. The work already carried out for concrete exposed in a marine environment should also be continued, by studies of the effect of thicker covers and longer exposure times on the chloride transport rate and the chloride threshold. 20 mm thick reinforced concrete slabs have been field exposed since 1992 and are available with 40 and 55 mm cover, for SRPC concrete with 0 and 5 % silica fume and for OPC concrete, w/c ratios 0.35 and 0.40.

B) Systems for improving the chloride threshold, either by eliminating or minimising defects at the steel – concrete interface, by developing the reinforcing material, or by developing long term effective and non poisonous inhibitors.

C) Cement or concrete additives or mix designs which aims at reducing the chloride penetration rate, without affecting negatively the resistance to freezing and thawing.

## 11.3 The propagation phase

D) Laboratory studies of the permissible reinforcement cross section loss at a corrosion pit in various structural concrete members. Field and laboratory exposure tests for identification of mechanisms, quantification of relevant parameters and modelling.

E) Systems for reducing the reinforcement cross section loss by pitting corrosion in concrete, both for uncracked and cracked concrete, by developing the reinforcing material, cement or concrete additives (without affecting negatively the resistance to freezing and thawing), or by developing long term effective and non poisonous inhibitors.

## 12. REFERENCES


1. Dunker, K.F., Rabbat, B.G., "Why America's bridges are crumbling", Scientific American, Vol 268, No 3, pp. 66-72, 1993.

2. Stix, G., "Concrete Solutions", ", Scientific American, Vol 268, No 4, pp. 102-112, 1993.

3. Luping, T., "Chloride Transport in Concrete - Measurement and Prediction", Publication P-96:6, Chalmers Univ. of Tech., Dept. of Building Materials, Sweden 1996.

4. Tuutti, K., Corrosion of steel in concrete, CBI Fo 4:1982. Swedish Cement and Concrete Research Institute, Stockholm 1982.

5. Hansson. C., "Comments on electrochemical measurements of the rate of corrosion of steel in concrete", Cement and Concrete Research, Vol 14, pp. 574-584, 1984.

6. Mattsson, E., Electrochemistry and corrosion science, Swedish Corrosion Institute, Roos Produktion AB, Stockholm 1992 (in Swedish).

7. Shreir, L.L., Jarman, R. A., Burstein, G.T. (Eds), Corrosion, Butterworth-Heinemann, Oxford 1994.

8. Arup, H., "The mechanisms of the protection of steel by concrete", Proceedings Corrosion of Reinforcement in Concrete Construction, Ellis Horwood Ltd., Chichester, June 1983, pp 151-157.

9. Danish Road Directorate, "Chloride initiated corrosion - field studies of chloride corrosion in bridge columns" (in Danish), Copenhagen 1991.

10. Norwegian Road Directorate & Building Research Institute, "Chloride durability of concrete coastal bridges" (in Norwegian), Oslo, 1993.

11. Mangat, P.S., Molloy, B.T., "Prediction of long term chloride concentration in concrete", Materials and Structures, 27, pp. 338-346, 1994.

12. Masters, L., W., Brandt, E., "Prediction of service life of building materials and components", CIB W80/RILEM 71-PSL Final Report, 1987.

13. Maage, M., Helland, S., Carlsen, J.E., "Chloride penetration in high performance concrete exposed to marine environment", Proceedings 3rd Int. Symp. on Utilization of High Strength Concrete, Lillehammer, Norway 1993.

14. ASTM E632, "Standard practise for developing accelerated tests to aid prediction of the service life of building components and materials, 1988.

15. Glass, G.K., Buenfeld, N.R., "The presentation of the chloride threshold for corrosion of steel in concrete". Corrosion Science 1997, 39, No. 5, 1001-1013.

16. Yonezawa, T., Pore Solution Composition and Chloride-Induced Corrosion of Steel in Concrete, British Ph D Thesis, Victoria University of Manchester, Corrosion and Protection Centre, 1988.

17. Hausmann, D.A., "Steel corrosion in concrete", Materials Protection, Nov. 1967.

18. Page, C. L., Treadaway, K. W. J., "Aspects of the electrochemistry of steel in concrete". Nature 1982, 297, 109-115.

19. Mammoliti, L. T., Brown, L. C., Hansson, C. M., Hope, B. B., "The influence of surface finish of reinforcing steel and pH of the test solution on the chloride threshold concentration for corrosion initiation in synthetic pore solutions". Cem. & Concrete Res. 1996, 26, No. 4, 545-550.

20. Pettersson, K., "Service Life of Concrete Structures - In saline environment". CBI Report 3:96. Swedish Cement and Concrete Research Institute, Stockholm 1996.

21. Broomfield, J. P., "Assessing corrosion damage on reinforced concrete structures" Proceedings Corrosion and Corrosion Protection of Steel in Concrete. Swamy, R., N., Ed, Sheffield Academic Press, 1994, pp 1-21.

22. Elsener, B,, Wojtas, H., Böhni, H., "Galvanostatic pulse measurements – rapid on site corrosion monitoring". Proceedings Corrosion and Corrosion Protection of Steel in Concrete. Swamy, R., N., Ed, Sheffield Academic Press, 1994, pp 236-246.

23. NT BUILD 443. In Concrete, hardened: Accelerated chloride penetration, part 6.4.4 Profile grinding.

24. Tang, L., Sandberg, P. "Chloride penetration into concrete exposed under different conditions" In Durability of Building Materials and Components 7, II. Sjöström, C., Ed., E & FN Spon, London, 1996, pp 453-461.

25. Arup, H., Sørensen, H. E. "A proposed technique for determining chloride thresholds". In Chloride Penetration into Concrete. Nilsson, L-O, Ollivier J.P., Eds., RILEM Publications, France, 1997, pp 460-469.

26. ACI Committee 309. "Guide for consolidation of concrete". ACI 309R-87. In ACI Manual of Concrete Practice, Detroit, Mich. 1990.

27. Arfvidsson, J., Hedenblad, G. Calculation of moisture variation in concrete surfaces. Lund Inst. of Tech., Building Materials & Building Physics, 1991.

28. Tang, L., Nilsson, L-O., "Chloride binding capacity and binding isotherms of OPC pastes and mortars", Cement and Concrete Research, Vol 23, pp 247-253, 1993.

29. Sandberg, P., Larsson, J., "Chloride binding in cement pastes in equilibrium with synthetic pore solutions", Proceedings Nordic Seminar on Chloride Initiated Reinforcement Corrosion in Concrete, Gothenburg, Sweden, January 13-14, 1993.

30. Arya, C., Newman, J.B., "An assessment of four methods of determining the free chloride content of concrete", Materials and Structures, 23, pp. 319-330, 1990.

31. Sergi, G., Yu, S.W., Page, C.L., "Diffusion of chloride and hydroxyl ions in cementitious materials exposed to a saline environment", Magazine of Concrete Research, 44, No. 158, pp. 63-69, March 1992.

32. K. Byfors, Chloride Initiated Reinforcement Corrosion, Chloride Binding. CBI Report 1:90. The Swedish Cement and Concrete Research Institute (1990).

33. J. Tritthart, Chloride Induced Steel Corrosion in Concrete" (in German). HEFT 346, Bundesministerium für Wirtschaftliche Anlegenheiten, Strassenforschung, Wien (1988).

34. Collepardi M, Marcialis A & Turriziani R. "The kinetics of chloride ion penetration in concrete" (in Italian). Il Cemento, Vol 67, pp 157-164 (1970).

35. Nilsson L-O, Poulsen E, Sandberg P, Sørensen H E & Klinghoffer O. A system for the prediction of chloride ingress and corrosion in concrete. HETEK, The Danish Road Directorate, Report No.83, 1997.

36. Sørensen, H., Frederiksen, J.M., "Testing and modelling of chloride penetration into concrete", Nordic Concr. Res, Trondheim 1990, pp. 354-356.

37. Sarukawa, Y., Sakai, K., Kubouchi, A., "Japan´s 100-Year-Long Otaru Port Breakwater Durability Test". Concrete International, May 1994, pp. 25-28.

38. Sandberg, P. "Kloridinitierad armeringskorrosion i betong" (in Swedish). In Report TVBM 7032, Lund Inst. of Tech., Building Materials, 1992.

39. Fagerlund, G. "Durability to freezing and thawing" (in Swedish), In Betonghandboken Material. Ljungkrantz, C., Möller, G., Petersons, N., Eds., Svensk Byggtjänst and Cementa AB, 1994, pp. 727-783.

40. Sandberg, P. "Resistance to salt scaling" In Öresundscement. Carlsson, C-A., Ed., Cementa AB 1995.

41. Pettersson, K. "Chloride threshold value and corrosion rate in reinforced concrete" In Concrete 2000. Dhir R. K. & Jones M. R., Eds., London: E&FN Spon, 1993, Vol 2, s. 461-471.

42. Fidjestøl, P., Jørgensen, O., Pettersson, K., Sandberg, P. and Tuutti, K. "Reinforcement corrosion" (in Swedish). In Swedish Manual for High Performance Concrete. Ljungkrantz, C., Petersons, N., Eds. Stockholm 1998.

43. Nilsson, L-O., Rodhe, M., Sahlén, S. And Roczak, W., Moisture distributions in marine concrete structures as a basis for service life prediction. Parts 4, 5 and 7. Working reports. Chalmers University of Technology, Division of Building Materials, 1994-95.

44. Swedish Concrete Assosiation. Durable concrete structures (in Swedish). 2nd revised edition. Stockholm 1998.

45. Nilsson L-O, Poulsen E, Sandberg P, Sørensen H E & Klinghoffer O. Chloride penetration into concrete. State of the Art. HETEK, The Danish Road Directorate, Report No.53, 1996.

# APPENDIX

## Appendix

Photographs 1-17 show the microstructure and chloride penetration in concrete corrosion cells. Concrete with chloride was visually identified by spraying freshly cut surfaces with a 0.1 M $AgNO_3$ solution. The formation of light grey AgCl precipitate in chloride rich areas provides a visual indication of the chloride penetration.

Photographs 18-20 show the design of a corrosion cell and the potentiostat used for the potentiostatic control of steel electrodes.

Photograph 21 shows the equipment used for sampling of concrete at various depths from the exposed surface, as used for the analysis of a total chloride distribution profile.

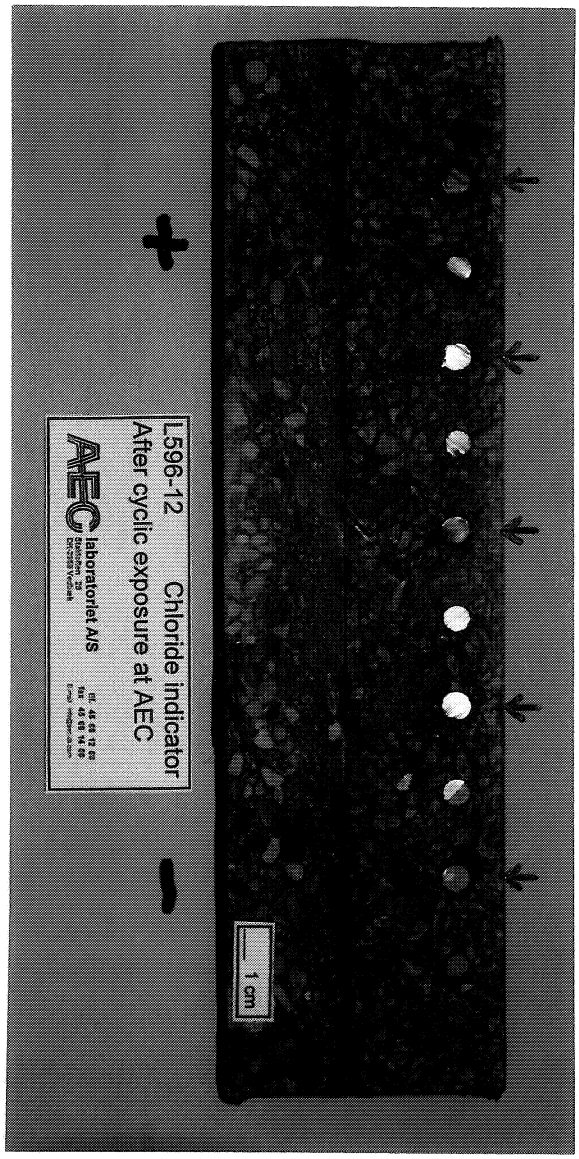


Photo 1. Microstructure and chloride penetration in concrete corrosion cell. SRPC w/c ratio 0.40, after 8 months exposed to cycles of 2 hours wetting in a 16 % NaCl solution and 22 (-) or 166 (+) hours drying in the laboratory at room temperature. See Figure 6.5 for exposure conditions. Arrows (←) indicate steel electodes with filter paper defect.

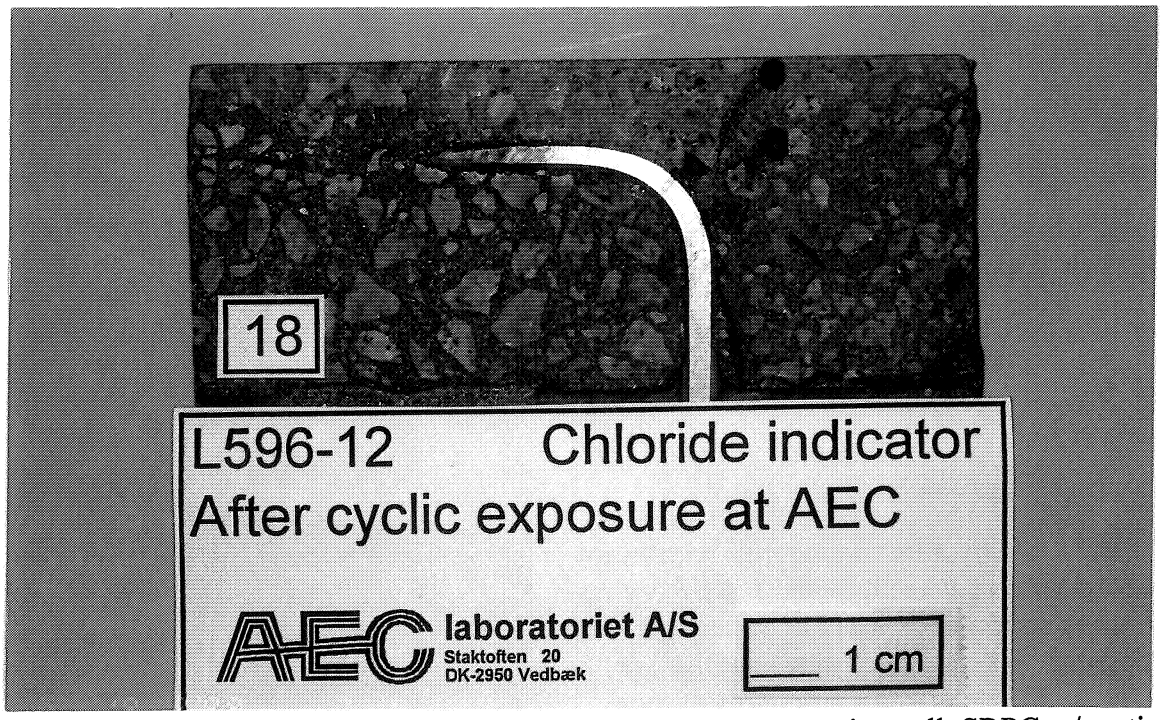


Photo 2. Microstructure and chloride penetration in concrete corrosion cell. SRPC w/c ratio 0.40, after 8 months exposed to cycles of 2 hours wetting in a 16 % NaCl solution and 22 hours drying in the laboratory at room temperature. Electrode without filter paper defect.


Photo 3. Microstructure and chloride penetration in concrete corrosion cell. SRPC w/c ratio 0.40, after 8 months exposed to cycles of 2 hours wetting in a 16 % NaCl solution and 22 hours drying in the laboratory at room temperature. Electrode with filter paper defect.

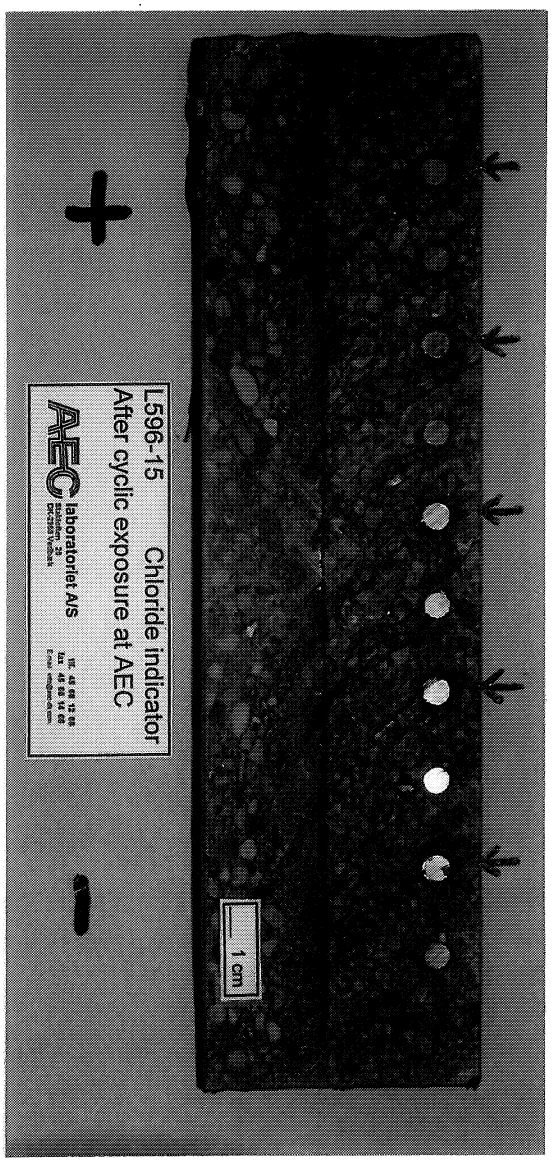


Photo 4. Microstructure and chloride penetration in concrete corrosion cell. SRPC 5 % SF w/c ratio 0.40, after 8 months exposed to cycles of 2 hours wetting in a 16 % NaCl solution and 22 (-) or 166 (+) hours drying in the laboratory at room temperature. See Figure 6.5 for exposure conditions. Arrows (←) indicate steel electodes with filter paper defect.

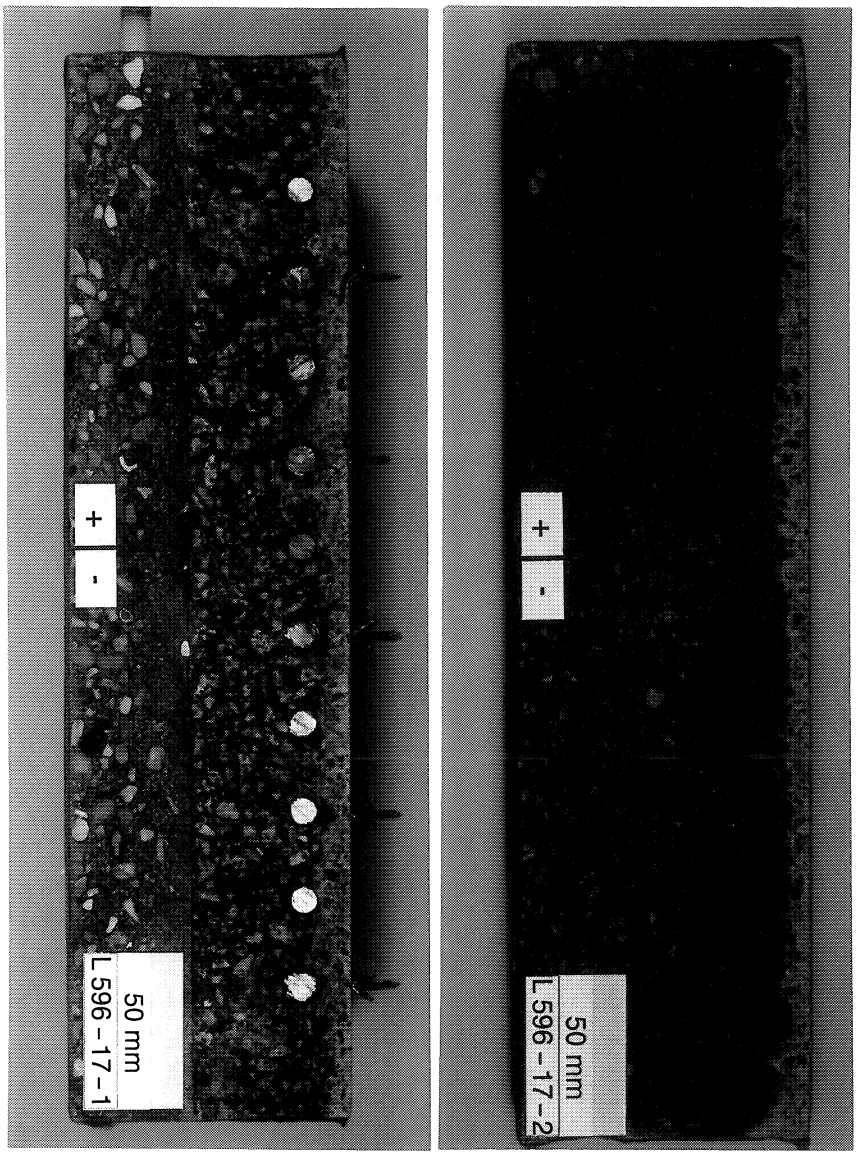


Photo 5. Microstructure and chloride penetration in concrete corrosion cell. Slag cement w/c ratio 0.40, after 8 months exposed to cycles of 2 hours wetting in a 16 % NaCl solution and 22 (-) or 166 (+) hours drying in the laboratory at room temperature. See Figure 6.5 for exposure conditions. Arrows (←) indicate steel electodes with filter paper defect.


Photo 6. Microstructure and chloride penetration in concrete corrosion cell. Slag cement w/c ratio 0.40, after 8 months exposed to cycles of 2 hours wetting in a 16 % NaCl solution and 166 hours drying in the laboratory at room temperature. Electrode without filter paper defect.

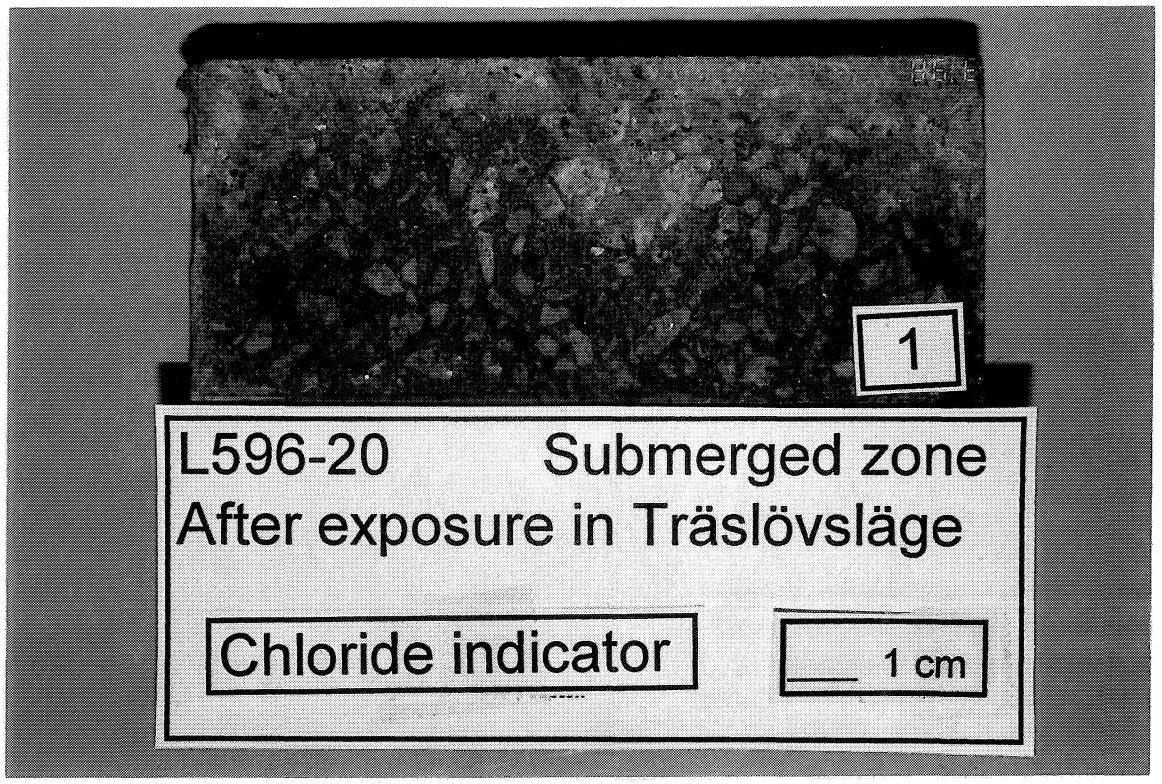


Photo 7. Microstructure and chloride penetration in concrete corrosion cell. SRPC w/c ratio 0.40, after 2 years submerged exposure at the Träslövsläge Marine Field Station. Concrete close to electrode with filter paper defect.

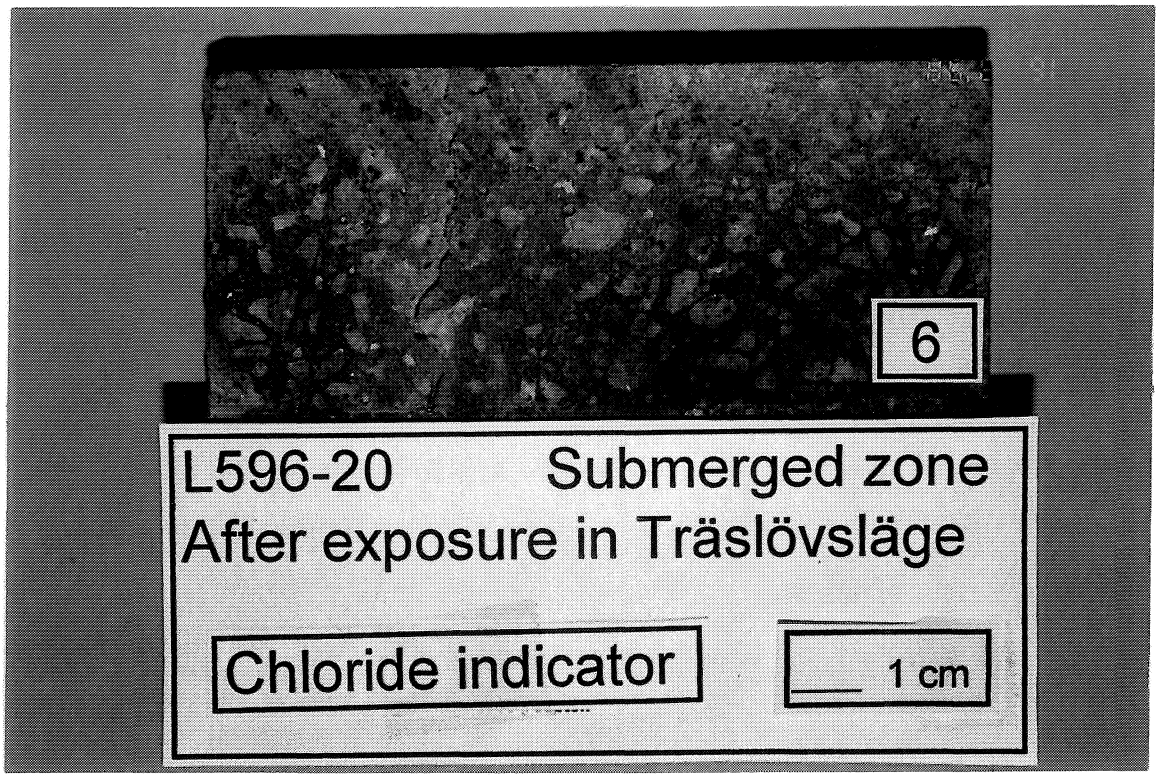


Photo 8. Microstructure and chloride penetration in concrete corrosion cell. SRPC w/c ratio 0.40, after 2 years submerged exposure at the Träslövsläge Marine Field Station. Concrete close to electrode without filter paper defect.

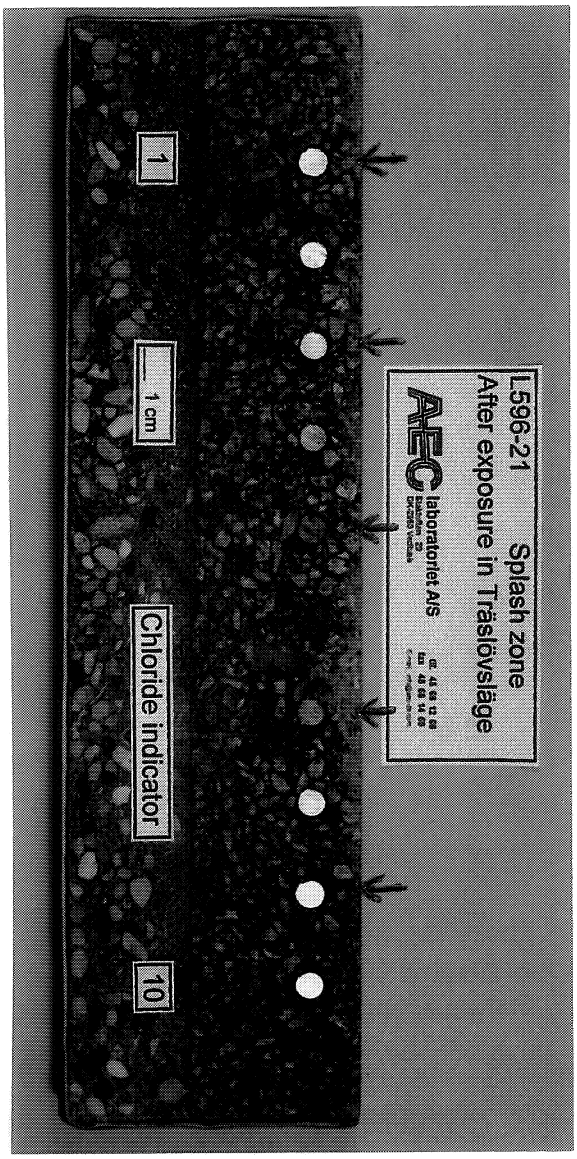


Photo 9. Microstructure and chloride penetration in concrete corrosion cell. SRPC 5 % SF w/c ratio 0.40, after 2 years exposure in the splash zone at the Träslövsläge Marine Field Station. Arrows (←) indicate steel electodes with filter paper defect.


Photo 10. Microstructure and chloride penetration in concrete corrosion cell. SRPC 5 % SF w/c ratio 0.40, after 2 years exposure in the splash zone at the Träslövsläge Marine Field Station. Concrete close to electrode without filter paper defect.

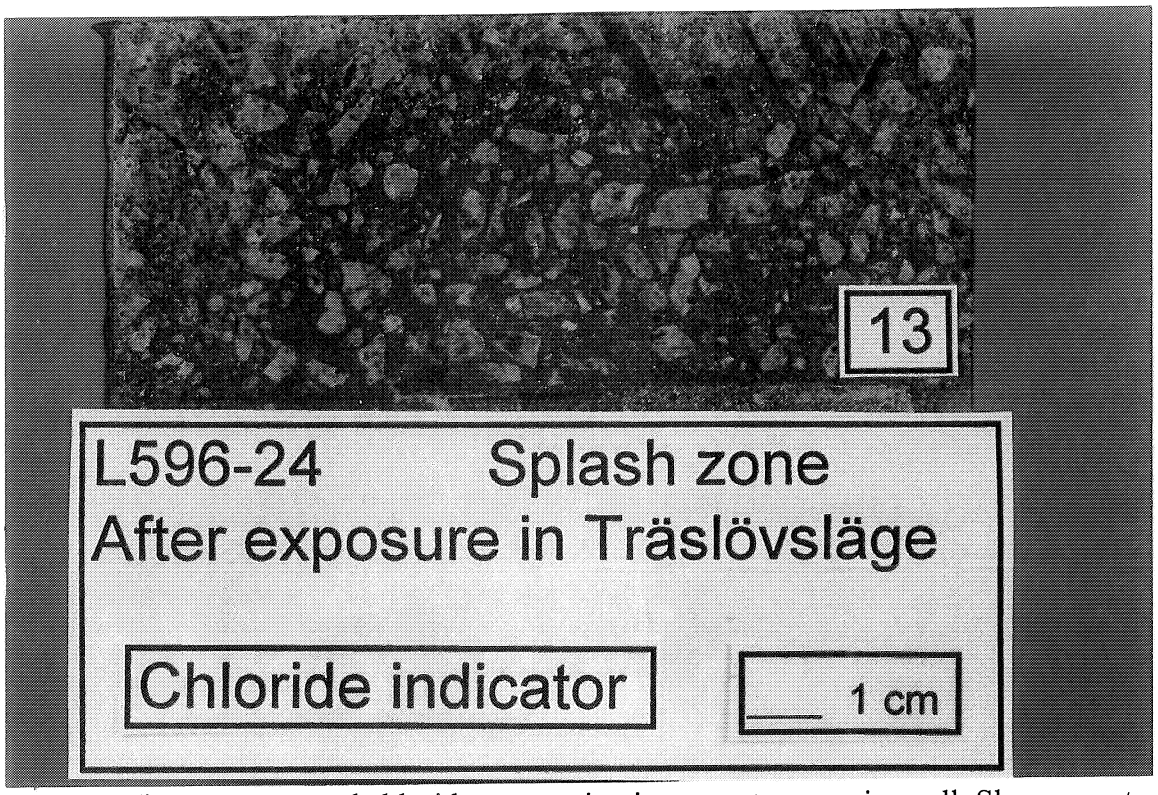


Photo 15. Microstructure and chloride penetration in concrete corrosion cell. Slag cement w/c ratio 0.40, after 2 years exposure in the splash zone at the Träslövsläge Marine Field Station. Concrete close to electrode with filter paper defect.


Photo 16. Microstructure and chloride penetration in concrete corrosion cell. Slag cement w/c ratio 0.40, after 2 years submerged exposure at the Träslövsläge Marine Field Station. Arrows (←) indicate steel electodes with filter paper defect.

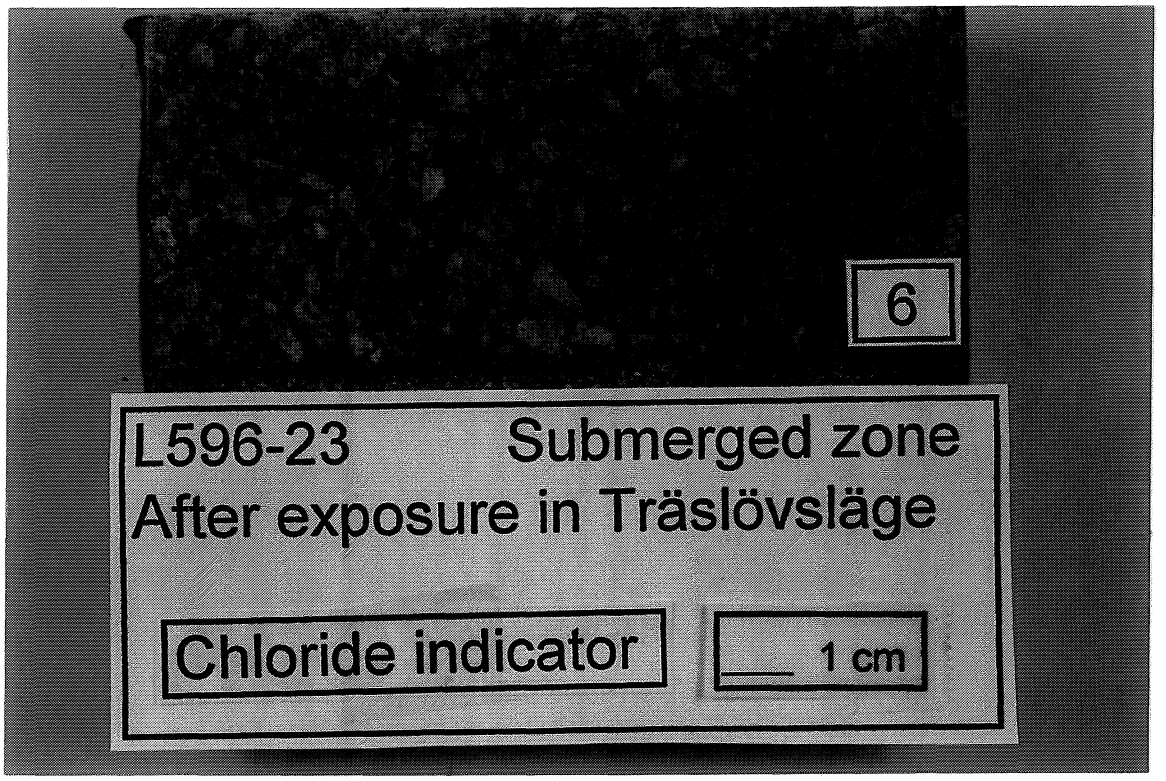


Photo 17. Microstructure and chloride penetration in concrete corrosion cell. Slag cement w/c ratio 0.40, after 2 years submerged exposure at the Träslövsläge Marine Field Station. Concrete close to electrode without filter paper defect.

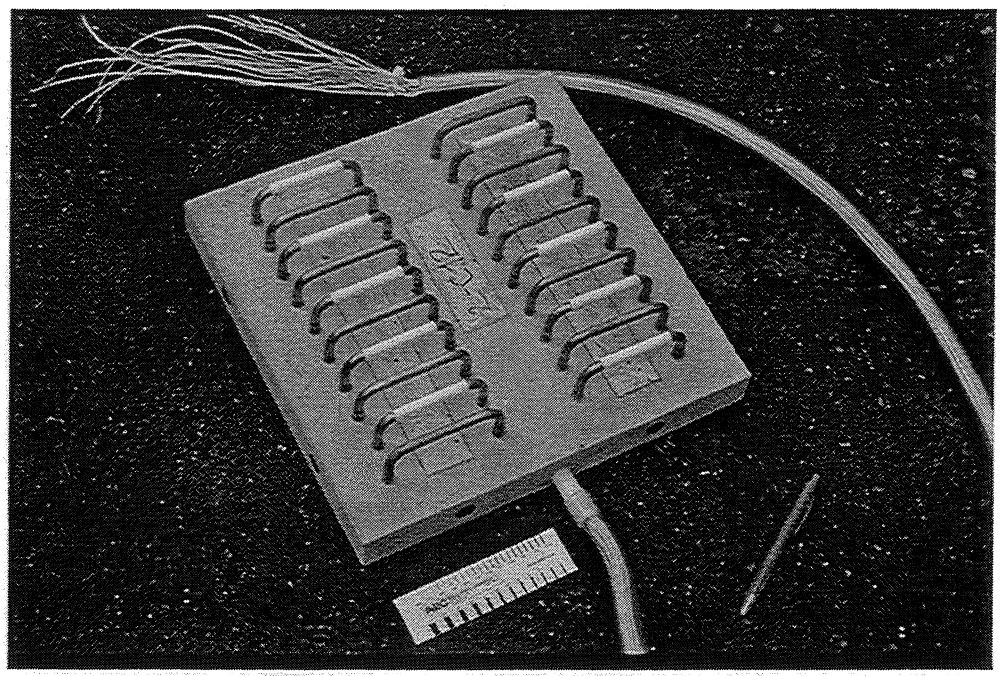

Photo 18. Steel electrodes with and without filter paper defects applied on the steel surface, mounted on a Densit mortar specimen holder prior to casting of test concrete.

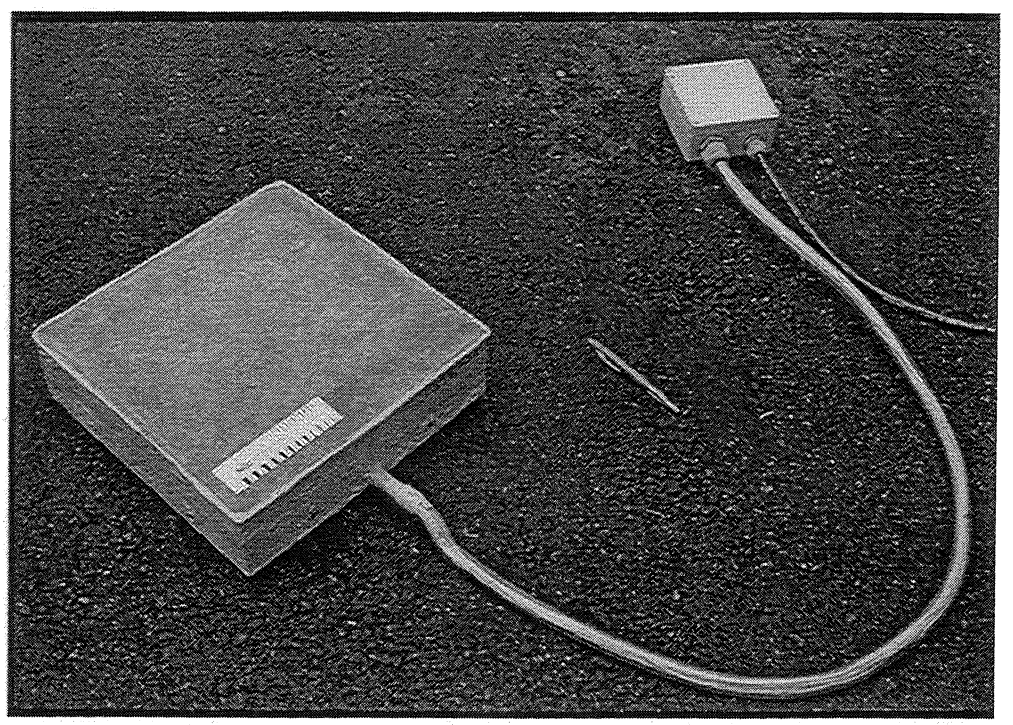

Photo 19. Corrosion cell with cables connected to a datalogger system prior to exposure at the Träslövsläge Marine Field Station

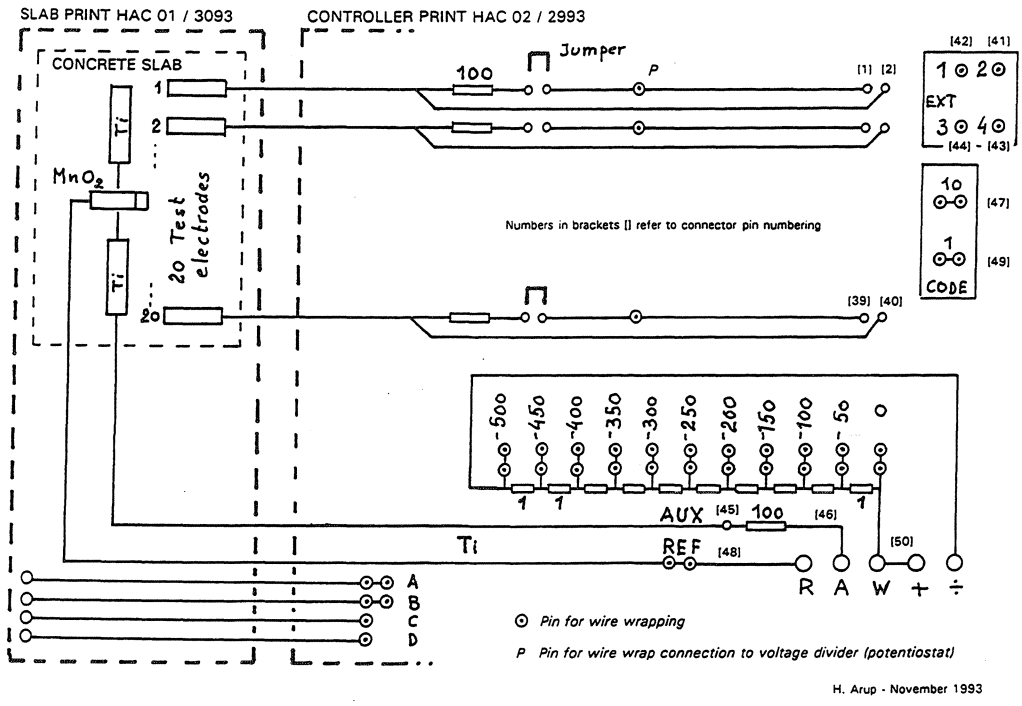


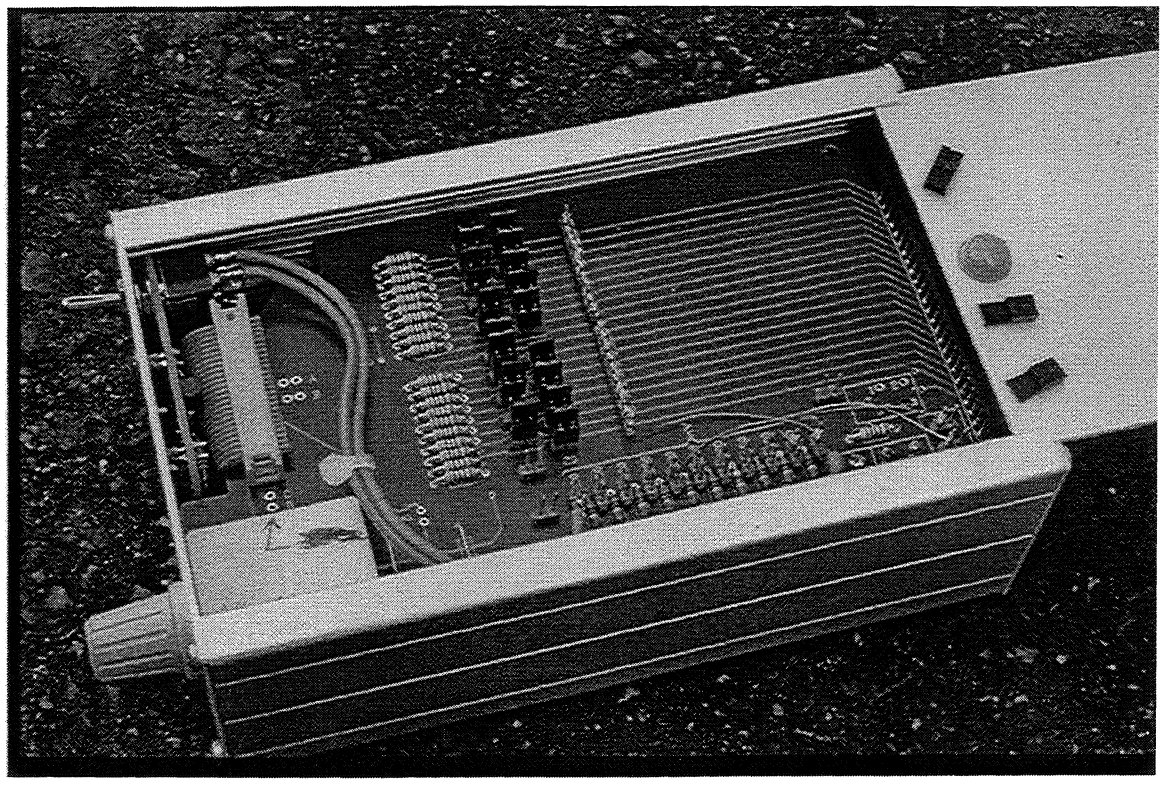

Photo 20. Potentiostat with jumpers for connecting and disconnecting the potentiostat to each steel electrode in a corrosion cell.

Photo 21. Equipment used for profile grinding, e.g. the successive abrasion of concrete from the exposed surface and inwards. The concrete core is fixed in a lathe while 0.7-2 mm thick layers of concrete are abraded by a rotating diamond tool.